THE PLEISTOCENE GLACIAL HISTORY OF THE LAKE WELLMAN AREA, DARWIN MOUNTAINS, ANTARCTICA

A thesis submitted in partial fulfilment

of the requirements for the

Degree of Master of Science in Geology

at the University of Canterbury

by David J. Hood

University of Canterbury

May 2009

Frontispiece

The Lake Wellman area, Darwin Mountains, Antarctica

"A view of the past may be a glimpse of the future"

- Peter Barrett -

Abstract

The Darwin and Hatherton Glaciers form a major system that drains a significant portion of the East Antarctic Ice Sheet (EAIS) through the Transantarctic Mountains (TAM) into the Ross Sea. Flow lines along their length demonstrate that they connect back to Dome Cirque on the Polar Plateau. Very little is known about the way these outlet glaciers have drained the EAIS in the past. However, information on their previous behaviour in response to global climate change and EAIS activity is recorded in their geomorphology. An ice-free region adjacent to Lake Wellman contains a well preserved sequence of moraines that provides evidence of glacial ice fluctuation related to earlier climates. Consequently, this area has potential as an appropriate site for investigating past glacial movement and change. A study was therefore conducted in the Lake Wellman area in order to examine the drift material left behind as the Hatherton Glacier retreated. This was done to obtain information that would help explain the manner and timing of glacial recession.

A geomorphology map was constructed using data obtained from a series of transects placed across the drift moraine material. The transects were located at different elevations ranging between 800 m and 1200 m a.s.l., and were at distances between 4 and 8 km from the present glacier edge near Lake Wellman. Field data were collected from clast material sampled at regular intervals along each transect. These records consisted of assessments and measurements of clast lithology type, average size, hardness measured with a Schmidt hammer, angularity or roundness, and degree of weathering.

The field data demonstrated that for clasts of dolerite and sandstone, angularity decreased and roundness increased significantly with altitude. No such trend occurred with clasts of gabbro, granite or basalt. The field observations therefore indicated that clasts at higher elevations and greater distances from the present glacial ice had been freed from the receding ice earlier and hence exposed for longer periods to the effects of atmospheric weathering. This effect was more apparent on the less durable sandstone and dolerite lithologies.

Rock samples were also collected in the field for subsequent Surface Exposure Dating (SED). These consisted of sandstone and granite rocks which contain a high level of quartz, and care was taken to ensure that the samples chosen had been transported by glacial ice. The rock samples were prepared in the laboratory at the University of Canterbury, Christchurch, New Zealand. The processed samples were sent for cosmogenic dating at the Australian Nuclear Sciences Technology Organisation (ANSTO), in Sydney, Australia, using ^{10}Be and ^{26}Al isotope analysis. Difficulties were experienced with the removal of aluminium from the quartz during the processing of some samples with excessive levels of this element, which interferes with the dating process, possibly leading to an underestimation of the true age. Also, for some samples there were significant differences in the ages determined by the two isotopes. Data were only accepted if there was agreement between the two values and there was no technical or physical reason to doubt the age determined.

These results confirmed those from the clast weathering data and clearly demonstrated the past retreat of the Hatherton Glacier over a period of 2 Ma from an elevation of 1600 m a.s.l. down to its present altitude of ca. 800 m a.s.l. in the vicinity of Lake Wellman. In general, there was a trend of increasing age of exposure with greater elevation and distance from the present glacial edge. Between 800 and 1000 m a.s.l., rocks had been exposed for 1-60 ka. Between 1000 and 1200 m a.s.l., rocks were dated within the range 75-400 ka before present (B.P.) and between 1200 and 1600 m a.s.l., ages ranged up to a maximum around 2 Ma B.P.

The dates obtained in this study are generally greater than those recorded in an earlier published study from the same area in which a different dating technique was used. In particular there is a discrepancy in the position of the ice during the Last Glacial Maximum (LGM; 18-20 ka B.P.). Instead, the results of this study support an alternative modelling analysis that indicates a thinner Hatherton Glacier during the LGM. This conclusion implies a more rapid recession of the Ross Ice Shelf as a result of rising sea levels during an increasingly warmer climate.

Suggested future work to refine the outcomes from this study would include the collection of more samples for SED dating, particularly in the region of the greatest extent of ice during the LGM.

Acknowledgements

I would like to give special thanks my supervisors. Professor James Shulmeister and Professor Bryan Storey! Jamie, you were always ready to offer ideas and support. Your shrewd decisive judgment and quick Irish humour a blessing in stressful moments. Bryan, thanks for the discussions in your office. Your wisdom and responsible steadiness were essential in the learning process. All the best on future trips to Antarctica.

Thank you to: Antarctica New Zealand, Gateway Antarctica, the Department of Geological Sciences and the Royal Society of New Zealand all whom provided thesis and conference funding. Their support made this project possible!

Thank you to LINZ and Geosciences Australia for providing ALOS imagery (© JAXA 2007); and to ANSTO and David Fink for cosmogenic dating. The following people from the department are also thanked: Rob Spiers for getting me started on sample preparation; James the cosmogenics technician; Olivia Hyatt, for advice regarding my many Arc map headaches; John Southward; Anekant Wandres; Travis Horton; Pat and Janet. Thanks, also, to my field assistant Mette; to Irfon Jones for help with GIS solutions; and to Wolfgang Rack and Mike Bentley, thank you.

Thanks to all the geology boys: Daniel (Santa) an inspiring force, Tim O'Toole always ready for a laugh, Andy (The Ginger) an example of calm under stress; and Tom, Sam, Darrel, Nick, Jesse, Kurt, Sean, Cooksey, cheers guys.

My friends and family provided much encouragement, for which I am grateful. Thanks to my family, always there offering support and help. My girlfriend Angie you are an inspiration, always ready to share your honest opinion, thanks for all your keen optimism, support and being there for me. My friends, the crew, you know who you are… Luis, Bree, Max, Amira, Simon, Pepita, Anton (the Destroyer); you were always ready to take me on another climbing, surfing or snow boarding adventure, not to mention mountain biking. Thank you everyone who supported me.

Abbreviations

ALOS Advanced Land Observing Satellite

AMS Accelerator Mass Spectrometer

ANSIE Australian National Science Institute of Engineering

ANSTO Australian Nuclear Sciences Technology Organisation

a.s.l. above sea level

EAIS East Antarctic Ice Sheet

DEM Digital Elevation Mmodel

GIS Geographic Information Systems

GM ground moraine

GPS Global Positioning System

HM hummocky moraine

IPCC International Panel on Climate Change

JAXA Japan Aerospace Exploration Agency

LGM Last Glacial Maximum

LINZ Land Information New Zealand

LGP Latitudinal Gradient Project

m metres

MIS Marine Isotope Stage

PPG polygonal pattern ground

PPM parts per million

SED Surface Exposure Dating

TAM Transantarctic Mountains

WAIS West Antarctic Ice Sheet

WGS World Geodetic System 1984

List of figures

List of tables

Table of contents

1. Introduction and background literature

This chapter introduces the thesis topic. It describes the study area and reviews our present understanding of the geological and glacial history of the region as reported in the literature. Significant issues are brought into focus, and the chapter concludes with a list of questions that the work of this project was designed to address.

1.1. The Lake Wellman area

The Lake Wellman area is a relatively ice-free locality situated on the northern margin of the Hatherton Glacier in the Transantarctic Mountains (TAM), Antarctica (Figure 1). The Hatherton Glacier and the Darwin Glacier to the north, are separated by the Darwin Mountains, but join as a unit just before they emerge eastwards into the Ross Sea immediately north of the Britannia Range and the Byrd Glacier (Figure 1). The Darwin-Hatherton system thus channels polar plateau ice through the TAM from the East Antarctic Ice Sheet (EAIS) to the Ross Ice Shelf. This is demonstrated by flow lines which run the full length of each glacier, projecting back deep into the interior of the EAIS where they originate at Dome Cirque on the outer margin of the Ross Sea catchment. Very little is known about the way the Darwin and Hatherton Glaciers have drained the EAIS in the past, or how their behaviour is influenced by climate change.

In order to predict the response of the EAIS to future climate change a better understanding of its behaviour and response to past climate variation is required. It is therefore important to investigate the way the outlet glaciers have functioned over time, and the ice-free nature of the area around Lake Wellman makes it an ideal site to examine this question. The valleys in this locality are blanketed by vast glacial drifts consisting of well-preserved ice-margin deposits that display clear evidence of activity by the Hatherton Glacier in the recent past. For the purpose of this thesis we are particularly interested in the deposits which were laid down during the period spanning the Last Glacial Maximum (LGM) 18-28 ka before present (B.P.). This is a key marker in relation to global climate change since it is from that time that the climate has generally warmed and sea levels have risen.

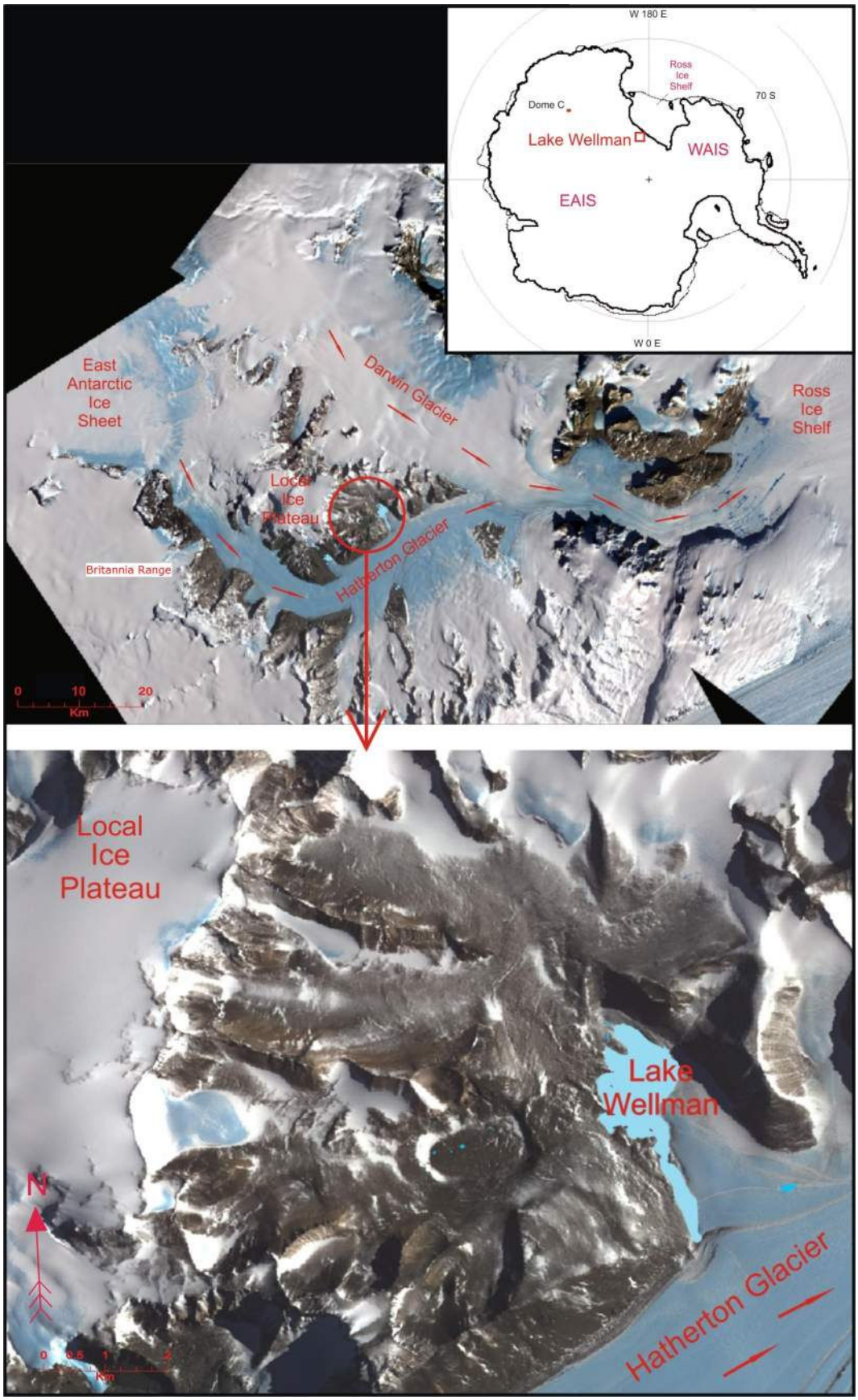

Figure 1. The location of the Lake Wellman area in the Darwin Mountains, TAM, Antarctica; Image source: Antarctica New Zealand.

The glacial deposits adjacent to Lake Wellman reach elevations up to 800 m above the present ice surface, indicating the extent of the past glacial ice limit. They are primarily composed of locally derived boulders of Ferrar Dolerite and Beacon Sandstone (see below). Besides these, however, many granite boulders are also found within the drifts left in this area and in the adjacent valleys. These rocks are erratics, exotic to this region, as no granitic basement rocks are exposed in outcrops at Lake Wellman or in the Darwin Mountains. A brief description of physiography of the Lake Wellman study area is presented in the next section.

1.2. The physical and geological setting

The geological study of Antarctica is hampered by the thick layer of ice that permanently covers nearly the entire continent. However, rocks are accessible in exposed outcrops in large mountains which protrude through this ice layer. Of these, the most extensive are the Trans Antarctic Mountains (TAM), which form one of the largest mountain chains in the world. The TAM are described by Stern and Ten Brink (1989) as a rift-shoulder mountain range with gently-tilted, faulted blocks. They follow a line of intersection between two ‘continents’ of separate geological origin, and thus divide Antarctica into two distinct parts, East and West (Stern and Ten Brink, 1989). The TAM extend 3500 km across the entire width of the Antarctic continent from Coats Land (adjacent to the Ronne Ice Shelf at the head of the Weddell Sea) to northern Victoria Land, and therefore act as a barrier, 100 km - 300 km in width, that separates the East Antarctic (EAIS) and West Antarctic Ice Sheets (WAIS). There are over 4000 peaks in the TAM, the highest reaching an elevation of 4500 m a.s.l.

The glacial history in the TAM is linked to the geological and tectonic evolution of Antarctica, as well as to the past climate. Tectonic activity and related uplift influence ice sheet dynamics (van den Berg et al., 2006) and any basal melting is affected by geothermal flux (Hulbe and MacAyeal, 1999). Therefore, before discussing the nature and development of the glacial aspects of Antarctica and the TAM, the geology of the region is examined in a broad outline.

1.2.1. Early tectonic activity

East Antarctica is older than West Antarctica, and was tectonically stable for most of the Pre-Cambrian. Historically it has existed as a component of a number of successive super-continents, including Rodinia (ca. 1100 Ma B.P.), and later Pangea (Paleozoic and Mesozoic) and then Gondwana. West Antarctica developed as an accretion of terranes during the Late Proterozoic and Palaeozoic. Over this same period, the margin of East Antarctica was subjected to deformation and intrusive activity, with orogeny events occurring in both East and West Antarctica (Anderson, 1999). The TAM first formed along a paleo-Pacific margin of the East Antarctic Craton. Strongly deformed and folded sedimentary and igneous plutonic (granite) rocks which now make up the basement of these mountains date back to the Precambrian and Palaeozoic eras (ca. 440-800 Ma B.P.; Stern and Ten Brink, 1989). These basement rocks formed during the Ross Orogeny which began in the early Paleozoic (ca. 500 Ma) as a single deformation event which continued on during the late Cambrian and Ordovician times (Storey et al., 1996). The dominant cover unit immediately above the basement rocks in the TAM is made up of the Beacon Super Group sequence exposed on the edge of the East Antarctic Craton, which dates back to the Devonian (ca. 400 Ma B.P.) (Barrett and Kohn, 1975).

During the Permian-Triassic the break up of the super-continent Pangea was initiated. Associated global tectonic activity continued during the Jurassic and early Cretaceous with rifting between west and east Gondwana occurring in the middle Jurassic (ca. 170 Ma B.P.). This caused uplift along the West Antarctic Craton, ca. 145 Ma B.P. (Behrendt and Cooper, 1991). During the Jurassic, voluminous magmatic activity formed extensive basaltic sills (referred to as the Ferrar Dolerite), which intruded into the Beacon Super Group and basement rocks of the TAM (Anderson, 1999). Widespread deposition of Jurassic and Cretaceous shales was also occurring at this time.

During the late Cretaceous (ca. 67 Ma B.P.), break up of Gondwana had begun with the separation of India and Africa, but Antarctica remained still joined to South America and Australia. At this time subduction commenced along the

Pacific Antarctic margin, initiating further uplift of the TAM (Anderson, 1999). Oblique convergence and deformation along the TAM is demonstrated by slaty cleavage that transects the variably plunging folds (Storey et al., 1996). There are varying views on uplift rates ranging from episodic uplift of approximately 1 kilometre every 1 Ma (Behrendt and Cooper, 1991) to approximately 100 metres every 1 Ma. There is also debate as to whether the plate boundary that caused this uplift still exists in Antarctica today (Smith 1985; Drewry 1986).

During the Eocene (ca. 40 Ma B.P.) Antarctica was centred in a polar position with fully developed continental margins (Anderson, 1999). Extensive ice sheets had formed by the Oligocene - Miocene (ca. 30-24 Ma B.P.) as a result of global climate change (see below). This cooling effect was enhanced by the development of a circum-polar current as Antarctica separated and became isolated from South America and Australia (Windley et al., 1984).

1.2.2. The Darwin Mountains

As elsewhere in the TAM, a granite complex of Paleozoic–Precambrian age makes up the basement formation at Lake Wellman in the Darwin Mountains (Table 1). Between this basement layer and the overlying Beacon Supergroup is a major unconformity, the Kukri Peneplain (McKelvey et al., 1977). This developed as a result of mass erosion at ca. 400 Ma B.P. (Allibone et al., 1991).

Higher in the stratigraphic sequence is the Hatherton Sandstone, a 450 m thick sequence divided into two members (Table 1). The basal member consists of well-bedded white quartz sandstone, with beds up to 6 m thick. The upper member contains microfossils and displays current bedding structures. Both the upper and lower members grade into one another (Haskell et al., 1964). The Darwin Tilite disconformably overlies the Hatherton Sandstone. It consists of angular, unsorted sandstone with weathered and rounded erratics of Beacon and basement groups. In the middle parts there are alternating beds containing ripple marks which resemble varves (annual layers of sedimentary rock; Haskell et al., 1964). Overlaying the Darwin Tilite, the Misthound Coal Measures are composed of irregular bands of basal conglomerate indicating a disconformable contact. The 30 m thick Ellis

Formation is the youngest formation in the sequence separated from the Misthound coal measures by 300 m of Ferrar Dolerite sill (Haskell et al., 1964). Numerous sills of the Ferrar Dolerite Group intruded into the Beacon Group during the Jurassic (Haskell et al., 1964), and can be seen in frequent exposures flanking Lake Wellman and at the heads of adjacent valleys.

Table 1**.** Correlation and stratigraphic subdivision of the Beacon Group in the Darwin Mountains area (adapted from Haskell et al., 1964).

Formation	**Lithology and fossils (thickness in metres)**	**Age**
Ellis	Siltstone, sandstone, conglomerate (30 m +)	Upper Permian (?)
Misthound Coal Measures	Current – bedded, sub-arkosic sandstone. Interbedded carbonaceous sandstone, shale and coal. *Gangamopteris* flora (93 m)	Lower Permian
Darwin Tillite	Fluvio-glacial sandstone erratic boulders. Varved sandstone and siltstone (27 m)	Permian/ Carboniferous (?)
Hatherton Sandstone	Current-bedded quartz sandstone. *Beaconites antarcticus* Vialov and other ichnofossils (230 m). Overlies well bedded quartz sandstone with occasional ichnofossils (220 m)	Carboniferous? /Devonian (?)
Brown Hills Conglomerate	Interbedded conglomerates and current-bedded sandstones with a few carbonaceous beds (34 m)	Devonian (?)
	Major Unconformity – the Kukri Peneplain	
Basement Complex	Weathered granite. Mainly granodiorite and granite with small area of metasediments	Paleozoic / Precambrian

1.3. Holocene glacial and ice sheet activity

1.3.1. The West Antarctica/Ross Ice Sheet

During the Eocene (50 Ma B.P.), when the earth was about 6^{o}C warmer than at present, ice sheets were absent in the Antarctic, and the continent was covered in areas of forest and green vegetation. Substantial ice developed at the end of the Eocene (34 MA B.P.) accompanied by a large drop in sea level, as the earth's temperature fell 3-4^{o}C. The Antarctic ice sheets apparently fluctuated in size until the present stable situation was reached ca. 14 Ma B.P. During the uplift of the TAM in the Eocene, major ice streams such as the Byrd Glacier formed in the geologically weaker zones, catching the majority of the flow from the EAIS. Many of the adjacent valleys were left with slow moving streams such as the Darwin and Hatherton Glaciers (Denton, 1979). As uplift of the TAM continued the pre-existing ice sheets responded throughout by increased gravitational flow which shaped deep-transverse valleys. Ice spilled over from existing plateaus breaching adjacent valleys and eventually connecting neighboring ice streams (Denton, 1979). At the same time isolated nunataks formed between ice lobes, and were uplifted or eroded (Denton, 1979). The flow of ice through the TAM was influenced not only by the source in the EAIS but also by the level of obstructing grounded shelf ice at the glacial outlets in the Ross Sea which regulated their outflow. This, in turn, was affected by the supply from the West Antarctic Ice Sheet (WAIS). Sea floor drilling has indicated more than 60 cycles of advance and recession of the Ross Ice Shelf grounding line in the McMurdo Sound area during the past 14 Ma. The grounding line represents the limit of contact with the underlying bed rock beyond which there is sufficient water depth and natural buoyancy for the ice to separate free from the underlying surface.

Reconstructions of the Ross Ice drainage system and the position of the grounding line of the Ross Ice Shelf during the LGM have been presented by Anderson et al. (2004), Bockheim et al. (1989), Conway et al. (1999), Denton and Hughes (2000), and Kellogg et al. (1996). A model for the advance of the Ross Ice Sheet into the Ross Embayment was proposed by Kellogg et al. (1996); this suggested that during advance, ice from the WAIS occupied sub-glacial troughs in the inner Ross Embayment. These troughs are oriented in a northwest-southeast direction and the

largest troughs are aligned with major ice stream from the WAIS (Anderson, 1999). Today these ice free troughs extend all the way to the edge of the continental shelf (Bentley and Jezek, 1981). As sea level began to rise following the LGM, the ice retreated along the submerged troughs to its present position. The retreat of the grounding line occurred faster than the calving front resulting in the formation of the Ross Ice Shelf (Denton and Hughes, 2000).

At the height of the LGM, glacial termini in the Dry Valleys were well inland of the Ross Ice Shelf. In this unique situation grounded ice from the Ross Ice Shelf spread inland into the valley mouths, causing the formation of numerous pro-glacial lakes due to damming by the grounded ice (Conway et al., 1999).

Previous positions of the grounding line of the WAIS can be estimated by reconstructing the size and form of the glaciers flowing through the TAM. This is because when blocking their outlets the grounded ice acts as a dam where merging occurs, impeding movement and resulting in thickening. However, estimates of the rate of retreat of the Ross Ice Shelf grounding line during the Holocene have varied. Conway et al. (1999) proposed a swing gate model for the movement of the grounding line back to its present position (Figure 2). They believed that the grounding line of the WAIS was situated seawards almost to Coulman Island during the LGM (approximately 20 ka B.P.), 1300 km closer to the outer coast than its present position. Their model shows the retreating grounding line passing the Darwin- Hatherton outlet at 6.8 ka B.P. (Figure 2), this was based on data from ^{14}C dating (Bockheim et al., 1989).

On the other hand, Anderson et al. (2004) modelled a more rapid retreat of the Ross Ice grounding line past the Darwin outlet as occurring at 7.9 ka B.P., about a thousand years earlier. This was several centuries before the Darwin-Hatherton Glacier reached equilibrium at 7.1 ka B.P. A more rapid retreat was more recently supported by Todd et al. (2007) who deduced that ice at the mouth of the Reedy Glacier, further south in the TAM, thinned from ca. 7 ka B.P. By contrast, at this earlier time (between 9.4 and 7.6 ka B.P.), Conway et al. (1999) had placed the grounding line position as still in the McMurdo Sound area, indicating a slower rate of recession, as noted. They pictured ice filling the Ross Embayment and

merging with glacial ice on land as far as the southern Scott Coast, close to the McMurdo Sound area where it terminated on land 450 km south of Coulman Island at the mouth of the Taylor Valley and other Dry Valleys (Conway et al., 1999).

The rate of retreat must therefore fall into one of these two scenarios, with the grounding line position at the Darwin-Hatherton Glacier outlet being earlier (7.9 ka B.P.; Anderson et al., 2004) or later (6.8 ka B.P.; Conway et al., 1999: Denton and Hughes, 2000). Information on the thickness of the Darwin and Hatherton glaciers during these periods is therefore necessary, in order to help resolve this issue.

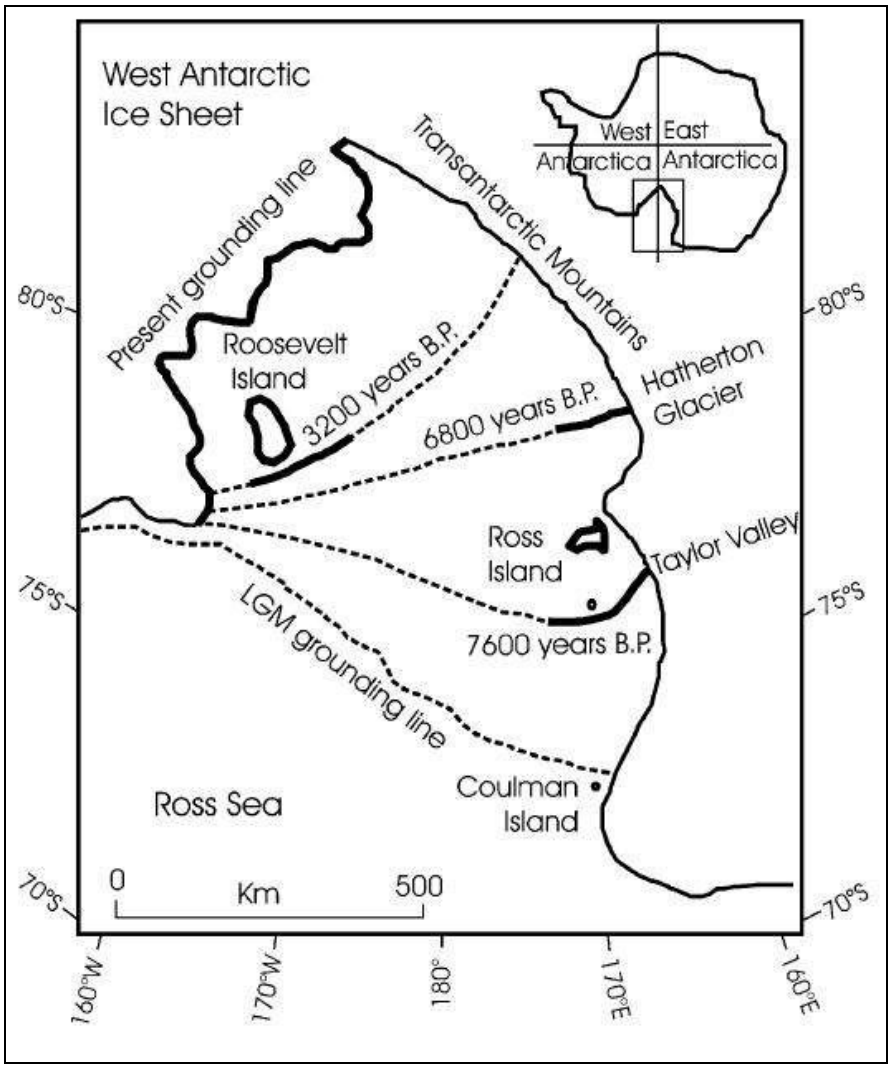

Figure 2. The swinging gate model and grounding line position on the Ross Ice Shelf, proposed by (Conway et al., 1999).

1.4. Previous studies of The Lake Wellman area

It was shown in the previous section that establishing the correct timing of the retreat of the Ross Ice Shelf entails understanding the past magnitude of the EAIS outlet glaciers over time. This section reviews what has already been learned of the past size and behaviour of the Darwin and Hatherton Glaciers, and considers what information is still required.

Bockheim et al. (1989) identified a glacial sequence of five moraine drifts deposited adjacent to Lake Wellman in the Darwin Mountains by the Hatherton Glacier. These were named (from youngest to oldest) the Hatherton, Britannia I, Britannia II, Danum and Isca drifts (Bockheim et al., 1989). The locations of the deposits in this sequence are presented in Figure 3.

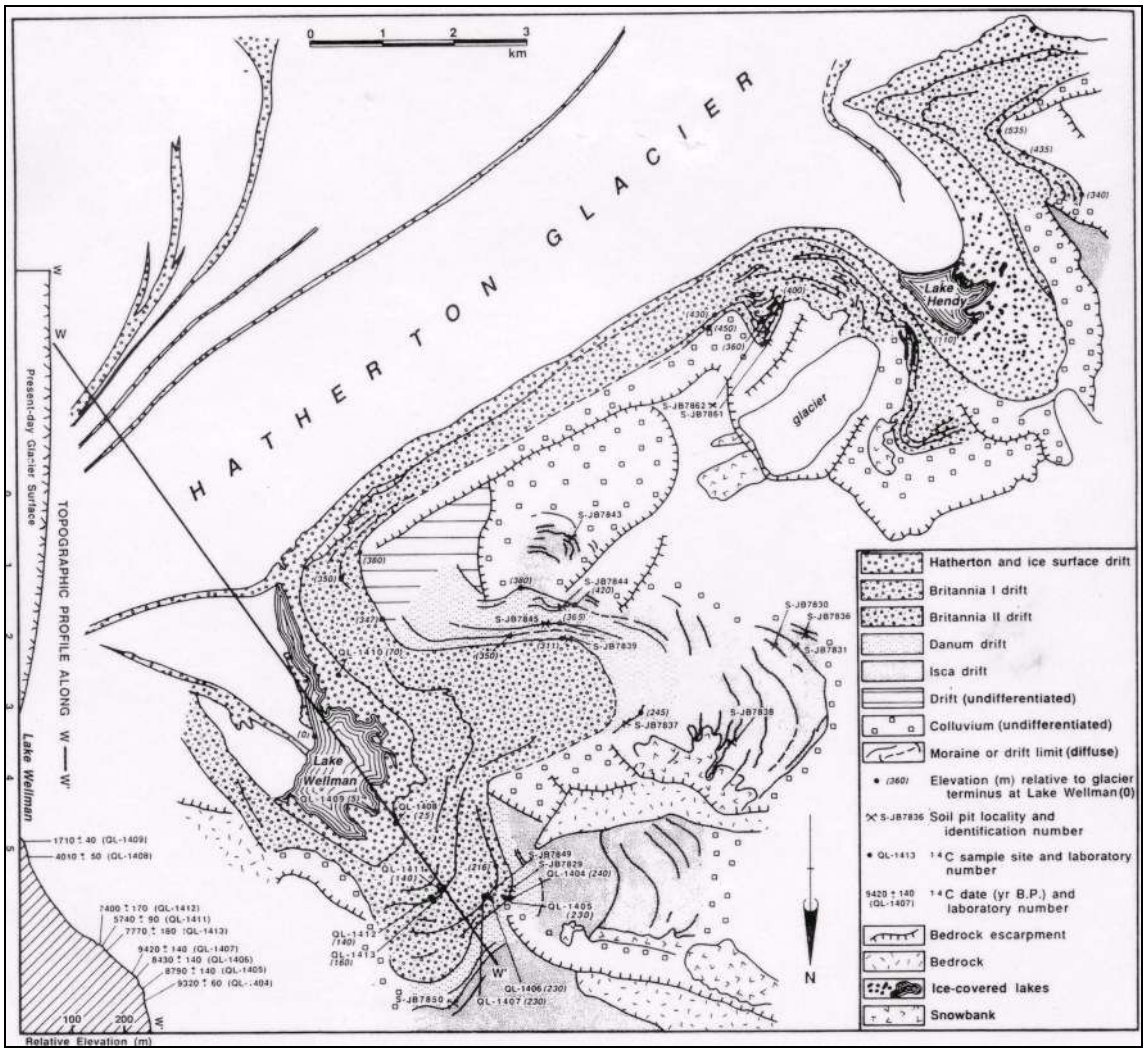

Figure 3. Glacial drift sequence and moraines at Lake Wellman (Bockheim et al., 1989).

By projecting horizontally from the present upper limit elevations of these ice-free moraines, Bockheim et al. (1989) reconstructed a vertical profile along the length of the Hatherton Glacier indicating the elevation of the ice surface at the time each was deposited (Figure 4). They found that the Hatherton drift is uniformly 20 – 70 m above the present ice surface; the Britania I drift is 50 - 100 m above the present ice surface at the central part of the glacier; and the Britannia II drift is 100 m and 450 m above the present ice surface in the upper and mid sections, respectively. It was determined that the Britannia I and Danum ice surfaces had remained uniformly parallel to the Britannia II Drift (Figure 4). At the lower end of the glacier, the extrapolated Britannia II drift position implied a former ice surface elevation of 1100 m above the present Hatherton Glacier where it interfaced with the Ross Ice Shelf. It was believed that this substantial depth of glacier ice resulted from damming by grounded Ross Shelf ice. The comparatively small change in thickness at the upper end of the glacier indicated that the thickening was not caused by an increase in ice flow from the EAIS (Conway et al., 1999).

Bockheim et al. (1989) used ^{14}C dating, and dug pits to observe soil properties, in order to determine stages of development and so deduce the past retreat and advance movements of the glacier. These properties included depth of soil staining, thickness of layers showing strongest coloration due to oxidation, and the position of soil consolidated by the accumulation of weathering products. They recognised a number of buried soils, apparently covered by temporary re-advances and subsequent retreats of the glacier, which they distinguished by changes in hue in buried ventifacts (rocks abraded, pitted, or polished by wind-driven sand or ice crystals). From these buried soils they inferred, for instance, at least four glacial advances within the Danum drift. This and related work was collated by Moriwaki et al. (1992) in an attempt to match glacial features over a wider area. Sequences identified in the Darwin Mountains by their contrasting soil properties and changes in surface morphology were correlated with those in the adjacent Britannia Ranges (Figure 1) to the south and the Brown Hills to the north, and more widely with profiles from the Beardmore, Reedy, McMurdo Dry Valleys, Terra Nova Bay, and Rennick Glacier regions. The correlations are displayed in Table 2.

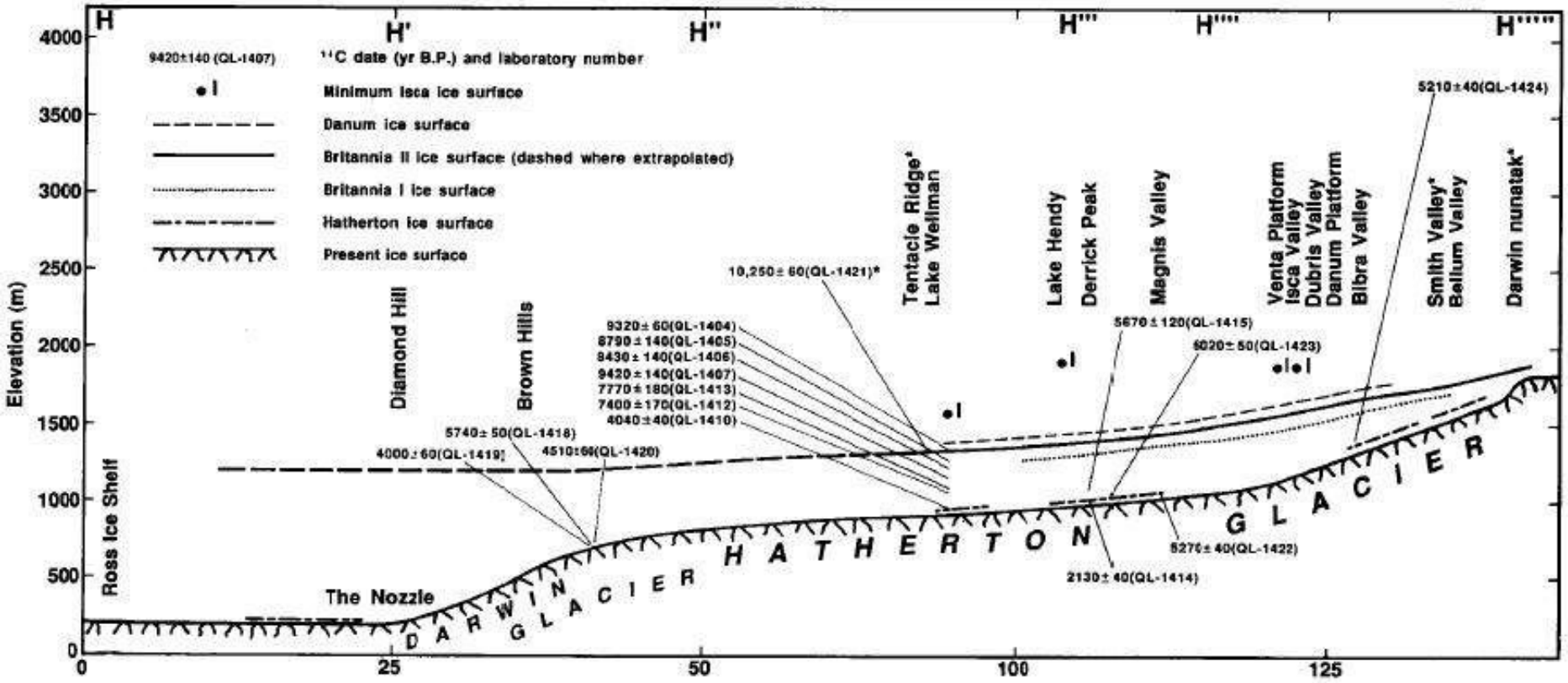

Figure 4. Present and former profiles along the Hatherton Glacier, with ^{14}C dating locations identified (Bockheim et al., 1989).

Table 2. Likely correlation of glacial events in the Transantarctic Mountains (Moriwaki et al., 1992).

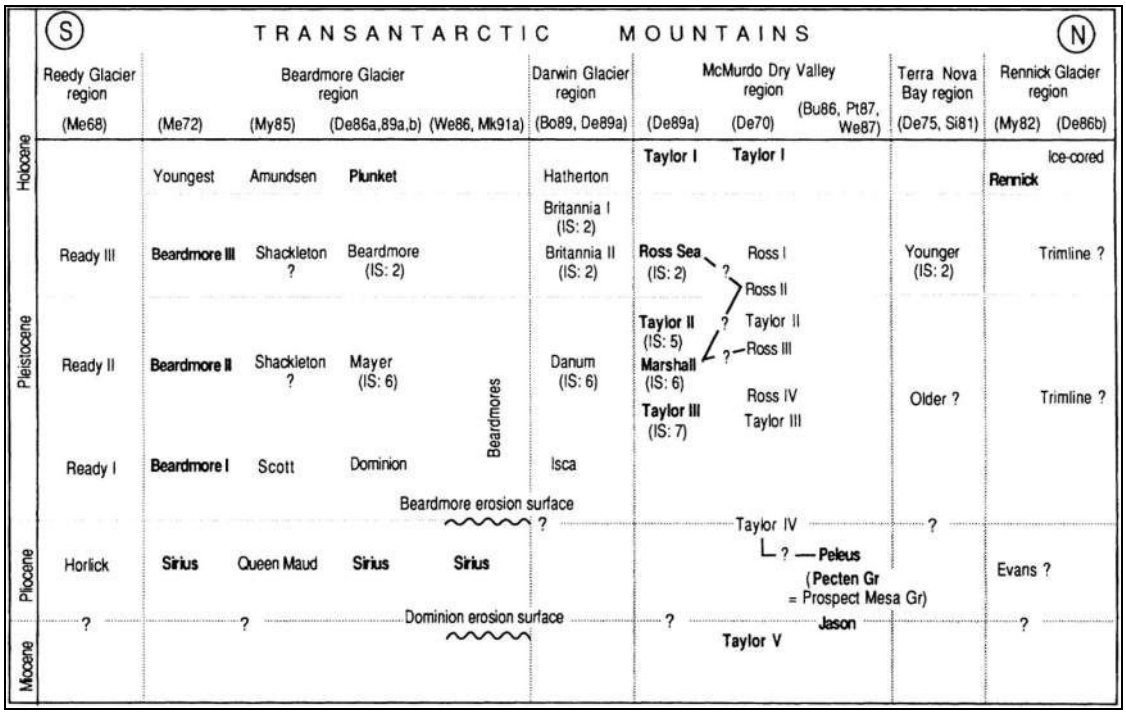

Secondly, Bockheim et al. (1989) used ^{14}C dating to fit a time scale to the ice profiles of the Hatherton Glacier (Figure 4). Numerous ponds today occur in depressions and kettle holes in the Hatherton and Britannia drifts or as a result of damming by this debris from the Hatherton Glacier. Blue-green algae that once inhabited similar ponds are now preserved beneath surface clasts within the glacial drifts in the same region. These were used for ^{14}C dating to identify the minimum age of the overlying Britannia and Hatherton drifts.

In this way, Bockheim et al. (1989) estimated the age of the Hatherton drift at 5.2 ka B.P., or older. By correlating the Hatherton, Britannia and Danum drifts with corresponding outer Ross Sea profiles they concluded that the Britannia II drift represents a temporary glacial thickening (advance) during the late Wisconsin (marine oxygen isotope stage, MIS 2; 16-20 ka B.P.[1]), at the time of the LGM.

[1] Glacial and interglacial periods can be classified by the ratio of the stable oxygen isotopes $^{18}O/^{16}O$ in foraminifera microfossils present at different depths in cores from sediments in deep ocean basins; due to different rates of evaporation and condensation between the lighter $H_2{}^{16}O$ and heavier $H_2{}^{18}O$ water molecules in sea water, this ratio is higher during colder and lower during warmer eras, whereas the reverse pattern occurs on land ice formed from past precipitation. MIS 2 to MIS 4 refer collectively to the last glacial.

Subsequent recession was than followed by a smaller Britannia I re-advance, superimposed on the older Britannia II profile. In the same way it was deduced that the Danum drift represented thickening of the Hatherton Glacier due to grounding of the Ross Ice Sheet during MIS 6 (ca. 130-200 ka) (Bockheim et al., 1989). The younger Britannia thickening persisted until between 8.4 and 9.4 ka B.P., but than dropped to its present level by 5.7-6.0 ka B.P. These estimates were the basis for assuming that the Ross Ice Shelf grounding line had retreated past the Darwin-Hatherton Glacier outlet by 6.8 ka B.P. (Conway et al., 1999).

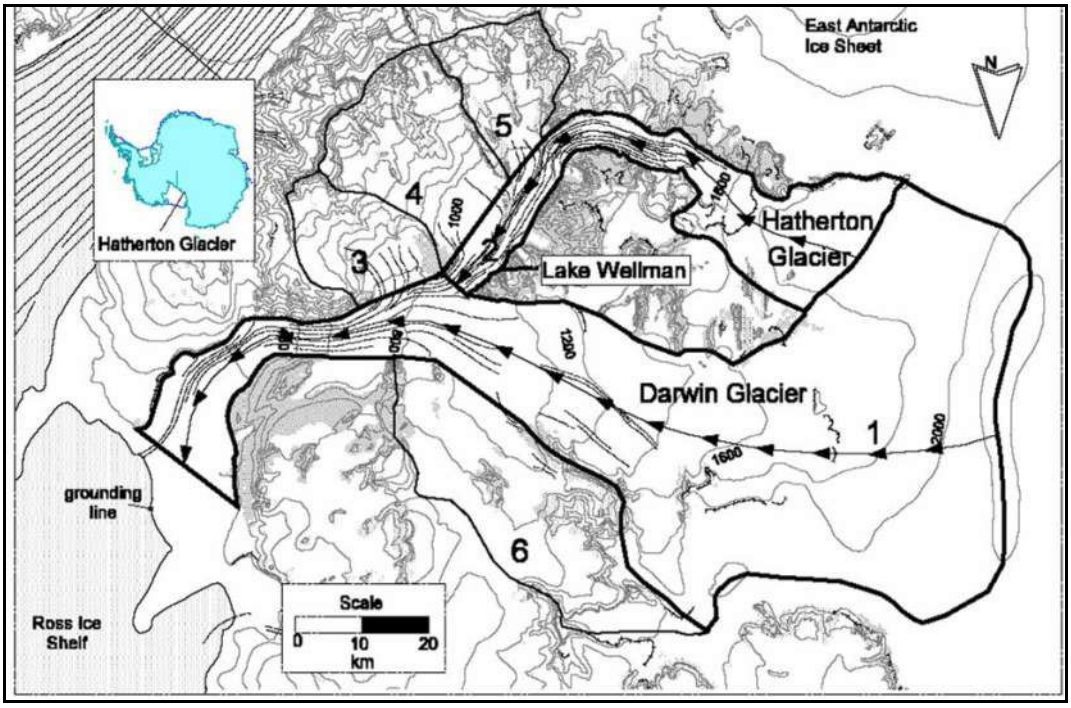

Figure 5. Location of Lake Wellman, the Darwin and Hatherton Glaciers, and ice flow lines of glacial ice movement (Anderson et al., 2004).

Anderson et al. (2004) modelled the Hatherton-Darwin Glacier system by projecting from the current surface to create former ice surface profiles for a glacier in equilibrium over a range of ice elevations between 0 and 1100 m. During the LGM, the best fit profile was found to occur when the ice elevation was 800 m ± 100 m higher than the present Ross Ice shelf surface (Figure 6) (Anderson et al., 2004). The modelled elevations derived by Anderson et al. (2004) therefore did not fit those obtained by Bockheim et al. (1989). The 800 m profile of Anderson et al. (2004) was lower than the position of the Britannia II drift at the outlet of the

Hatherton Glacier (Figure 4), which was where Bockheim et al. (1989) had placed the position of the ice surface during the LGM. Anderson et al. (2004) therefore concluded that the Britannia II surface extrapolation for the LGM by Bockheim et al. (1989) was unrealistic. It was also noted that no allowance had been made for a lag period while the glacier system responded after release from grounded shelf ice, which could help to explain their later estimate of the grounding line retreat. Anderson et al. (2004) decided that the outlet ice elevation had fallen to its present level 7.9 ka B.P., which they therefore inferred was when the Ross Ice Shelf grounding line had passed the Darwin-Hatherton outlet.

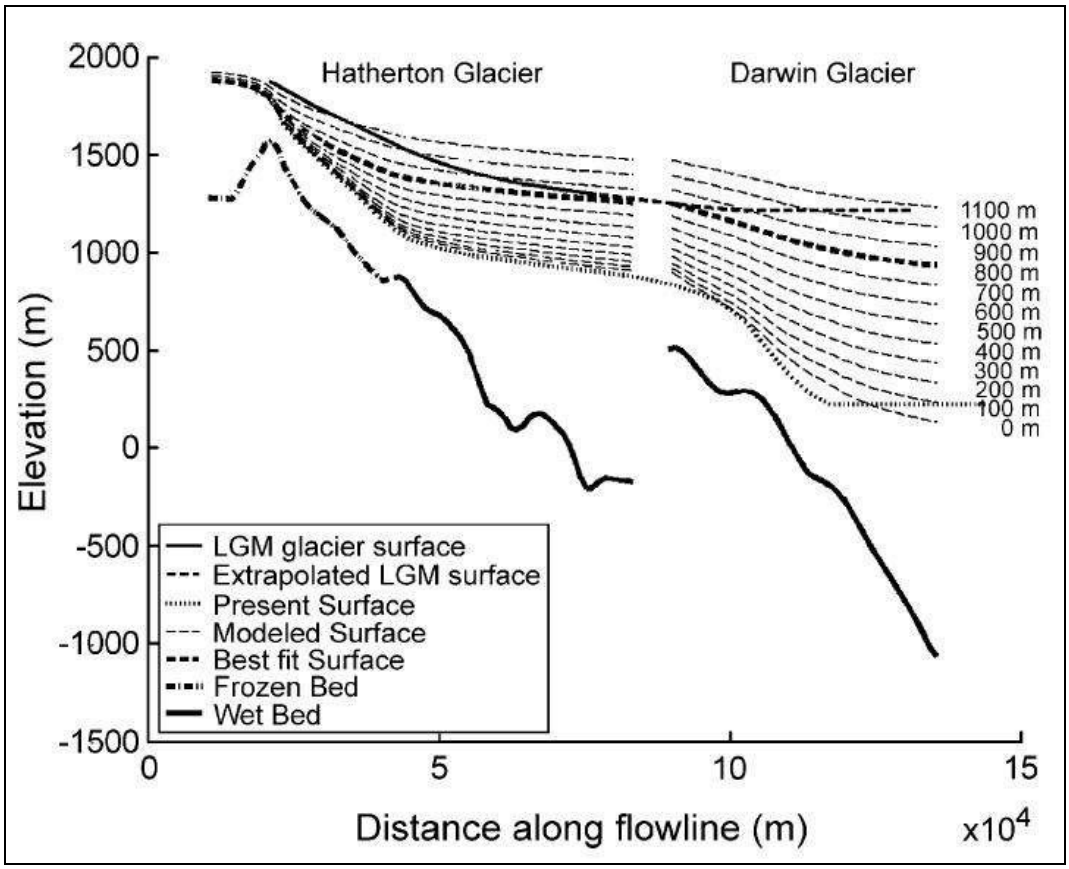

Figure 6. The Darwin-Hatherton Glacial system equilibrium profiles. The thin dashed lines represent 100 m contour intervals. The 800 m profile is marked with a heavy dashed line representing the best fit to the LGM surface (Anderson et al., 2004).

A reconstruction by Denton and Hughes (2000) shows ice stream flow lines feeding fast moving ice from the polar plateau into the Ross Ice Shelf (Figure 7). The position of the LGM and present grounding line positions of the Ross Ice

Shelf are marked (Figure 7). At the Darwin-Hatherton outlet the ice surface contours are influenced by the 1100 m glacier elevation of Bockheim et al., (1989), and as a result the flow lines are much steeper and more concave than elsewhere in the TAM. Anderson et al. (2004) suggested that at this position the elevations presented by Denton and Hughes (2000) are unrealistic and forced because during the LGM the height of the Darwin outlet surface was actually lower. This is more consistent with an earlier and more rapid retreat of the grounding line past the Darwin Glacier.

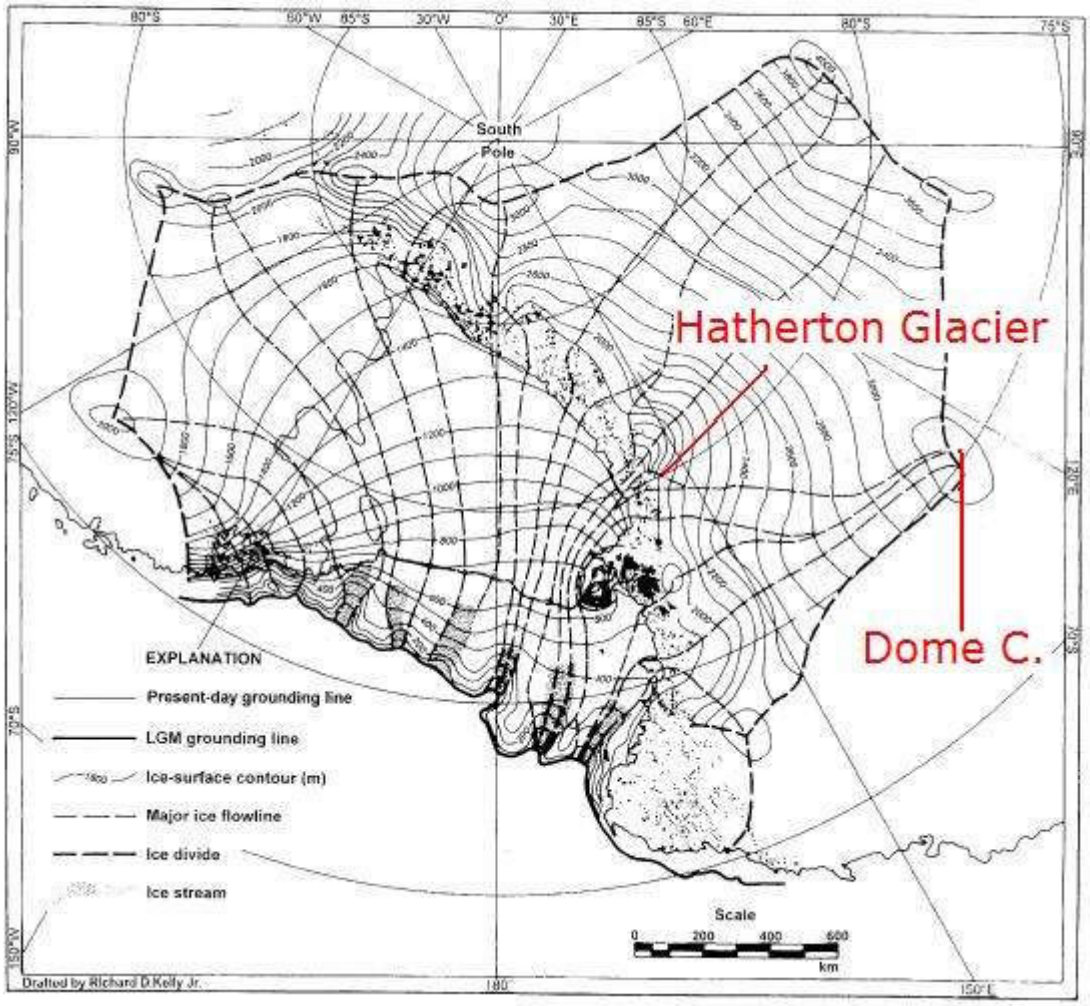

Figure 7. Reconstruction of the Ross Ice Shelf drainage system as at the LGM (Denton and Hughes, 2000). The Hatherton Glacier and Dome Circe (marked in red) are inter-connected by glacial flow lines (indicated by dashed line).

1.4.1. Conclusion

During the LGM, glaciers flowing through the TAM experienced significant thickening as they merged with ice from the Ross Ice Shelf. When grounded, the Ross Ice Shelf acts as a dam impeding the outflow of the Darwin and Hatherton Glaciers. According to Conway et al. (1999) the dating of three points within the Ross Sea Embayment indicates that most of the grounding line recession occurred during the Holocene (0 - ~ 10 ka) without any influence from climate or sea level. Therefore, ongoing recession is not affected by recent climate and sea level fluctuations. The maximum extent of ice during the most recent glacial cycle dates at around 18 – 24 ka B.P. in the Wisconsin. Glacial drift profiles presented by Denton et al. (1989) show that there was little elevation change of the polar plateau at this time. Bockheim et al. (1989) mapped glacial drift sequences and extrapolated former ice surface profiles suggesting that the ice elevation of the Darwin outlet to the Ross Ice Shelf was 1100 m thicker than today. However, Anderson et al. (2004) used a modeling approach to conclude that the ice elevation at the Darwin outlet was 800 m thicker than the present ice surface during the LGM. Study of the drift moraines adjacent to Lake Wellman will assist in clarifying this discrepancy and help to resolve the timing of the retreat of the Ross Ice Shelf following the LGM.

1.5. Aims and objectives

The influence of longer-term global climate change on the EAIS is recorded in the glacial deposits of the Hatherton and Darwin Glaciers. The Lake Wellman area displays a well-preserved sequence of moraines that retain evidence of past glacial ice fluctuation spanning the LGM period. The occurrence of undisturbed moraines adjacent to the outlet glaciers provides a rare and valuable opportunity to study past climate change in Antarctica. The aims of the thesis research were therefore:

I. To test the hypothesis that the Darwin-Hatherton Glacier System has retreated in stages during the Holocene to its present position.

II. To define the limits of stages of glacial recession or re-advance, based on surface morphology, erosion and weathering features in the Lake Wellman Valley in the Darwin Mountains.

III. To date the recession of individual glacial episodes using cosmogenic exposure age dating (SED), identifying (if possible) the location and elevation of the LGM recession.

IV. Compile a descriptive glacial geomorphology map detailing the location of different glacial moraines, drift sequences and past ice extent.

The methods used to achieve these goals are described in the next chapter.

2. Methodology

2.1. Introduction

A range of data was recorded in the field, and rock samples were systematically collected for subsequent processing in the laboratory at the University of Canterbury, Christchurch. The field data included information on the nature and properties of rocks sampled at regular intervals along transect lines on moraine ridges deposited by the Hatherton Glacier at different elevations and distances from the present ice surface. This was undertaken in order to resolve any possible altitudinal or spatial trends that might help explain past behaviour of the glacier. Some of the data were superimposed onto maps or aerial photographs in order to assist interpretation by helping to visualise potential trends. A detailed step by step explanation of the field work and laboratory work is presented in this chapter.

2.2. Fieldwork

An intensive ten day period of mapping, recording and sampling was undertaken in the study area during December 2007. Specific activities were:

I. Field mapping and observations.

II. Measuring and recording clast size, angularity and weathering information along selected transect lines throughout the study area.

III. Observing and recording the character of striations and their orientation on boulders within a selected moraine in order to determine the nature of the basal ice condition and the type of glacial flow in the study area.

IV. Determining surface hardness on a selection of rocks using a Schmidt Hammer in order to help interpret the relative age relationship between moraines at different elevations. Surface hardness is influenced by degree of weathering and hence by period of exposure in different drifts.

V. Collection of samples from different locations across the study area for processing in preparation for SED dating in order to identify the timing of glacial recession.

2.2.1. Field mapping

A geomorphology map of the study area (~ 40 km^2 in area) was prepared as part of the project. This map was based on a satellite image supplemented by ground based observation and recording. The satellite image was taken from the Advanced Land Observation Satellite (ALOS) in 2006 and made available by the Japanese Aerospace Exploration Agency (JAXA). Field data for the map were obtained during traverses of selected areas on foot. Locations of significant landforms were recorded, as well as the positions of transect lines and SED sample points (see sections below). These positions were precisely located using a Trimble Navigation Ltd global positioning system (GPS) unit (GEO-XM) for later importation onto the map. Polygon and digital elevation model (DEM) data for the map were provided by Land Information New Zealand (LINZ).

The JAXA image was also used for the initial planning of the field work by identifying focus areas and regions of potentially difficult terrain. The limited time available for field work, as well as uncertainties regarding weather conditions, necessitated good preparation during the preliminary stages for greatest effectiveness.

2.2.2. Field transects

Transect lines were placed across the field site in such a way as to cover the full sequence of previously identified glacial drifts (Figure 8). Within this stratified design, selection was randomised by throwing a hammer in order to determine the transect starting point. Transects were 50 m long, with sample points at 1 m intervals. They were oriented horizontally at precise elevations and ran parallel to the lines of moraine ridges which themselves tended to follow the contours (Figure 12).

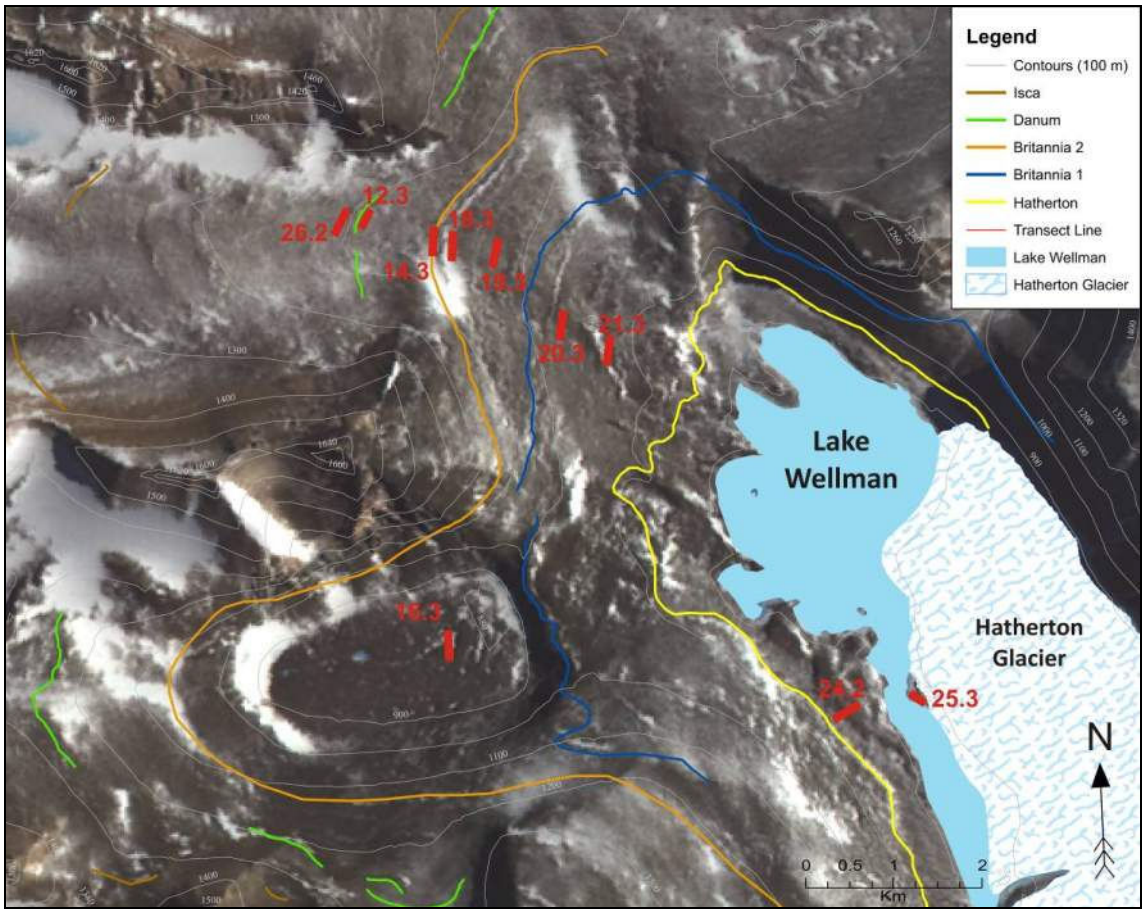

Figure 8. Positions of transect lines in the study area. Locations are indicated by the solid red lines. Ten transects were measured. The glacial drifts after Bockheim et al. (1989) are indicated by the coloured lines.

In total, 10 transects were placed at elevations between 800 and 1200 m a.s.l. (Figure 8). However, transects 14.3 and 16.3 were not used in the final evaluation, as they were each sited on drifts that represented different glacial processes from the main transect series. Transect 16.3 was located within the moraine of a local cirque glacier, and transect 14.3 was positioned on a large moraine ridge separate from the main sequence of transects (Figure 8). The data from the remaining eight transects were entered into spreadsheets for statistical analysis to assist in identifying any patterns and relationships that might be present. These transects were (Figure 8; Table 3): Hatherton drift (801 and 841 m a.s.l.; transects 25.3 and 24.2); Britannia I drift (930 and 967 m a.s.l.; transects 21.3 and 20.3); Britannia II drift (1021 and 1047 m a.s.l.; transects 19.3 and 18.3); Danum drift (1110 m a.s.l.; transect 12.3); and Isca drift (1194 m a.s.l.; transect 26.2).

Table 3**.** Transect positions in relation to moraine drifts and moraine ridges identified in this study (Section 3.2.4).

Drift	**Drift elevation (m a.s.l.)**	**Transect elevation (m a.s.l.)**	**Moraine ridges 1-6 elevation (m a.s.l.)**
Isca	1200 +	12.3 (1194 m)	
Danum	1100-1200	26.2 (1110 m)	Moraine 6 (1100 m) See figure 24.
Britannia II	1000-1100	18.3 (1047 m)	Moraine 5 (1064 m) See figure 26.
		19.3 (1021 m)	Moraine 4 (1010 m) See figure 27.
Britannia I	900-1000	20.3 (967 m)	Moraine 3 (980 m)
		21.3 (930 m)	
Hatherton	800-900	24.2 (841 m)	Moraine 2 (801 m) See figure 23.
		25.3 (801 m)	Moraine 1 (800 m) See figure 25.

2.2.3. Clast properties

Clasts were evaluated for physical characteristics along the transect lines, one rock being selected at each of the 50 points on all transects (Figure 9). To minimise inconsistency during assessment, all clasts were evaluated by one person. If no clast was present at the sample point, a record was made in the field notebook and a substitute clast was evaluated beyond the end of the transect in order to make up the full complement. The characteristics evaluated or measured on each clast were: lithology, angularity, size, and degree of weathering. For lithology, the clast was classified as dolerite, sandstone, gabbro, basalt or granite. Angularity was assessed on a shifting scale between angular and rounded as: very angular, angular, sub-angular, sub-rounded, rounded, or very rounded. The clast size was recorded by measuring the dimensions along the three, mutually perpendicular axes a, b, and c

axes using a tape. The degree of weathering on the rock surface was assessed as fresh, light, moderate, or high/iron-stained.

Figure 9. Measuring a transect line in the study area. The red line is the transect which has 1 m intervals marked along its length.

2.2.4. Measurement of rock surface striations

Records were made of the surface striations on each of 50 boulders located within the Hatherton ground moraine in a concentrated 150 m^2 area close to Lake Wellman. Properties evaluated were their general character and the direction or orientation as determined using a magnetic compass. This was done in order to aid the subsequent interpretation of ice condition during past glacial cycles, even though it was realised that the striation orientation would not reflect ice flow direction on boulders that had not been fixed to bedrock.

2.2.5. Measurement of surface hardness

Surface hardness was determined on a selection of boulders at sites between 800 m and 1600 m a.s.l. using a Schmidt hammer. Three boulders were arbitrarily selected at each of the transect site locations. The hardness of a boulder provides an indication of its period of exposure, since it reflects the length of time the boulder has been subject to atmospheric and weathering processes (Winkler, 2005). Rocks of two lithologies were sampled, Beacon Sandstone and granite, in order to compare their respective exposure ages. The Schmidt hammer is constructed in the form of a long column enclosing a pin driven by a spring. When the hammer is pressed against the rock surface, the pin is released allowing it to impact onto the rocks surface. The column then bounces away from the rock with a force proportional to the hardness of the surface. The column is calibrated allowing a rebound factor (R) to be recorded as a measure of the rock surface hardness. When using the Schmidt hammer in the field at each test location, it was important to ensure that:

I. The rock surface tested was flat.

II. The same rock types were compared.

III. The instrument was applied perpendicular to the surface being measured.

IV. The boulders that were tested did not move during the test.

Figure 10. Using a Schmidt hammer to measure the surface strength of a Beacon Sandstone boulder located in the Hatherton drift in the Lake Wellman study area.

2.2.6. Collection of samples for surface exposure dating (SED).

One of the main aims of the field work was the collection of samples for subsequent surface exposure dating, as discussed in greater detail in section 2.4 (refer page 34). SED dating is based on the length of time a boulder has been exposed to the effects of cosmic radiation after release from glacial ice. The resultant accumulation of ^{10}Be and ^{26}Al attenuates rapidly with depth, with greatest concentrations located within 5 cm of the clast surface.

Sampling was conducted in three zones, zone A, zone B, and zone C (Figure 11). Zone A was located in the Hatherton drift ground moraine close to Lake Wellman; zone B was sited on the slopes directly to the south and southwest of the lake, and placed so as to intersect a vertical sequence of glacier-formed benches; and zone C crossed a series of moraine ridge lines in the valley rising to the northwest (Figure 11). It was logical to collect the SED samples close to the positions of the transects (section 2.2.2), and hence the SED sample numbers are related to the transect line numbers.

An initial suite of up to three samples was collected at each sample point, giving rise to a total of 70 samples from the whole study area (Figure 11). However, the cost and time constraints involved with the subsequent laboratory preparation placed a limit on the maximum number that could be taken. Therefore, a subset of 25 samples was selected from the total collection (Figure 12). To maintain consistency two samples were retained from most sample points, as for example, samples 2.1 and 2.2 from position 2 (Figure 12).

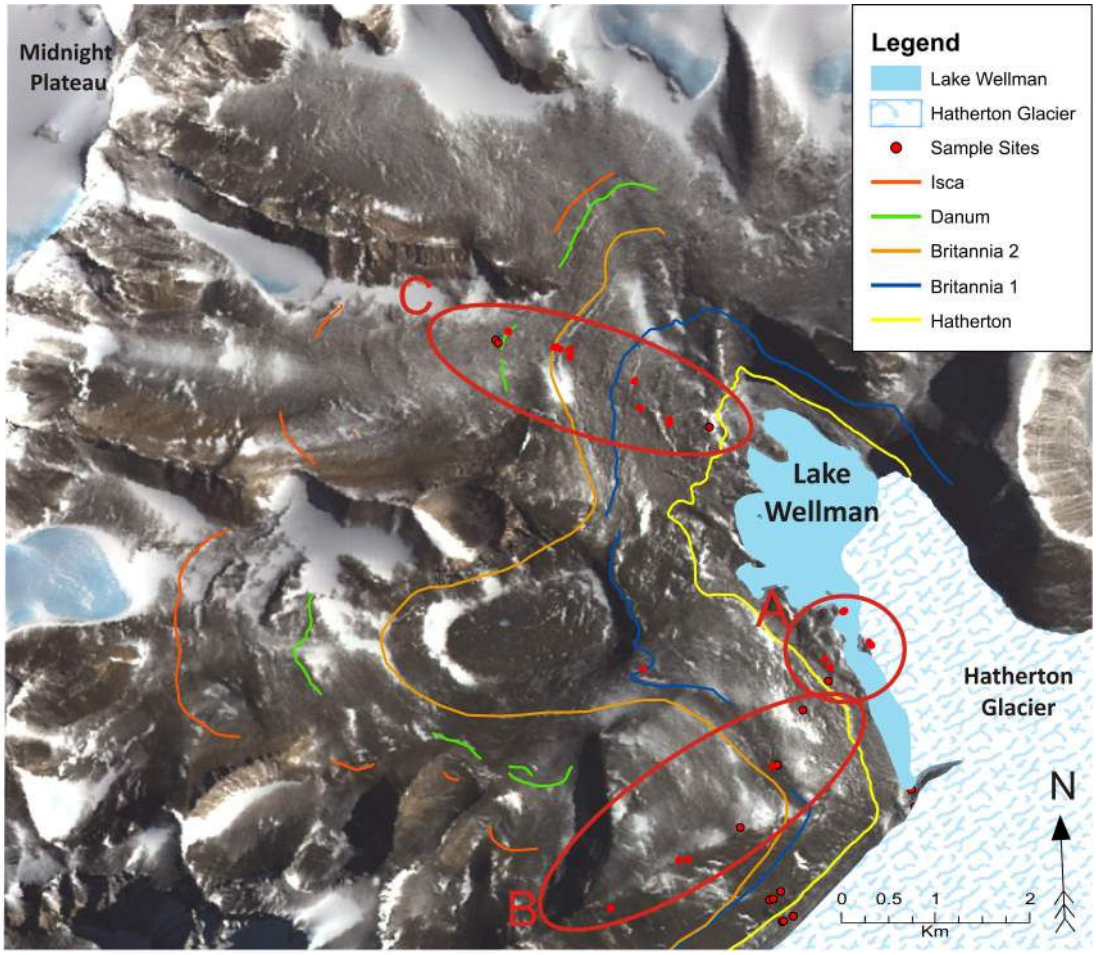

Figure 11. The location of all SED sample sites are marked by small red dots, and the sample zones A, B, and C are marked by the large red circles. The glacial boundaries after Bockheim et al. (1989) are indicated by the coloured lines.

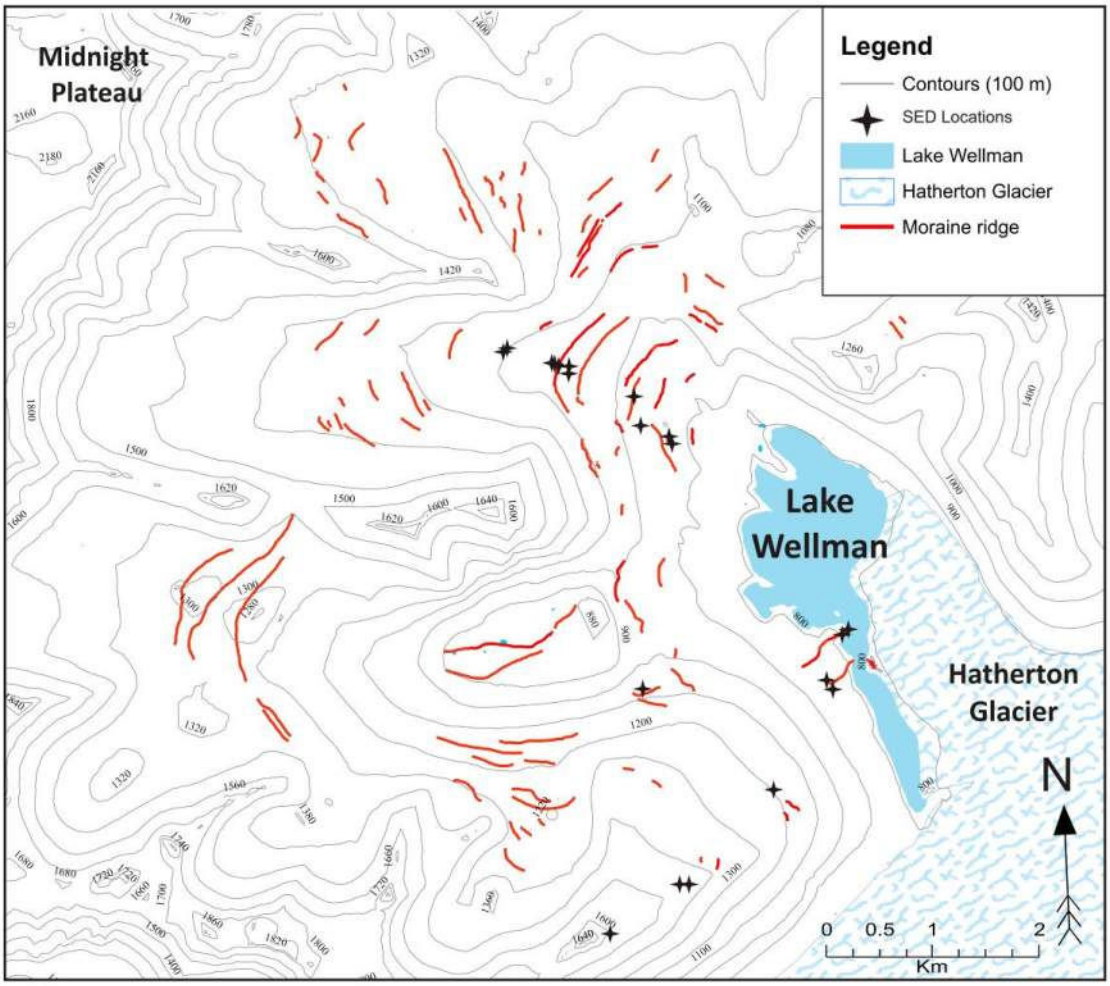

Figure 12. The subset of 25 SED samples prepared for cosmogenic dating area marked with the black stars. Moraine ridges are indicated with red lines.

There were additional constraints placed on the rocks chosen for sampling. The cosmogenic isotopes of ^{10}Be and ^{26}Al are found in greatest abundance within the crystal lattice of quartz. Hence, igneous rocks such as basalt, dolerite and gabbro are not suitable, and samples were only collected from boulders of Beacon Sandstone and granite. It was also paramount that the samples collected came from boulders that had been transported within the glacial ice, but had not been moved since the ice had retreated, and samples were therefore collected only where it was clear that these criteria applied. Evidence of glacial transportation included:

I. Perched blocks of differing lithology

There were many examples of perched blocks in the study area. These were treated as acceptable for sampling as having been transported into position as the ice

receded. For example, a sandstone boulder balanced on a dolerite boulder well above the moraine surface has clearly been transported and deposited by glacial ice (Figure 13). It is highly unlikely that such blocks arose by exhumation or by falling into position, even when located close to escarpments, steep slopes or even moraine ridges. Boulders perched level with the ground moraine surface might have been moved into position by frost heave processes, but such explanations can be eliminated at all sample sites because:

a. They were located within stable, level ground moraine.

b. Samples were taken from elevated perched blocks, which eliminate the issue of frost heave processes.

II. Large granite-erratic boulders

No granite is exposed as bedrock in the Lake Wellman area, so any granite boulders found in the valley were transported by glacier ice into the position. These boulders are referred to as granite erratics which provide undisputable evidence that glacial transportation had occurred (Figure 14).

III. Striations on boulder surfaces

There were numerous rocks displaying striations, which only form beneath glacial ice. This was certain evidence indicating that sub-glacial entrainment and transportation of boulders had occurred.

Figure 13. An example of a large perched Beacon Sandstone block in the Lake Wellman area, located at 156°47'49.151"E,79°55'18.43"S and 1085 m a.s.l. This is SED sample 15.1.

Figure 14. A large granite erratic boulder located at 156°52'9.001"E, 79°55'52.752"S and 1194 m a.s.l. This is an example of an exotic lithology foreign to study area and is SED sample number 2.1.

All of the SED sample sites were located across the floor of open valleys, and these provided an ideal situation for two reasons. Firstly, the boulders sampled were more likely to have remained in their original position on stable and level ground. Secondly, any obstructions present on the horizon leading to topographic shading were reduced. Shading from mountain ridgelines reduces the level of cosmic radiation reaching a sample, which affects the dating process. This effect is corrected by means of calculations based on the angular proportion of the 360^{o} horizon that lies more than 5°above the horizontal. These data were measured at each SED sample site using a compass (Appendix).

Samples were removed from large boulders using a hammer and chisel. Each sample collected weighed approximately 5 kg. Sampling was restricted to the upper surfaces which had full exposure to the sky, and sides of boulders were avoided. Any boulders with spalled surfaces or which were extremely weathered (Figure 15) were not sampled, since weathering may have removed cosmogenic nuclides from the outer surface. The field observations were recorded in notebooks and on sample identification sheets (Appendix). Each sample was photographed before and after sampling. The field records included the sample location, description, identifying characteristics, sky plots (to record the topographic shading), and image numbers.

Figure 15. An example of an extremely weathered and spalled granite bolder in the Lake Wellman study area. Boulders with weathering to this degree were avoided during SED sampling.

2.3. Data evaluation and processing

After the fieldwork was completed all of the samples and field data were taken to the University of Canterbury, Christchurch, New Zealand, where further work was conducted. This involved:

I. Completion of the geomorphology map of the Lake Wellman area using field data and satellite imagery (see map, back cover).

II. Graphing transect and surface hardness data to see if there were any obvious relationships between different variables with elevation. Statistical analyses undertaken to test the significance of any apparent relationships.

2.3.1. Geomorphology mapping

The comprehensive geomorphology map was created using ArcMap™ 9.2 and ArcView™ GIS software, based on field observations and photographic imagery

(section 2.2.1). The geomorphic landforms plotted on the map included: moraine ridges, ground moraine, hummocky moraine, debris cones, frozen ponds, glacial erratics, glacial benches, cirques, saddles, arêtes and nunataks. The SED sample sites and transect line positions were located using a GPS and the data were later uploaded and accurately imported onto the satellite image of the study area. It is important to realize that the contour information is provided in metres above the geodetic datum, as there was no contour data available in elevation above sea level. The World Geodetic System 1984 (WGS) datum was used as the reference ellipsoid. The measurements in metres above sea level (m a.s.l.) throughout the text were determined from the GPS locations made in the field.

2.3.2. Polygonal pattern ground

The polygonal pattern ground in the Lake Wellman area was mapped in very precise detail (Figure 68). This process was time consuming but important for the detection of any trends in distribution. The distribution of polygonal pattern ground was displayed in three size categories each with a different shade of green: large polygons (> 18 m diameter), medium polygons (12 – 18 m), and smallest polygons (> 10 m).

2.3.3. Evaluation and statistical analysis of transect data

Data from each transect were computed either as averages (clast size) or as proportions of clasts in each scale category, in order to make comparisons between transects on moraine drifts at different elevations. The statistics were conducted using Microsoft Excel® and R© software packages. The data were entered into a Microsoft Excel spread sheet and graphed. Comparisons of clast angularity, weathering and size data at were made visually between transects at different elevations for different lithologies, and for all taken together. The percentages of clasts of each lithology type at each elevation was visualised by means of pie graphs.

A chi-square probability distribution was conducted to test the significance of apparent trends in proportions of different variable categories between transect elevations. The clast variables examined in the chi-squared tests were lithology (for each lithology type), weathering and angularity. Assuming that the transect data were

normally distributed an analysis of variance (ANOVA) test was run to check on the significance of any relationships between data groups.

Data from two transects were excluded from the analyses, one (transect 14.3) because data were recorded from the apex of a large moraine ridge and were therefore not consistent with those from the other transects which were recorded within ground moraine. Another (transect 16.3) was also excluded since although near the other transects it was located out of line with them on a site associated with local glacial cirque processes inconsistent with those of the other transects. However, records from these two transects contributed additional information to the overall project.

2.4. Cosmogenic dating

The measurement of the concentrations of unstable isotopes in surface rocks allows quantification of the period the rocks have been exposed to cosmic radiation, as was first suggested by Davids and Shaeffer et al. (1955). The principle of cosmogenic exposure dating relies on the steady production of the nuclides ^{10}Be and ^{26}Al by this process over long periods. Cosmic rays are made up of several different high energy subatomic particles emitted extraterrestrially by star systems, which have bombarded the earth continuously throughout geological time. This radiation reacts with atoms in the earth's atmosphere giving rise to new unstable elements that can be used for cosmogenic dating when they reach the surface of the earth. However, other secondary sub-particles are also produced by this interaction process and when these reach the earth's surface they interact with atoms in surface rocks producing the cosmogenic isotopes of ^{10}Be, and ^{26}Al within the mineral lattice of the uppermost several metres of exposed rock (Bierman and Steig, 1996; Zreda and Phillips, 2000; Balco et al., 2008). The impact on O atoms in quartz gives rise to ^{10}Be and ^{26}Al is produced in the same way from Si atoms. These nuclides are produced at known rates depending on location, since the level of cosmic radiation varies with latitude and elevation a.s.l. (eg. ca. 5 ± 0.3 atoms produced/gm/yr for ^{10}Be in quartz at latitudes exceeding 58°). They also decay with time at regular rates, ^{10}Be having a half life of 1.4 Ma and ^{26}Al a half life of 720 ka. The accumulation of cosmogenic nuclide concentrations attenuates with depth, with the greatest abundance of isotopes

occurring in the outer 5 cm of exposed material (Bierman and Stieg, 1996, Balco et al., 2008). The accumulation rates are proportional to the concentration of the target nuclides in the material and the intensity of the cosmic rays (Zreda, 2000). Analyses of the quantities present in a sample can therefore be used to calculate a value for how long a clast has been exposed free from the protective ice cover of the receding glacier that has left it behind (Bierman et al., 1999). The dating technique measures the length of exposure to cosmic radiation or effectively the minimum age of exposure as ice recession is initiated (Balco et al., 2008). This assumes that the clast has been previously covered for sufficient time for any older cosmogenic isotopes to have decayed away. Or that a clast is subjected to sufficient glacial erosion (in transportation) that at least 3 m of material is removed from the outer rock surface, promoting the resetting of the cosmogenic clock.

The sample preparation in this study was conducted at the cosmogenics preparation laboratory at the University of Canterbury, Christchurch. This involved a series of pre-treatment cycles to concentrate 100 g of quartz from each sample. Next, the concentrated quartz was placed through a series of steps to extract the ^{10}Be and ^{26}Al needed to calculate the concentrations in each sample. The ^{10}Be and ^{26}Al concentrations were measured using the ANTARES- Accelerator Mass Spectrometer (AMS) at the Australian Nuclear and Science Technical Organisation (ANSTO), in Sydney, Australia.

2.4.1. SED sample preparation

The first stage of preparation involved weighing, numbering and photographing the samples. They were then crushed into a fine powder, and separated into different size fractions, and carefully placed into labelled sample bags. Out of the four size fractions created, only the 212 - 500 micrometre size fraction was used in the SED process. Each sample was washed in water until the liquid appeared clear and then dried ready for the acid digestion stage. The equipment used in the laboratory processing included:

- Sieves and shaking platforms
- Jaw crusher
- Pulveriser (plate grinder)

- Plastic sample bags and markers
- Hot plates
- Flasks
- Stirring rods
- Fume cupboards

2.4.2. Sample acid digestion

The goal of acid digestion was to remove impurities and concentrate the quartz grains in each sample. Quartz is very resistant to acid due to the stable structure of its mineral lattice. Each sample was therefore washed and digested in a series of intensive cycles using nitric acid (HNO_3), hydrochloric acid (HCI), sodium hydroxide (NaOH), and phosphoric acid (H_3PO_4) to concentrate the quartz by removing all other material in each sample.

The digestion process proceeded over a three-month period. The first stage of this procedure involved treatment in an ultrasonic bath with aqua regia (a mixture of concentrated nitric and hydrochloric acids), in order to remove many substances resistant to other reagents. This step removed any hydrous iron from the sample. The samples were then secured on a hot plate and boiled in phosphoric acid, followed by sodium hydroxide in alternating cycles that were repeated until the samples were clean. The samples and the acid solution were boiled on the hot plate at 250 ˚C and maintained at this temperature for 1½ hours (Figure 16). Careful rinsing of the samples with water between steps was necessary as any contact between the phosphoric acid and the sodium hydroxide would cause an explosion.

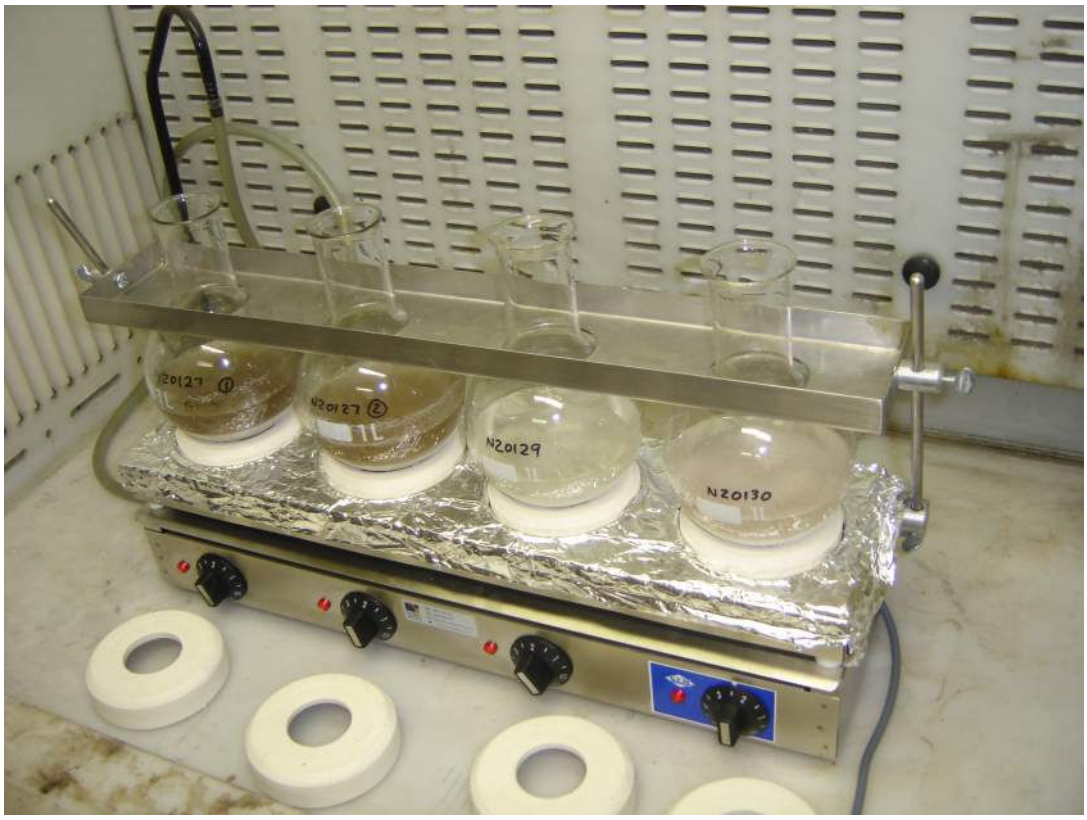

Figure 16. Samples in a phosphoric acid solution, fastened securely to a hot plate boiling at 250 ˚C in the cosmegenics preparation laboratory at the University of Canterbury. The left hand samples have reacted and have changed colour as a result.

2.4.3. Cosmogenic preparation

Once the samples were clean and the aluminium concentrations were below 500 ppm, they were ready for extraction of ^{10}Be from the crystal lattice. This stage of the processing was performed by a laboaratory technician in the cosmogenics preparation facility. First, ^{9}Be, which is referred to as the carrier, was added to the mix containing the ^{10}Be. The precise weight of the carrier was measured, in order to allow comparison of the ^{9}Be/^{10}Be ratio during cosmogenic dating with the accelerator mass spectrometer (AMS). The process in the laboratory involved: hydrofluoric acid dissolution and fuming, anion exchange separations, aluminium separation, cation exchange separation, followed by precipitation of ^{10}Be. The concentrated ^{9}Be/^{10}Be solution was sent to ANSTO for measurement using the ANTARES-AMS.

2.4.4. Accelerator Mass Spectrometer (AMS)

The ANTARES-AMS at the ANSTO facility in Sydney, Australia functions on the rule that charged particles passing through a magnetic field are deflected along varying paths depending on their atomic mass (Olmsted and Williams, 2006). Using a Cs^{+} beam, the atoms are passed through an electrical discharge plate, removing any electrons from the atoms (Figure 17). The ANTARES-AMS uses an 8 million volt accelerator, increasing the kinetic energy of the positively charged irons, accelerating them between two magnetic poles which channel them into a collector. The positively charged ions are separated in the collector based on their mass, since ions with a greater mass are deflected at a larger angle (Olmsted and Williams, 2006). As the atomic mass of beryllium is known, atoms other than beryllium were filtered out by adjusting the magnetic intensity accordingly allowing measurement of ^{10}Be and ^{26}Al nuclides concentrations (Budzikiewics et al., 2006).

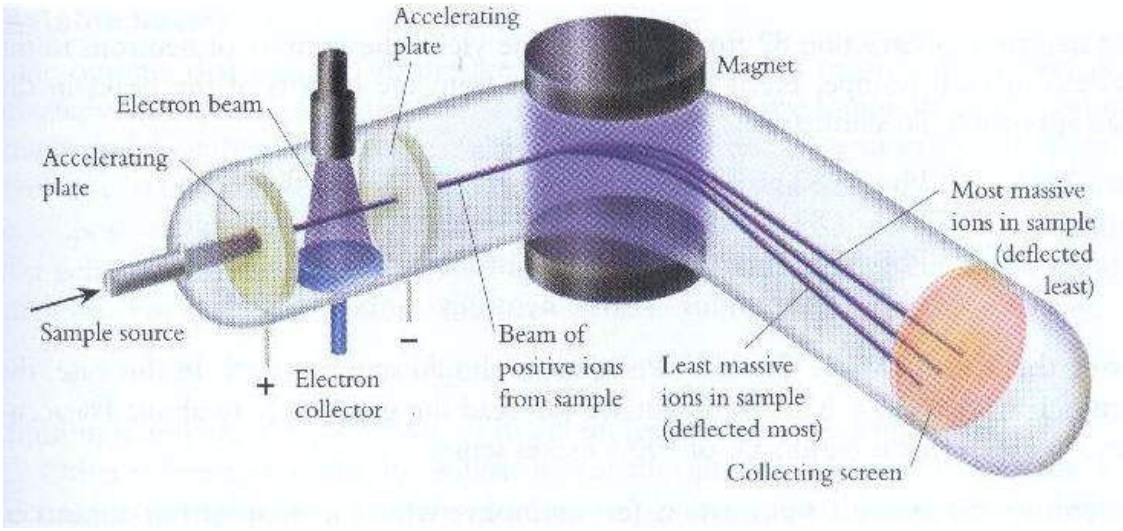

Figure 17. An example of an Accelerator Mass Spectrometer (Olmsted and Williams, 2006).

2.5. Interpretation of field data

Before moving on to describe in detail the results obtained, an account is provided of the various geomorphic landforms and glacial features encountered during the field portion of the project. An understanding of this aspect was important in interpreting the past glacial history in the Lake Wellman area. Because of its importance this topic is not included here but instead forms the subject of the next chapter, Glacial Geomorphology.

3. Glacial geomorphology

The Lake Wellman area displays exceptional preservation of past glacial geomorphology and periglacial landforms for two reasons. Firstly, the high topography has protected the valley from glacial ice to the south, which has therefore been unable to access and disturb existing formations. Secondly, the Antarctic continent is very dry and receives little annual precipitation. The lack of flowing water in such an arid and cold environment has minimised the erosion and destruction of the glacial landforms. In the study described in this thesis, field observations of the glacial features of the valley were identified and described, and results were later compared with information published in the literature. Previous studies in the Lake Wellman study area have been conducted by Denton et al. (1989) and Bockheim et al. (1989), who described some of the landforms. However, a comprehensive investigation was needed to understand and interpret their evolution and development. Satellite and photographic imagery were used to display these formations for examination in greater detail and their locations are depicted on a grid reference map (Page 39). In order to interpret their formation, it is necessary to have a full understanding of these glacial features.

3.1. Location of images on map

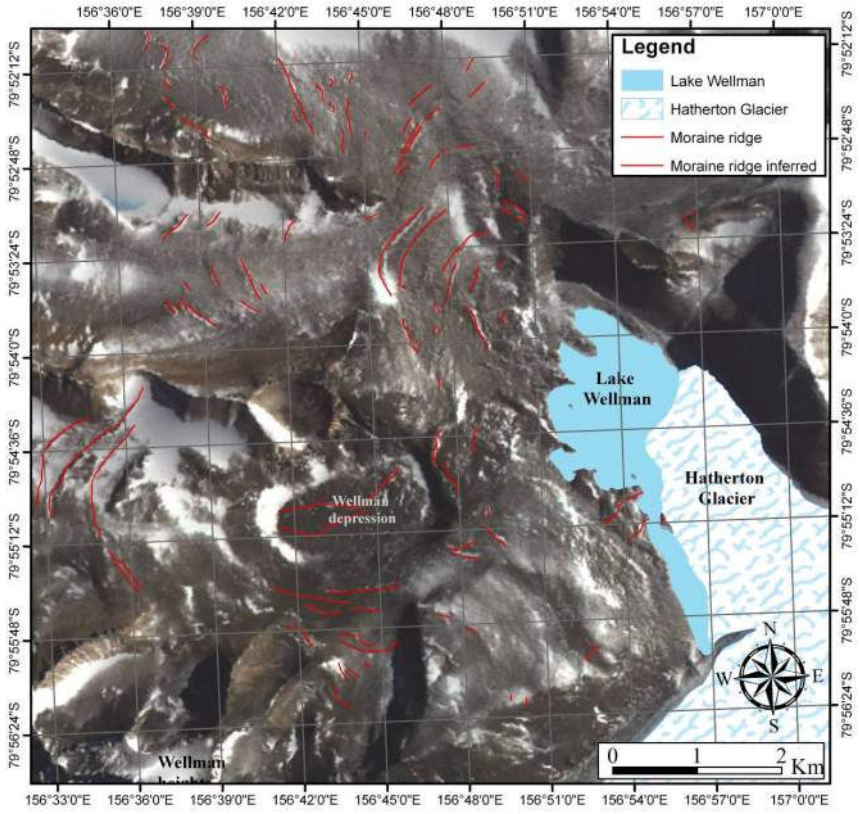

Figure 18. The Lake Wellman study area showing grid coordinates of latitude and longitude. (Image source: Antarctica New Zealand).

3.2. Glacial deposits

3.2.1. Moraine deposits

A moraine is defined as a glacial depositional landform produced by a wide variety of processes in marginal and supraglacial environments (Evans, 2002). Moraine deposits form the most prominent geomorphic features in the Lake Wellman area. They have a well formed structure and are easily identified in the landscape. The moraine deposits range from low relief ground moraine, through hummocky moraine, to very high relief end-moraines up to 11 m high. In this study the end moraines have been categorised into three types based on their appearance. Type A moraines are those with a moraine ridge that is symmetrical in shape; Type B moraines are defined as those with a ridge that is asymmetrical in shape; and Type C moraines have a ridge with a degraded appearance and low relief in the landscape.

3.2.2. Ground moraine

The term ground moraine is often misused. Here it is defined as a moraine with glacial and supra-glacial deposits that have low relief and a uniform appearance. The Lake Wellman area is blanketed with extensive glacial-derived ground moraines. These moraines are predominantly composed of sub-glacial material but also include pro-glacial debris and material that was entrained within the glacial ice. The ground moraines in the Lake Wellman area can be further sub-divided according to their weathering characteristics. At high elevations boulders display substantial levels of weathering and iron staining (Figure 19). At low elevations boulders are only lightly weathered and there are only limited quantities of iron-stained clasts present (Figure 20). The ground moraine is poorly sorted and includes rounded to sub-angular clasts of dolerite, sandstone, basalt, gabbro and granite. The ground moraine is described in detail in the results.

Figure 19. The ground moraines in the upper elevations of the Lake Wellman area are quite uniform in appearance. There are only a few granite erratic boulders and very few sandstone clasts present. This photo displays boulders with extensive weathering and iron staining at elevations between 1200 – 1300 m a.s.l. at grid reference 156°36'22.471"E, 79°53'36.313"S.

Figure 20. The ground moraine in mid elevations in the Lake Wellman area displays extensive weathering of clasts with less iron staining on boulders. There are numerous sandstone and granite boulders and a large proportion of fine material in the ground moraine. This photo was taken at 801 m a.s.l. at grid reference 156°55'29.447"E, 79°55'13.998"S.

3.2.3. Hummocky moraine

The hummocky moraines in the Lake Wellman area consist of mounds, ridges, and hollows. This type is found predominantly on gently dipping slopes at lower elevations between 850 m a.s.l. and 890 m a.s.l., although there are some patches at higher elevations. Hummocky ground is also found on flat terrain along the margins of Lake Wellman and in the Wellman Depression at grid references 156°51'15.226"E, 79°54'49.912"S and 156°44'59.856"E, 79°55'16.641"S, respectively. The slope between Lake Wellman and the Wellman Depression displays extensive hummocky ground. The hummocks range from 1 – 5 m in height and 3 – 4 m in width (Figure 21). These hummocks have a conical shape and the material within them is unsorted, containing angular and sub-rounded clasts, fine sediment, and large boulders up to 2.5 m in length (Figure 21).

Figure 21. Hummocky ground moraine located on the slope between Lake Wellman and the Wellman Depression at elevations between 800 - 900 m a.s.l. at grid reference 156°49'39.002"E, 79°54'49.961"S.

3.2.4. Linear moraine ridges

A summary geomorphology map of the Lake Wellman area is presented below displaying the location of prominent moraine ridges in the Lake Wellman area as mapped during the field work (Figure 22). The moraine types in the following sections include Type A, Type B and Type C moraines as defined for the purpose of this research. Type A represents symmetrical moraine ridges, Type B asymmetrical moraine ridges and type C are degraded and ice over run moraine ridges. The location of these features are included in the results as they indicate the nature of the past ice flow at different locations in the study area and are fundamental in its interpretation. In addition to this, six significant moraine ridges (some of which mark the boundary locations between the previously named sequences of glacial drifts) have been defined for the work in this study (Figure 22). Moraine 1 and Moraine 2 are located within the Hatherton drift. Moraine 3 is located at the upper limit of the

Britannia I drift. Moraine 4 lies in the upper half of the Britannia II drift and Moraine 5 represents the upper limit of this drift where it meets the Danum drift. Moraine 6 may be located near the boundary between the Danum and the Isca drifts (after Bockheim et al., 1989).

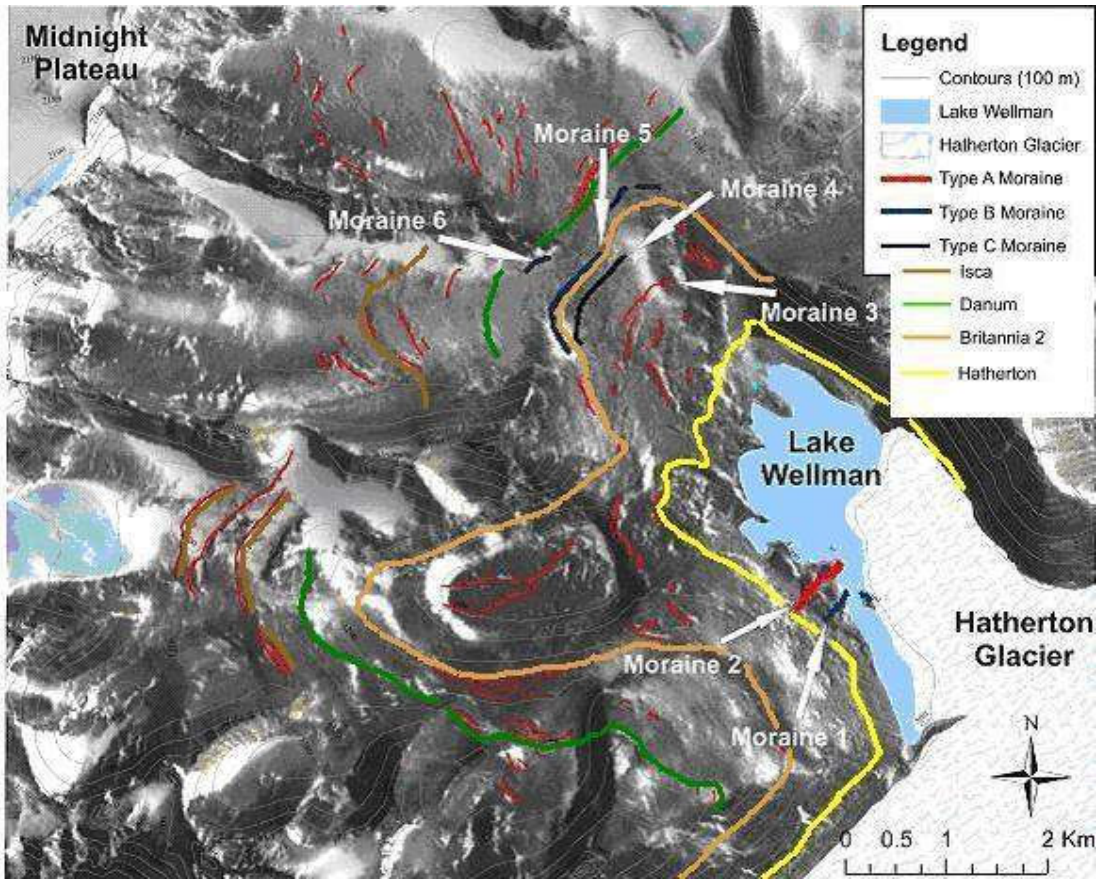

Figure 22. The location of prominent moraine ridges in the Lake Wellman area. The moraine ridges have been separated into Type A, B and C and moraine ridges 1 - 6 identified with the arrows.

3.2.5. Type A: Symmetric moraine ridges

There are many symmetrical moraine ridges in the Lake Wellman area, which are defined as Type-A moraine ridges (Figure 22). A good example this is the large moraine ridge located at 801 m a.s.l. This is referred to as Moraine 2 (Figure 23) and located at grid reference 156°54'42.884"E, 79°55'11.185"S (Figure 23). This moraine ranges from 2 – 3 m in height along its length and is 4.5 m in width. It runs continuously across the valley, but is cut part way along its length by a melt-water channel. The moraine is 764 m in length and contains dolerite, sandstone and granite

clasts. There is a small bench on the down-glacier side of the ridge, indicative of a secondary still stand phase following deposition of the main ridge.

Figure 23. An example of a Type A moraine which is symmetrical in shape. This ridge (Moraine 2) is located within the Hatherton drift at an elevation of 801 m a.s.l. at grid reference 156°54'42.884"E, 79°55'11.185"S. Glacial ice was located to the right of the large moraine ridge. A small bench is visible on the right side of the first moraine ridge.

There are also small Type A moraine ridges in the Lake Wellman area. One example is 1.5 m in height and 2-3 m wide (Figure 24). This is referred to as Moraine 6 and is located at an elevation of 1100 m a.s.l. at grid reference 156°47'33.351"E, 79°52'51.107"S. The ridge contains clasts of sub-rounded and sub-angular dolerite, sandstone and granite boulders and there is fine material present. The moraine ridge is symmetrical in shape with smaller boulders deposited down-glacier of the ridge and large boulder deposited up-glacier from the ridge (Figure 24).

Figure 24. An example of a small symmetrical, Type B moraine ridge (Moraine 6). Moraine 6 is located at an elevation of 1100 m a.s.l. at grid reference 156°47'33.351"E, 79°52'51.107"S. The large boulders are deposited on the up-glacier side of the ridge and the small clasts on the down-Glacier side of the ridge.

3.2.6. Type B: Asymmetric moraine ridges

In the Lake Wellman area there are 2 asymmetrical moraine ridges (Figure 22). These ridges range from 1.5 m to 11 m in height. There is an excellent example of a Type B moraine ridge at lake level (Moraine 1) at grid reference 156°54'42.884"E, 79°55'11.185"S (Figure 25). This large moraine ridge is the youngest in the Lake Wellman area. It is 11 m in height and very poorly sorted with a diverse range of clast diameters. Large boulders are 2-3 m in diameter. Smaller clasts are supported in a fine matrix of sand sized particles and quartz pebbles up to 5 cm in diameter. The moraine is asymmetric in shape with a steep scree slope on the down glacier side (Figure 25). Lithologies of granite, sandstone and dolerite are found in the ridge and there are numerous striated boulders which have had their edges spalled off.

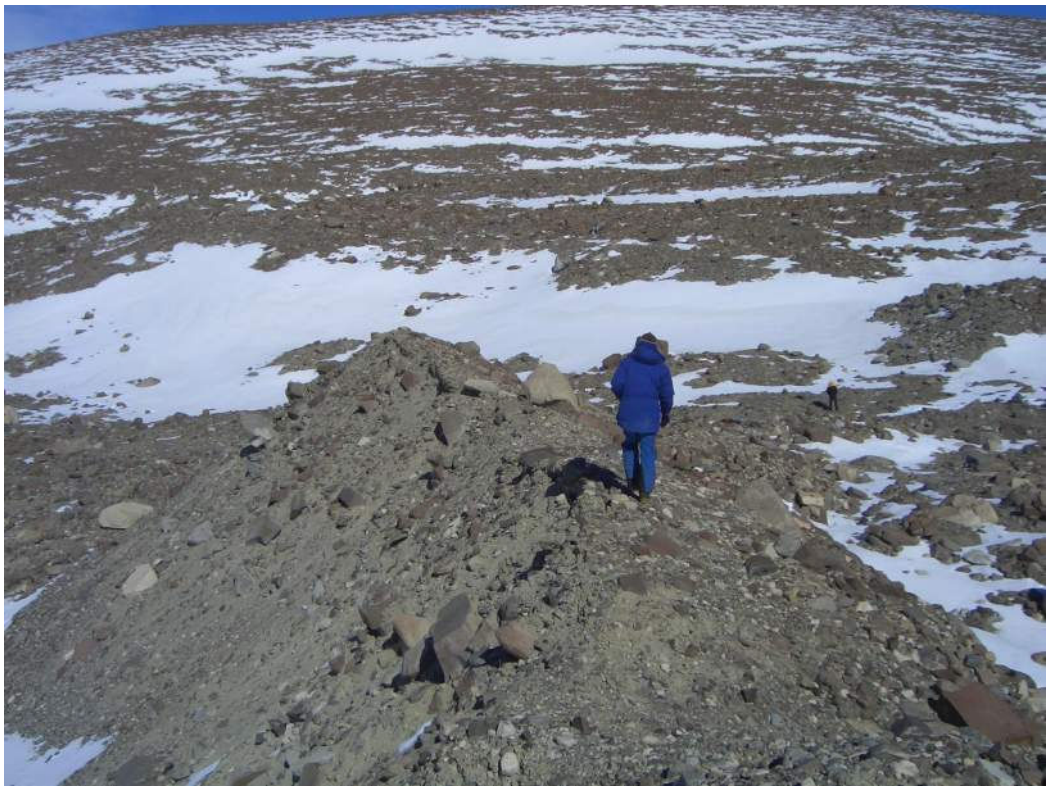

Figure 25. This is an example of an asymmetrical moraine ridge located near lake level in the Hatherton drift, at an elevation of 800 m a.s.l. (grid reference 156°54'42.884"E, 79°55'11.185"S). This is referred to as Moraine 1. The Hatherton Glacier was located on the left side the image.

Another example of a Type B moraine ridge in located in the upper part of the Lake Wellman area at an elevation of 1064 m a.s.l. (Moraine 5). This moraine ridge is approximately 1250 m in length and is located at grid reference 156°45'38.503"E, 79°53'26.402"S (Figure 26). Moraine 5 is approximately 5 m in height and 8 – 9 m wide. It contains very angular clasts of iron-stained Ferrar Dolerite and of Beacon Sandstone (Figure 26). Although all lithologies are present in the ridge, the clasts are predominantly composed of dolerite and sandstone with little granite. Many of the boulders are striated. The ridge is composed wholly of angular boulders, and a distinguishing feature is a distinct lack of fine sediment over its surface (Figure 26). The angle of the down-glacier slope of the ridge is 19° to horizontal and up-slope 32°.

Figure 26. An example of a large asymmetrical, Type B, moraine ridge at 1064 m a.s.l. is located at grid reference 156°45'38.503"E, 79°53'26.402"S. This is referred to as Moraine 5 (Figure 22). The ice advance was from left to right in the first image. The ridge extends across the valley for 1130 metres.

3.2.7. Type C: Degraded moraine ridges

This moraine with a low profile and a slightly degraded appearance has been defined as a Type C moraine ridge, and is referred to as Moraine 4 (Figure 22). Type C moraine ridges are symmetrical in profile and usually very small giving the impression that ice may have overtopped them. A good example is located at an elevation of 1010 m a.s.l. at grid reference 156°46'12.592"E, 79°53'32.102"S. This ridge is referred to as Moraine 4 (Figure 27). This moraine is not prominent in appearance, being less than 1 m high and 3 m wide. Clasts of angular and sub-rounded sandstone, dolerite, and granite are present in the degraded ridge. These clasts range in size from 5 cm – 200 cm in length and are larger in diameter than clasts located in the ground either side of the ridge (Figure 27). There is no change in appearance up slope or down slope of the degraded moraine ridge (Figure 27).

Figure 27. An example of a Type C moraine (Moraine 4). Moraine 4 is located at an elevation of 1010 m a.s.l. at grid reference 156°46'12.592"E, 79°53'32.102"S. The main ice body was located to the left of this image.

3.2.8. Erratic boulders

An erratic is defined as a rock fragment located far from its outcrop source and whose occurrence can only be explained by transportation using glacial processes (Evans, 2002). In the Lake Wellman area, large granite erratic boulders are found within and on top of moraine deposits. No outcrop exposures of granite occur in the Lake Wellman area. The basement granite rocks are stratigraphically located beneath the flat-lying Beacon Sandstone and Ferrar Dolerite intrusive, which are estimated to be 450 m and 960 m thick, respectively (Haskell, 1964). Glacial transportation is therefore the only explanation for the deposition of such large granite boulders, which being derived from beneath the EAIS must have been transported great distances. A good example of a large granite erratic boulder is pictured below (Figure 28). This large coarse grained erratic is approximately 3 m in height and 5.5 m long. It is located at an elevation of 1195 m a.s.l. at grid reference 156°52'6.363"E, 79°55'54.346"S. The mid portion of the boulder is bisected by a large course grained

pegmatite dyke. The dyke, by providing structural integrity, could explain why such a large boulder has remained intact during transportation.

Figure 28. A large granite erratic boulder located at an elevation of 1195 m a.s.l. at grid reference 156°52'6.363"E, 79°55'54.346"S.

3.2.9. Perched blocks

Perched blocks are rocks that have been deposited on top of other boulders as the ice retreated from the valley. These include blocks that were entrained in the ice and supraglacial material. Perched blocks vary greatly in size and placement, ranging from small pebble-sized clasts up to large boulders greater than 1 m in diameter; such as the perched dolerite boulder (Figure 29A). The lithology of these blocks may differ from the lithology of the boulder on which they are perched. Perched granite provides definite indication that the boulder has been deposited by receding ice (Figure 29B). The perched material varies considerably in angularity and weathering, blocks ranging from very angular to very round. Perched blocks at lower altitudes (Figure 29C) are less weathered than those at higher elevations (Figure 29D). Perched blocks are found extensively in the Lake Wellman area. The highest is

located at grid reference 156°52'4.94"E, 79°55'53.015"S at an elevation of 1200 m a.s.l. The composition of perched blocks varied in the study area and includes Ferrar Dolerite, Beacon Sandstone and granite, those of dolerite and sandstone being more common than those of granite. They often occur in groups and frequently three – four blocks occur together balanced on top of a larger boulder. At lower elevations, fine material is deposited on and amongst perched blocks.

A B C D

Figure 29. Examples of perched blocks in the Lake Wellman area. Figure A is a large, very angular perched dolerite boulder; figure B shows a pair of angular granite boulders; figure C has two perched rocks, one of sandstone and the other of dolerite; figure D is a rounded very iron stained dolerite boulder balanced on small pebbles which are perched on a large dolerite boulder.

3.2.10. Supraglacial debris

Evidence can be found in the Lake Wellman area of supraglacial material that did not enter within the ice during transportation, but was carried along on the glacier surface. A large elongate, basaltic boulder, 2.5 m long was found close to lake level

(Figure 30). This boulder is located at an elevation of 849 m a.s.l. at grid reference 156°55'22.483"E, 79°55'9.987"S. Its shape, orientation and composition indicate that its source most likely from an exposure of columnar jointed basalt ~ 2400 m to the south above the current limit of the Hatherton Glacier at grid reference 156°53'44.294"E, 79°56'22.619"S (Figure 30).

Figure 30. Columnar-jointed basalt carried supra-glacially to its resting position in the Lake Wellman valley (right), most likely derived locally from the large exposure on the margins of the Hatheron Glacier (left). The columnar boulder is 2.5 m in length, and 0.5 m in width.

3.2.11. Debris Cones

Debris cones are large mounds of glacial debris which exhibit characteristics that contrast with those of the surrounding ground moraine. The rocks in these deposits differ in angularity, composition and weathering history, reflecting a different origin and process of deposition. A concentration of debris cones was found on the slope between Lake Wellman and the Wellman Depression at grid reference 156°50'1.868"E, 79°54'45.271"S. Towards the top of this slope at 892 m a.s.l. there was a small debris cone 2 m in height and 15 m in diameter. The material within this cone had a scree-like appearance since there were no large or round boulders present, all clasts being angular (Figure 31). The dominant lithology was dolerite and there was no granite present (Figure 31). Further up the slope there was a large debris cone at 967 m a.s.l. just below the crest. This debris cone was 7 m in height and 20 m in diameter, and was composed of clasts of granite, dolerite and sandstone, which were rounded to sub-rounded and strongly iron-stained. Another good example of a debris

cone was found at 156°51'20.403"E, 79°54'50.708"S at an elevation of 870 m a.s.l. This cone was 3.8 m high and 6 m wide (Figure 32). Further examples are shown in Figure 33 and Figure 34. The positions of these debris cones were plotted on the large geomorphology map (see back pocket of thesis).

There are a number of possible explanations for the formation of these cones. They may have arisen when debris-laden floating ice-rafts overturned and dumped their material at a time when Lake Wellman was at a higher elevation. Alternatively, material may have been carried to the lake edge on a succession of floating ice fragments and left there in a steadily growing deposit as if placed by a conveyor belt. Another explanation is that debris within large blocks of ice cast off from the Hatherton Glacier as its margin receded were left in the form of cone-shaped deposits as the ice melted. However, entrainment in the ice not supported by the shape of the rocks which are very angular and not rounded as would be expected of glacial ice.

Figure 31. Examples of debris cones in the Lake Wellman area. The right hand image shows a close-up view of the side of a debris cone. The clasts are very angular and there is no granite present. This cone is located towards the top of the slope between the lake and Wellman Depression at elevation of 950 m a.s.l. at grid reference 156°49'14.993"E, 79°54'45.293"S.

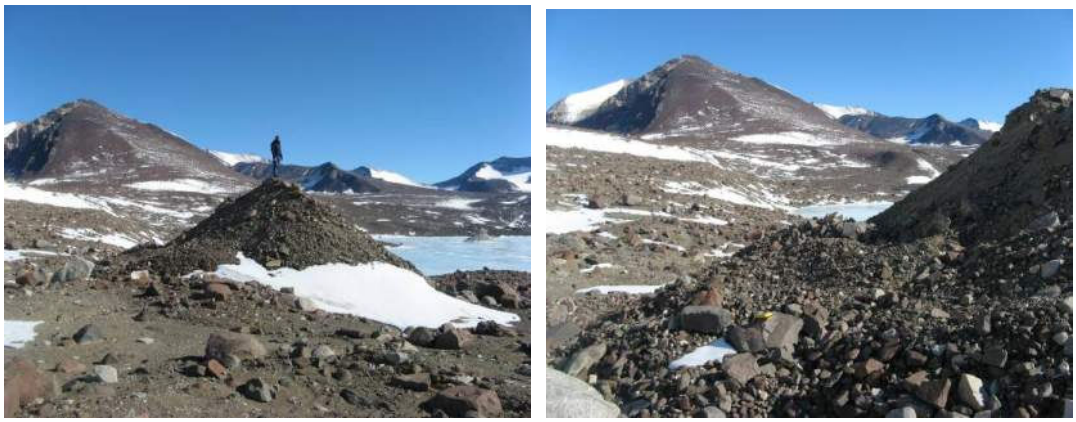

Figure 32. Debris cones at the base of the slope leading up from the lake to the Wellman Depression located at an elevation 870 m a.s.l. at grid reference 156°51'20.403"E, 79°54'50.708"S.

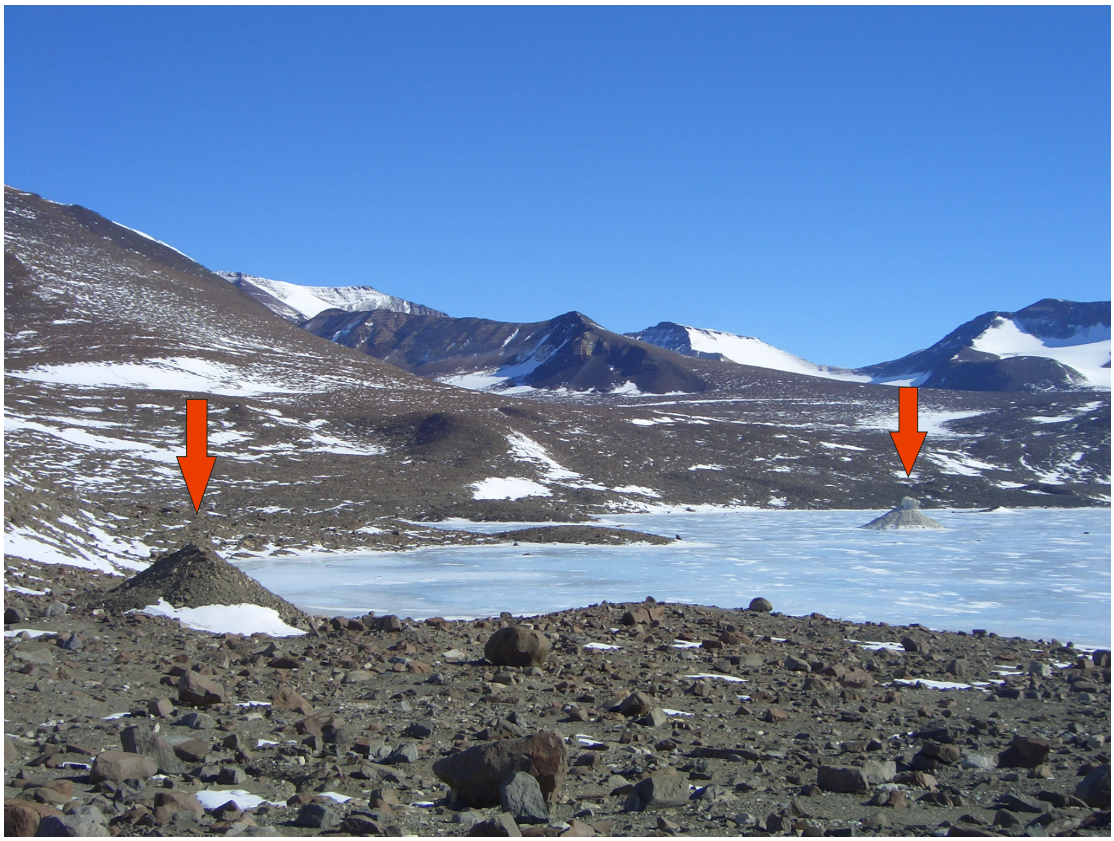

Figure 33. This image shows two large debris cones. The debris cone in the background (right) formed around a disintegrating Beacon Sandstone boulder trapped in Lake Wellman ice. The boulder is located at 790 m a.s.l. at grid reference 156°52'20.405"E, 79°54'26.625"S. The boulder in the foreground (left) is the same as the debris cone seen in Figure 32 above.

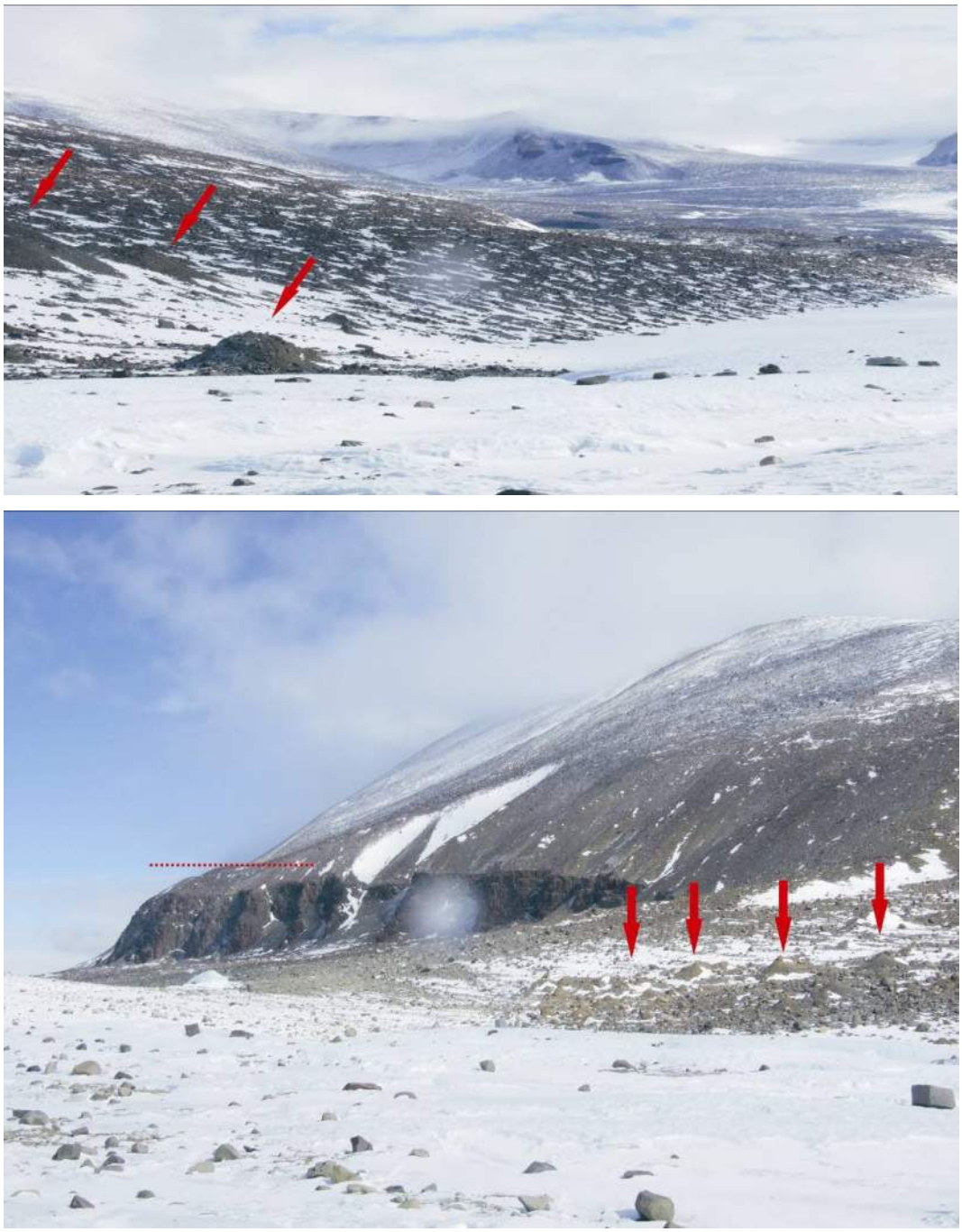

Figure 34. Debris cones at the end of Lake Wellman close to the current margin of the Hatherton Glacier. These are located at an elevation of 800 m a.s.l. at grid reference 156°56'11.906"E,79°56'6.783"S. The arrows indicate the location of each of the debris cones. An erosional debris-covered bench is also visible, indicated by the red dotted line.

3.3. Glacial erosion features

3.3.1. Cirques

Cirques are large, hollow, bowl-shaped depressions that were formed by erosion due to discrete masses of continuously moving ice. They may consist of enclosed rock basins or else connect with valley glaciers (Bennett and Glasser, 1997). These hollows are bounded up-slope by a steep headwall formed by plucking and freeze-thaw weathering, whereas down-slope they are open (Bennett and Glasser, 1997). The direction of cirque development is partly controlled by topographic shading and the influence of wind. There are numerous cirque hollows present in the Lake Wellman area. These features were observed at grid references 156°34'53.106"E,79°56'9.661"S, 156°37'51.563"E, 79°56'14.066"S, 156°41'2.054"E,79°56'35.936"S, 156°41'53.78"E,79°54'23.1"S, and 156°59'1.68"E,79°53'30.016"S at respective elevations of 1400 m, 1320 m, 1400 m, 1450 m and 1350 m a.s.l. (Figure 35). All elevations were measured from the centre of the cirque floor. A developing cirque basin presently containing ice was located at grid reference 156°36'9.271"E,79°52'52.84"S. The largest cirque hollow observed in the Lake Wellman area was 1030 m wide and 1300 m long (Figure 35) located at grid reference 156°34'44.362"E,79°56'9.955"S at an elevation of 1500 m a.s.l. A profile line through a prominent cirque basin is presented below (Figure 35).

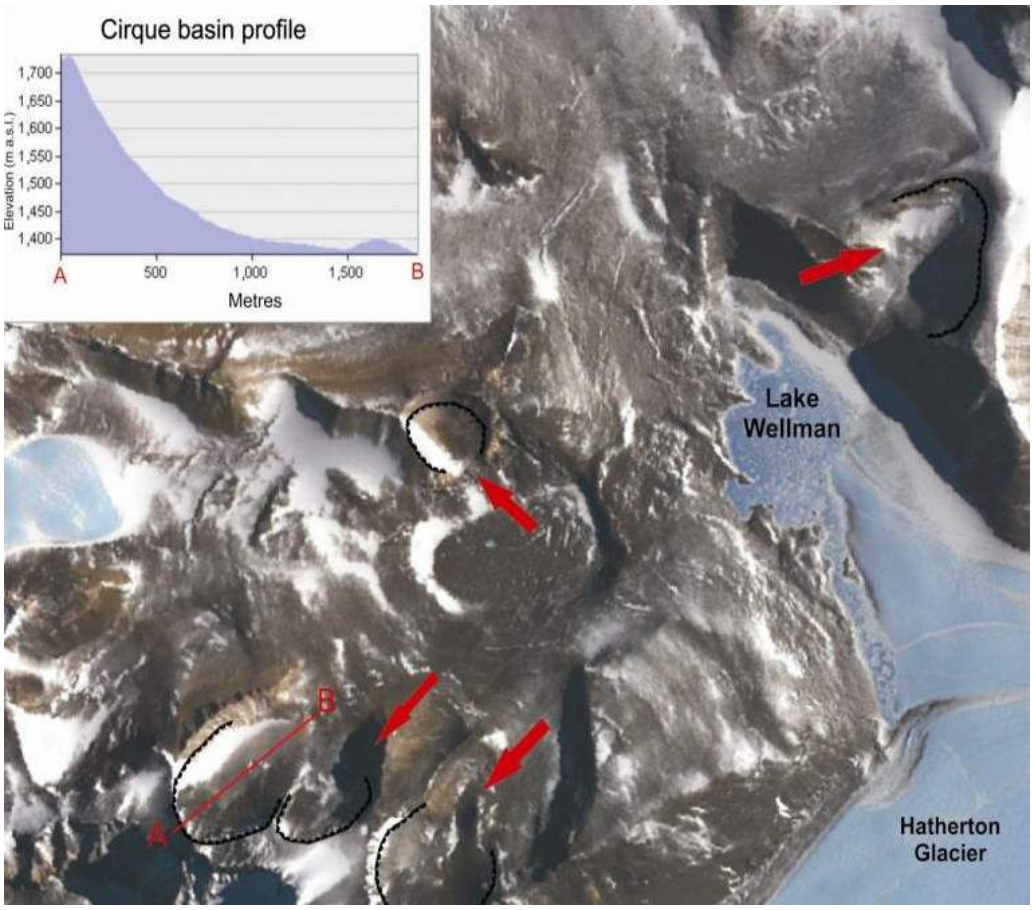

Figure 35. The location of prominent cirque basins in the Lake Wellman area. The red arrows indicate the cirques, which are outlined with the black line. The inset shows the elevation profile of a cirque basin (along the red line A – B).

3.3.2. Arêtes

Arêtes are sharp rock ridgelines with steep sides that are typically formed by the glacial back-erosion and eventual meeting of two parallel valley systems. They can also form when two cirque glaciers erode back the headwall of their respective valleys. However, in this latter situation a cirque will often produce a rounded transition stage between the two valleys known as a saddle (Benn and Evans, 1998). Arêtes have formed due to past glaciation in the upper valleys in the Lake Wellman area, and were observed at grid references 156°39'22.845"E/79°54'17.116"S, 156°33'17.484"E/79°54'5.461"S, and 156°41'6.846"E,79°52'48.625"S at elevations close to 1600 m a.s.l. There is also an example of a saddle formed at an elevation of 1600 m a.s.l. at 156°36'37.624"E/79°54'5.97"S. The adjacent arêtes merge into the saddle and indicate that the ice in the adjacent valleys once met in this location.

3.3.3. Nunataks

Tips of mountains that rise above the ice levels are referred to as nunataks. There is a sharp nunatak on a mountain peak in the Lake Wellman area (Figure 36). During the penultimate glaciation this nunatak protruded out above the ice and indicates the maximum ice elevation here was 1450 m a.s.l. Although ice has reached elevations of 1590 m a.s.l. at Lake Wellman (as previously mentioned) this site is down-glacier, and at a lower level relative to Lake Wellman. This accounts for the lower elevation of the penultimate ice level. The nunatak is located at grid reference 157°1'14.457"E, 79°53'13.064"S and composed of a Ferrar Dolerite sill overlain by Beacon Sandstone. There is no evidence suggesting these benches were formed by late Holocene ice and were very likely formed much earlier. Unfortunately we were unable to access this location for SED sampling. There is a series of glacial cut benches indicated by the red dotted lines. Each bench indicates a different glacial event as the ice receded down either side of the nunatak.

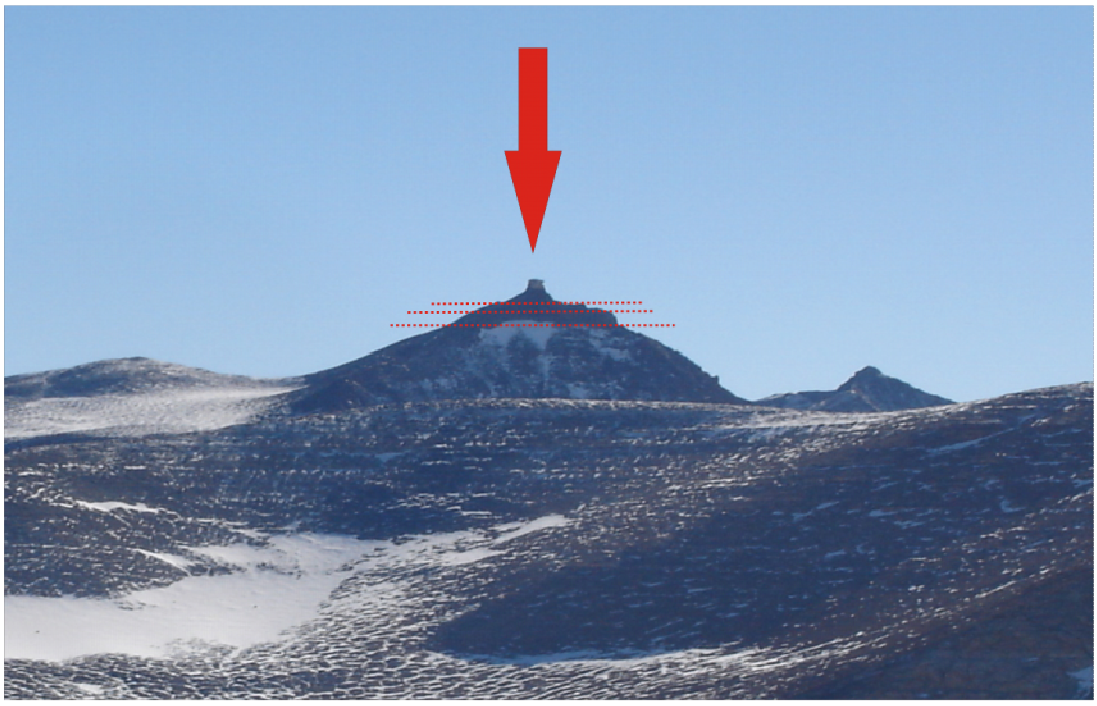

Figure 36. A classic example of a glacially-carved nunatak at a maximum elevation of 1450 m a.s.l. at grid reference 157°1'14.457"E/79°53'13.064"S. The red arrow indicates the nunatak, and the red dotted lines are glacial cut erosional benches.

3.3.4. Glacial cut benches

The glacial erosion power of the late Holocene glaciers is demonstrated by the large erosional cut benches located on the slopes to the southwest of Lake Wellman at 156°51'53.812"E/79°55'41.903"S. There are a total of five benches situated between elevations of 900 m a.s.l. and 1595 m a.s.l. A cross-sectional profile illustrates the angle of the slope in relation to the level benches (Figure 37). Each bench can be linked to the previously identified glacial drifts after Bockheim et al. (1989); Bench 5 = Isca, Bench 4 = Danum, Bench 3 = Britannia II, Bench 2 = Britania I and Bench 1 = Hatherton.

These glacial benches are large features, the longest being 1669 m long and 365 m wide. Each bench is blanketed with debris which consists of deposits analogous to ground moraine, which are composed predominantly of dolerite and sandstone. Numerous granite erratics are strewn over this slope up to a maximum elevation of 1595 m a.s.l.

The orientation of these benches in relation to the Hatherton Glacier suggests that the benches were carved as the Hatherton flowed into the Lake Wellman valley. There formation could be a result of the original geology and structural control. However the Ferrar Dolerite, Beacon Sandstone succession are flat lying; There is no evidence that they have been faulted in a manner that would form a series of benches as seen in Figure 37.

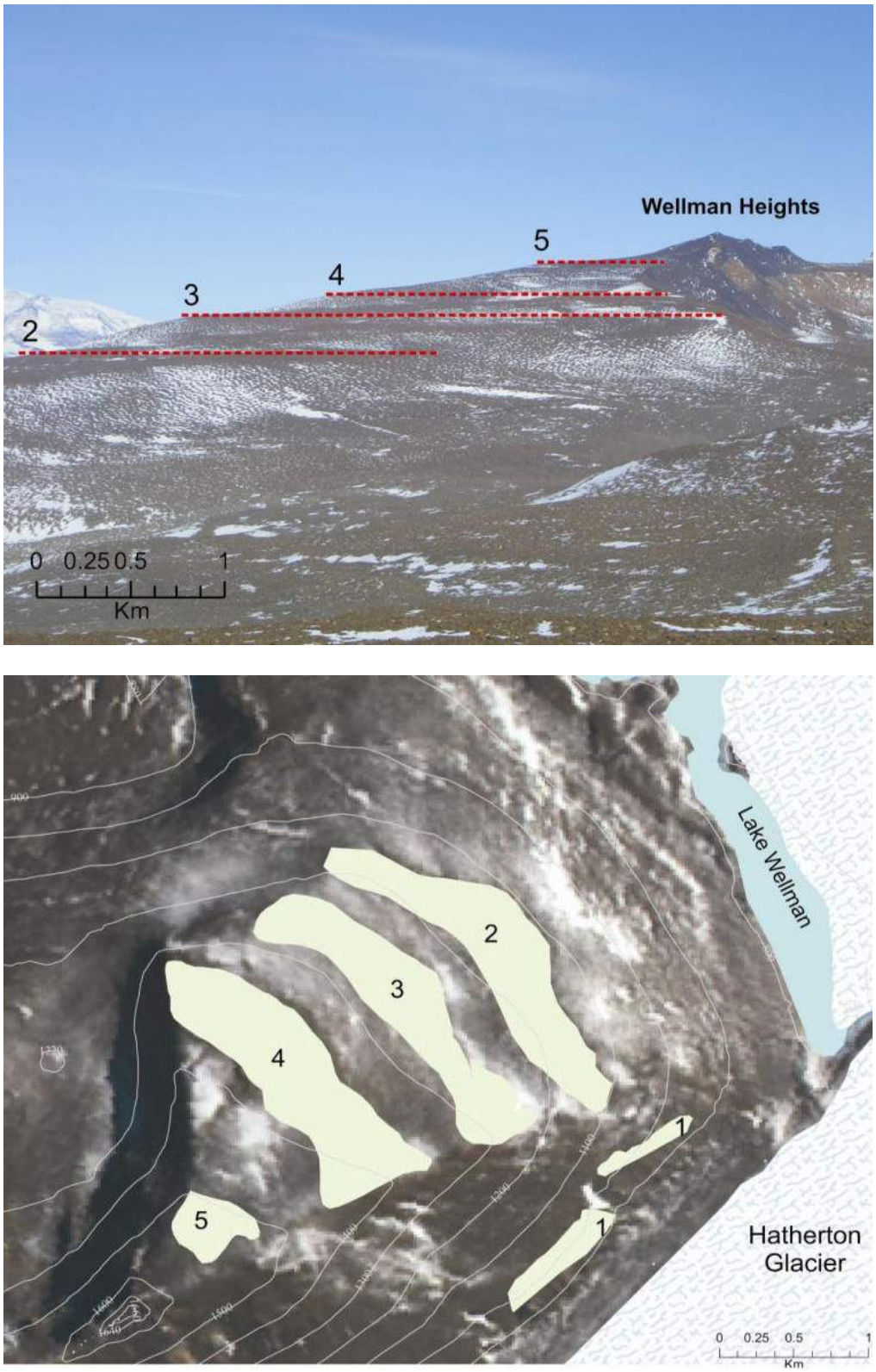

Figure 37. The slope to the south of Lake Wellman shows the locations of erosional drift-covered benches. Five levels are identified (represented by white shading) at elevations between 900 and 1595 m a.s.l. at grid reference 156°51'53.812"E/79°55'41.903"S.

3.4. Micro-scale glacial landforms

3.4.1. Bullet-shaped boulders

Bullet-shaped boulders with an elongate form and a smooth nose were found within the ground moraine in the study area (Figure 38). These boulders formed in the basal ice-flow under immense pressure, which caused them to develop their elongate appearance as a result of glacial abrasion (Figure 38) (Bennett and Glasser, 1997). There are many examples in the Lake Wellman area of such smooth, polished and plucked bullets indicating that these boulders had been carried within the glacier (Figure 38). It is not possible to discern the ice flow orientation from these boulders, but the presence of bullet-shaped boulders is indicative of fast moving, warm-based glacial ice.

Figure 38. Examples of well-formed bullet shaped boulders. The boulders have been carried in the ice parallel to their long axis indicated by the red arrows.

3.4.2. Glacial Abrasion

Abrasion occurs on a boulder when glacier ice moves over its surface. There were many examples of boulders that have been gouged and rounded by abrasion processes in the Lake Wellman area (Figure 39). Evidence of rounding was often present at the more exposed corners and edges where the rock had been removed. In many cases gouging and rounding had uncovered a new weathering surface beneath an iron-stained, outer layer. This suggested that there had either been multiple weathering exposures or that the boulder experienced weathering prior to glacial transportation (Figure 39).

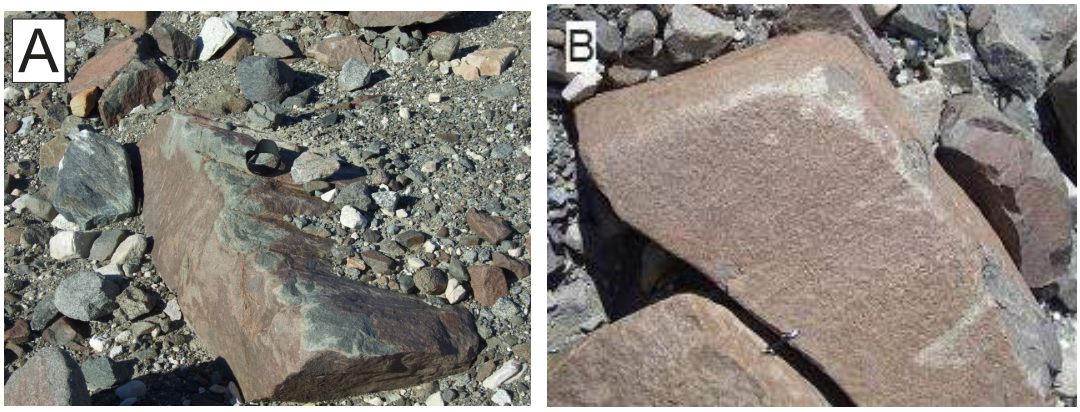

Figure 39. Examples of gouged and rounded boulders with their edges removed by glacial abrasion. Glacial ice was present on the right of image A, which is located within the Hatherton Drift at grid reference 156°55'19.869"E/79°55'9.574"S at an elevation of 830 m a.s.l. Image B is located within a Type B moraine ridge, also in the Hatherton Drift, at grid reference 156°54'35.275"E,79°55'13.689"S at 860 m a.s.l.

3.4.3. Striations

Abrasion of debris trapped in the ice results in the production of grooves and scratches across its surface as it is dragged over rock at the base of the glacier (Sugden and John, 1985). These features are known as striations (Evans, 2002). Striations occurred at numerous locations in the Lake Wellman area and in a variety of forms (Figure 40). They were found extensively on boulders around the margins of the lake and up to a maximum elevation of 1550 m a.s.l. Those observed were usually only a few millimetres in depth and populated boulders in great density, often oriented in more than one direction, indicating either the occurrence of multiple events or that the boulders had moved around during glacial transportation (Figure

41). The striations ranged in length from a few centimetres up to 40-50 cm. Some striations may have been much longer when they were first formed, but appeared shorter as continued glacial erosion reduced the size of the boulder. Many boulders displayed chatter marks formed from multiple closely spaced and downward directed impacts (Figure 42). There were also examples where striations were observed to cut through an existing weathering rind exposing a new surface (Figure 43). This indicated variation in the timing of striation emplacement relative to that of the weathering processes. Striations were not observed on bedrock in the study area, all those seen being located on boulders within moraines. Because of this, the orientation of striations was not indicative of the direction of previous ice flows. Striations do not usually form, or are at best only weakly developed, in cold-based glacial ice (Waller, 2001; Atkins, 2004; Atkins et al., 2002). In addition, the concentration of those observed on boulders suggested that the ice was fast moving in the study area.

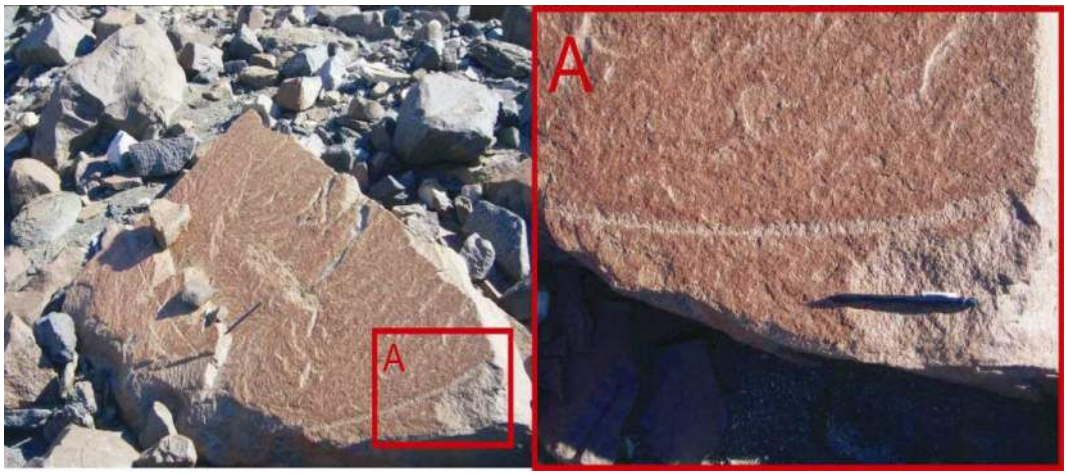

Figure 40. A striated boulder in the Lake Wellman area, located at an elevation of 880 m a.s.l. at grid reference 156°45'46.872"E/79°55'2.714"S.

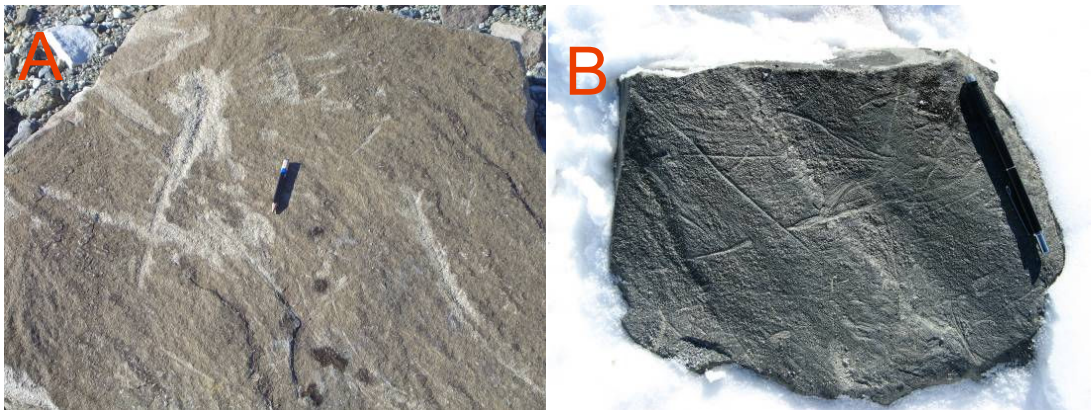

Figure 41. Cross-cutting striations. Image A depicts a rock located within the ground moraine at an elevation of 790 m a.s.l. Image B shows a boulder located within the lake ice 790 m a.s.l. at grid reference 156°54'51.893"E/79°54'55.587"S.

Figure 42. Chatter marks formed when this block was moving through basal ice and was impacted by multiple downward directed impacts. This bolder is located in a Type A moraine ridge with in the Hatherton Drift at 820 m a.s.l. grid reference 156°54'43.609"E/79°55'12.58"S.

Figure 43. A well-formed striation on a dolerite boulder. The contrast in degree of weathering between the striation and the outer surface indicate this boulder was weathered before the striation was formed.

3.5. Periglacial features

3.5.1. Patterned ground

Polygonal-patterned ground occurred at many locations in the Lake Wellman area (Figure 44). A great proportion of the ground moraine, especially in the low-lying valley regions was dominated by this landform, which is formed by a process related to frost heave (Figure 45). The material within the polygons was generally unsorted and contained angular debris. Small polygons ranged in size from 5 – 10 m in diameter and the large polygons were greater than 20 m across. A detailed map of the locations of patterned ground indicated that polygon size is a function of age. There was a trend for progressively larger polygons to occur with increasing elevation, younger ground tending to have small polygons. However, at lower elevations there were also a few random patches of large well-developed polygons that were nested amongst areas of smaller polygons (see geomorphology map in pocket, inside back

cover). These features were best observed from a distance and, mirage-like, they disappeared as you walked towards them.

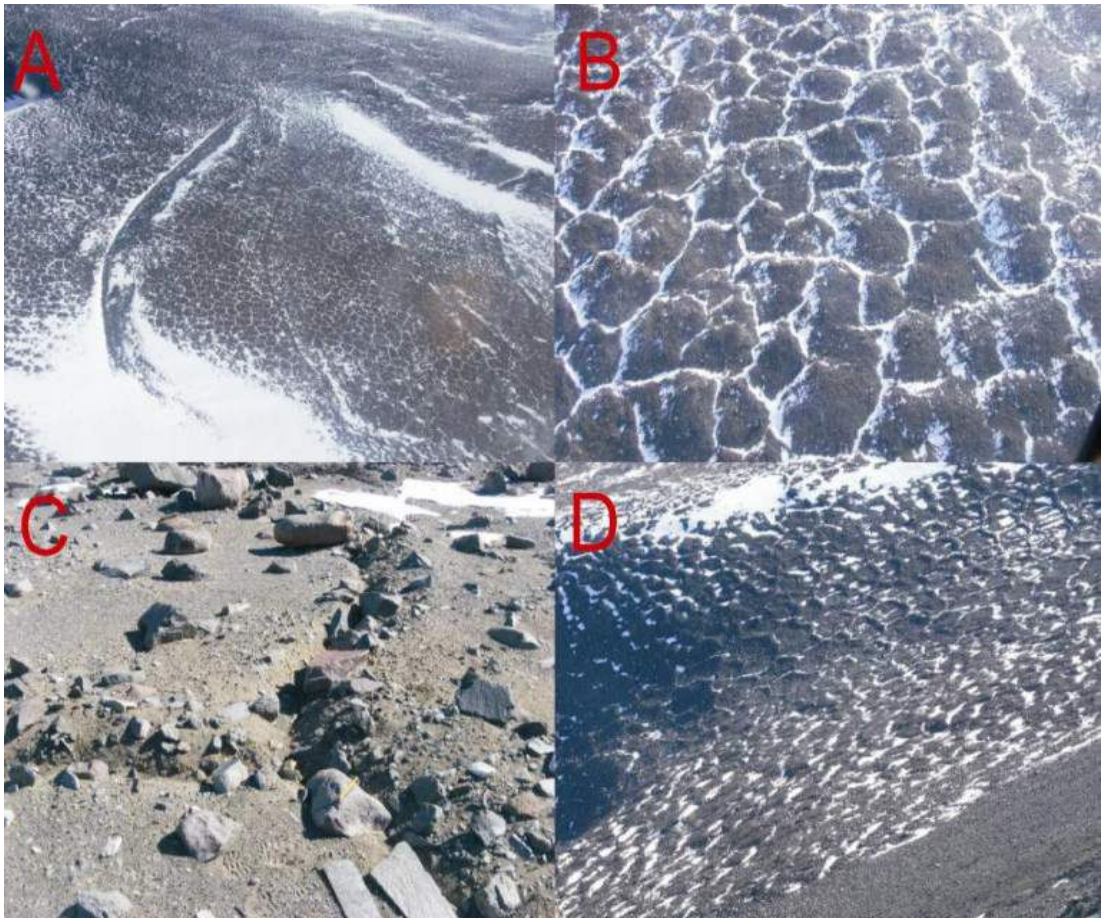

Figure 44. Polygonal-patterned ground. Image A displays patterned ground on either side of the ridge (Moraine 5) at 1064 m a.s.l. at 156°45'48.65"E/79°53'24.497"S (Figure 24). Image B shows polygons that are approximately 15 m in diameter at 1290 m a.s.l. at grid reference 156°41'33.825"E/79°53'25.871"S. Image C represents a close-up view of the frost wedge polygon border at 805 m a.s.l. at grid reference 156°55'26.199"E 79°55'13.714"S. Image D displays an unusual reverse phenomenon in which the borders of the polygons were raised relative to the lower relief of the interior at grid reference 156°51'9.314"E 79°53'30.233"S.

3.5.2. Frost heave

Frost heaving is the predominately upward movement and sorting of soil and debris caused by the fluctuating pressure exerted on it due to the repeated expansion and

contraction of water during freezing and thawing (Washburn, 1973). Freeze thaw processes are responsible for the formation of pattern ground (previous section).

There is evidence for frost heave affecting material in the Lake Wellman area. An exposure located close to lake level can be seen in Figure 45. This exposure is located at 850 m a.s.l. at grid reference 156°56'21.11"E,79°56'5.363"S. The lower section is dominated by fine-grained material, with few large clasts. In the upper part angular clasts of granite, dolerite and sandstone are observed (Figure 45). The large angular clasts may have been exhumed to the surface by frost heave processes, and this could explain the reverse grading. This affect is also observed in debris flows which cause large clasts to migrate upwards. However, it is unlikely this is a debris flow. But it is debateable weather this exposure has been affected by frost heave at all? With separation of the exposed section into two units, an upper and lower, it can be argued that each has a separate depositional history, i.e. an upper layer of course angular supra-glacial material that was deposited over the fine grained material below.

Another similar example is found in the Wellman Depression at an elevation of 880 m a.s.l. at grid reference 156°44'27.079"E**,**79°54'58.112"S (Figure 46). This exposure occurs in the top of a 7 metre high moraine ridge. There is sorting and vertical alignment of some of the clasts which could be attributed to frost heave. It is also possible this exposure was not affected by frost heave at all. Another explanation is deposition of course supra-glacial material over a layer of ablation till. This was the only exposed section along the ridge, making it difficult to confirm or deny these explanations. Figure 45 and Figure 46 are the only cross section exposures we observed in the Lake Wellman area.

Figure 45. An exposure of fine material overlain by course angular debris, located at 850 m a.s.l. It is likely that this material has been sorted by frost heave processes.

Figure 46. A cross-section through a large, sinuous moraine located in the Wellman Depression at an elevation of 880 m a.s.l. This exposure is at the top of a 7 metre high moraine ridge.

3.6. Non-glacial features

3.6.1. Undifferentiated talus

Undifferentiated talus was observed in concentrated masses down-slope from large scarp exposures of Ferrar Dolerite and Beacon Sandstone in the Lake Wellman area (Figure 47). This talus occurred on slopes adjacent to the lake and within the upper valleys. It consisted of very angular and poorly sorted material with clasts ranging from 20 cm to 1 m in size. The clasts were composed of dolerite and sandstone.

Figure 47. Undifferentiated talus sourced from a Ferrar Dolerite sill exposure adjacent to Lake Wellman located at grid reference 156°54'55.378"E/79°53'41.643"S.

3.6.2. Ponds

There were many ponds in the Lake Wellman area located within the Wellman Depression and around the margins of the lake. These ponds were often found close to moraine ridges which form a dam that traps any melt water. The ponds ranged in size from 1 - 14 m in diameter but their depth has not been measured (Figure 48).

Figure 48. A large pond located within the Wellman Depression at 880 m a.s.l. at grid reference 156°43'24.886"E/79°54'59.649"S.

3.6.3. Pond deposits

Pond deposits were found at numerous locations in the Lake Wellman area, and were evidence of former ponds that have dried up (Figure 49). These deposits were dominated by very fine sediment which consist of carbonate material and algal remains. Scattered boulders were also present, ranging in diameter between 30 cm up to 1 m (Figure 49). The finer sediment displayed desiccation cracks 7 cm wide. Pond deposits in the Lake Wellman area were found at grid references 457168/1129536 and 458386/1127203 at elevations of 960 and 800 m a.s.l. respectively. The pond deposits did not show signs of patterned ground indicating that the deposits were younger.

Figure 49. Areas where ponds may have once existed in the Lake Wellman area. The images are located at 960 m a.s.l. in the Britannia I Drift. The pond deposits occur upglacier of large moraine ridges which may have dammed water during glacial recession.

3.6.4. Melt-water channels

Melt-water channels are a seasonal feature occurring in the summer when higher temperatures cause snow to melt and frozen ground to thaw. The amount of moving free water is generally small and melt-water channels therefore develop slowly over many thousand years. Melt-water channels were seen in the Lake Wellman area at 156°45'9.902"E/79°55'13.148"S, 156°59'15.65"E/79°55'32.242"S, 156°47'6.942"E/79°52'36.667"S, and 156°56'44.799"E/79°53'52.61"S (see also section 3.2.5). In some cases, melt-water channels appear to have eroded through moraine ridges. A very prominent melt water channel is located in a cirque depression adjacent to Lake Wellman, this extends into the upper level of the valley head at 1150 m a.s.l. (Figure 50). This channel is approximately 1600 m in length.

Figure 50. A melt-water channel exiting from a cirque depression adjacent to Lake Wellman at an elevation of 950 m a.s.l. at 156°57'31.669"E/79°53'43.883"S. The channel is indicated by red arrows, and a red dotted line to the left delineates a glacial erosional bench. A nunatak peak is visible in the distance.

3.7. Weathering features

3.7.1. Honeycomb weathering

Pitted, honeycomb features are a surface phenomenon formed by a combination of wind and salt weathering (Mustoe, 1982; Rodriguez-Navarro et al., 1999). Strong, continuous wind-flow across the surface of a boulder promotes the growth of salt crystals as water evaporates, which causes cavities to form. The air pressure over the cavities is reduced, increasing the airspeed within them, which accelerates evaporation and salt growth, intensifying erosion (Rodriguez-Navarro et al., 1999). Honeycomb features were not found on freshly weathered surfaces at low elevations. The honeycomb cavities occur in concentrated groups on each boulder and range in size from 1 - 9 cm in diameter (Figure 51). They appear to occur equally on rocks of different lithologies. Honeycomb formations were found on dolerite and sandstone boulders in upper elevations in the Lake Wellman area. The affected boulders were

often strongly iron-stained with a varnished appearance on their outer surface which is the result of little precipitation and strong winds.

Figure 51. Boulders with honeycomb weathering. The upper left and lower right images are very iron stained and polished on their outer surface.

3.7.2. Cavernous weathering

Many boulders displayed cavernous weathering in the Lake Wellman area. Cavernous weathering is a chemical weathering process which occurs as a result of extreme cold temperatures combined with frequent strong winds carrying fine sediments that have a sand blasting effect on the boulder surface. The affected boulders are gradually broken down from beneath, resulting in extreme exfoliation and disintegration (Figure 52). This is quite different to honeycomb weathering which affects the upper surfaces of boulders in the form of concentrated groups of small erosion pockets. The weathering phenomenon equally affects boulders of dolerite, sandstone and granite, but because those of sandstone are less resistant they disintegrate rapidly. Cavernous weathering was more prolific at higher elevations, where rocks had been exposed longer after being freed from the ice, and was not

seen at low elevations. It was always observed on the undersides of boulders of various sizes and shapes (Figure 52).

Figure 52. Extreme cavernous weathering of a dolerite boulder, left, and a sandstone boulder, right.

3.7.3. Freeze-thaw shatter

Large blocks of Beacon Sandstone were observed displaying shattering characteristics caused by freeze-thaw weathering processes (Figure 53). These boulders were weakest along their bedding planes where shatter had occurred due to expansion and contraction pressures created by extremely cold temperatures and thawing.

Figure 53. Freeze-thaw shatter along the bedding planes layers within boulders of Beacon Sandstone. Both examples illustrated were located within close proximity of each other at 970 m a.s.l. at 156°48'25.415"E/79°53'21.522"S.

3.7.4. Subglacial conduits

Two very rounded Beacon Sandstone boulders were located within glacial drift surrounded by very angular material (Figure 54). No other boulders with this degree of rounding were observed in the field. Both examples are located within the Hatherton sequence at 800 m a.s.l. at 156°55'19.714"E/79°55'10.01"S (Figure 54). The presence and rarity of these rocks raised questions about their depositional history. Their surfaces were of a polished veneer, with no sign of wind erosion and no striations, and the degree of rounding indicated abrasion by fluvial processes rather than glacial entrainment.

One possible explanation is that these boulders are much older than the surroundings, being the remnants of a paleo river bed, and have been exhumed to the surface by frost heave processes over millions of years. However, this seems unlikely. Alternatively, the boulders may have been deposited by a series of sub glacial conduits. Transport within a network of conduits by sub glacial water would explain the degree of rounding, but more boulders of a similar nature would then be expected in the surrounding drifts. This explanation would also suggest that the glaciers were warm based at the time of deposition of these boulders, which would have implications with respect to glacial and climate fluctuations on the wider scale. The

most likely explanation is that these boulders were eroded locally from a nearby conglomerate, the Brown Hills Conglomerate (Table 1, Page 6). The Brown Hills Formation is stratigraphically just below the Hatherton Sandstone Formation.

Figure 54. Two extremely rounded Beacon Sandstone boulders. The extreme rounding and the absence of striations imply formation and deposition by sub glacial fluvial processes, rather than glacial entrainment. These boulders are located in the Hatherton drift at 800 m a.s.l. at 156°55'19.714"E/79°55'10.01"S.

4. Results

4.1. Introduction

In this chapter the results from the field and laboratory studies are presented. The outcomes from the processing and investigation of the field data from the Lake Wellman area are described in detail.

4.2. Geomorphic mapping

The detailed geomorphology map of the Lake Wellman area created from the field data and showing the locations of significant land forms and glacial features is presented in Figure 55. A large copy of this map can be found within the pocket on the inside back cover of the thesis for more detailed reference.

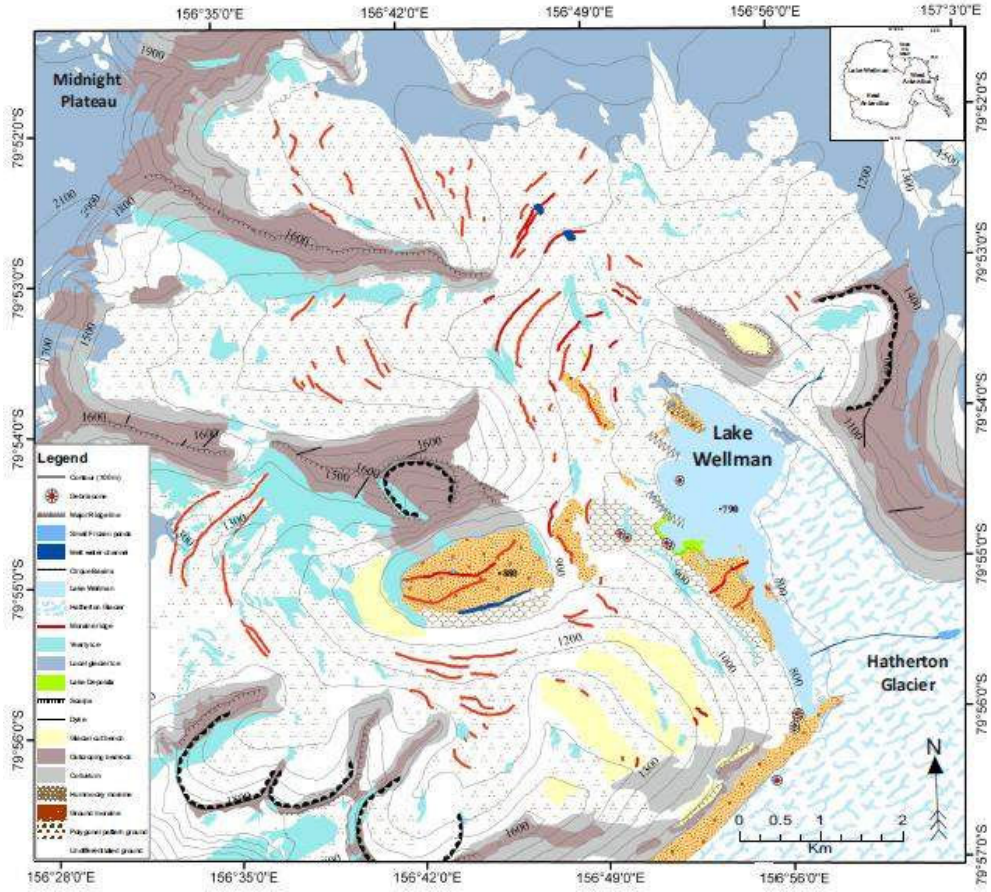

Figure 55. Geomorphology map of the Lake Wellman area. Moraine ridges are indicated by the solid red lines. Valley regions with expanses of polygonal pattern ground are indicated by the blue, triangular-patterned stipple. Hummocky and adjacent ground moraines dominating areas of low elevation are indicated by a blue and white scale pattern and yellow/brown stipple, respectively. The full-sized map was produced at a 1:50000 scale using satellite imagery

A geological map of the Darwin Mountains, after Haskel et al. (1964), showing the locations of Beacon/Dolerite outcrops and glacial deposits in the Lake Wellman area, is presented for comparison purposes (Figure 56). Close examination of Lake Wellman in Figures 55 and 56 (cf. Figure 1) indicates that the shape of Lake Wellman has changed during the last 4-5 decades. Either there has been a recession of the Hatherton Glacier or the lake level has risen and covered part of the glacier margin and associated moraine features.

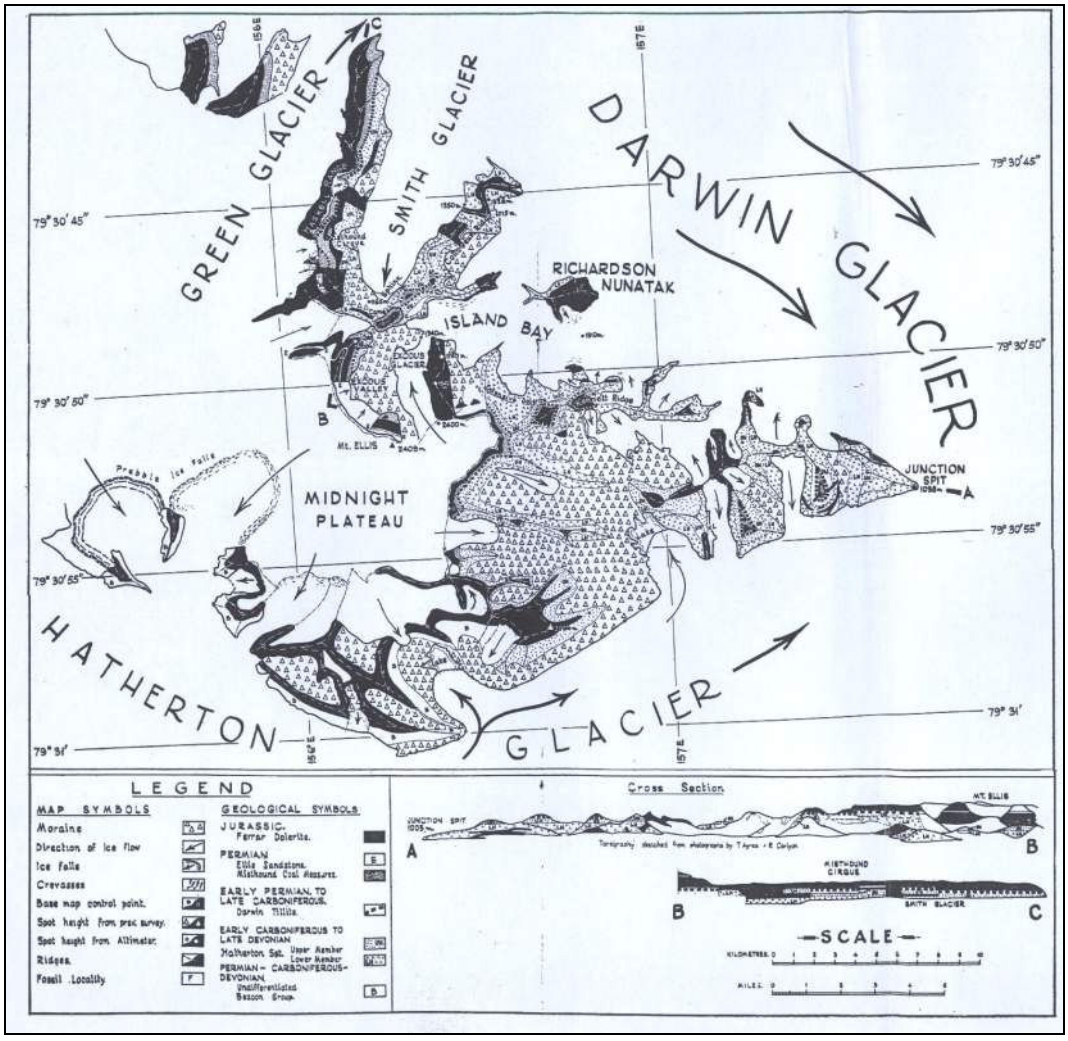

Figure 56. Geology of the Darwin Mountains, Transantarctic Mountain Range, Antarctica (from Haskell et al., 1964).

4.3. Sedimentology

The data on lithology, angularity, weathering and clast size of the rocks sampled along eight of the transect lines are presented below in the form of graphs. Since the

most common lithology types present consisted of dolerite, sandstone and gabbro, they were used to make comparisons between sites. The clast dimensions are presented as averages of all points per transect.

4.3.1. Lithology proportions

Results showing the proportions of lithology types among the rocks sampled in the study area are presented in Figure 57. Overall, the most common lithology types present were dolerite, sandstone and gabbro, while basalt and granite rocks were also present in smaller amounts at all elevations. It was found that although differences occurred between some transects, there were in general no consistent patterns between rock lithology and either elevation or distance from the present glacier. This lack of a trend among the relative proportions therefore initially suggested that the weathering process had occurred in a balanced way across all lithology types over the full range of elevations (Figure 57). Nevertheless, it was also observed that rocks in the drifts at high elevations were generally more weathered than those at low altitudes, which were only lightly weathered (see subsequent sections).

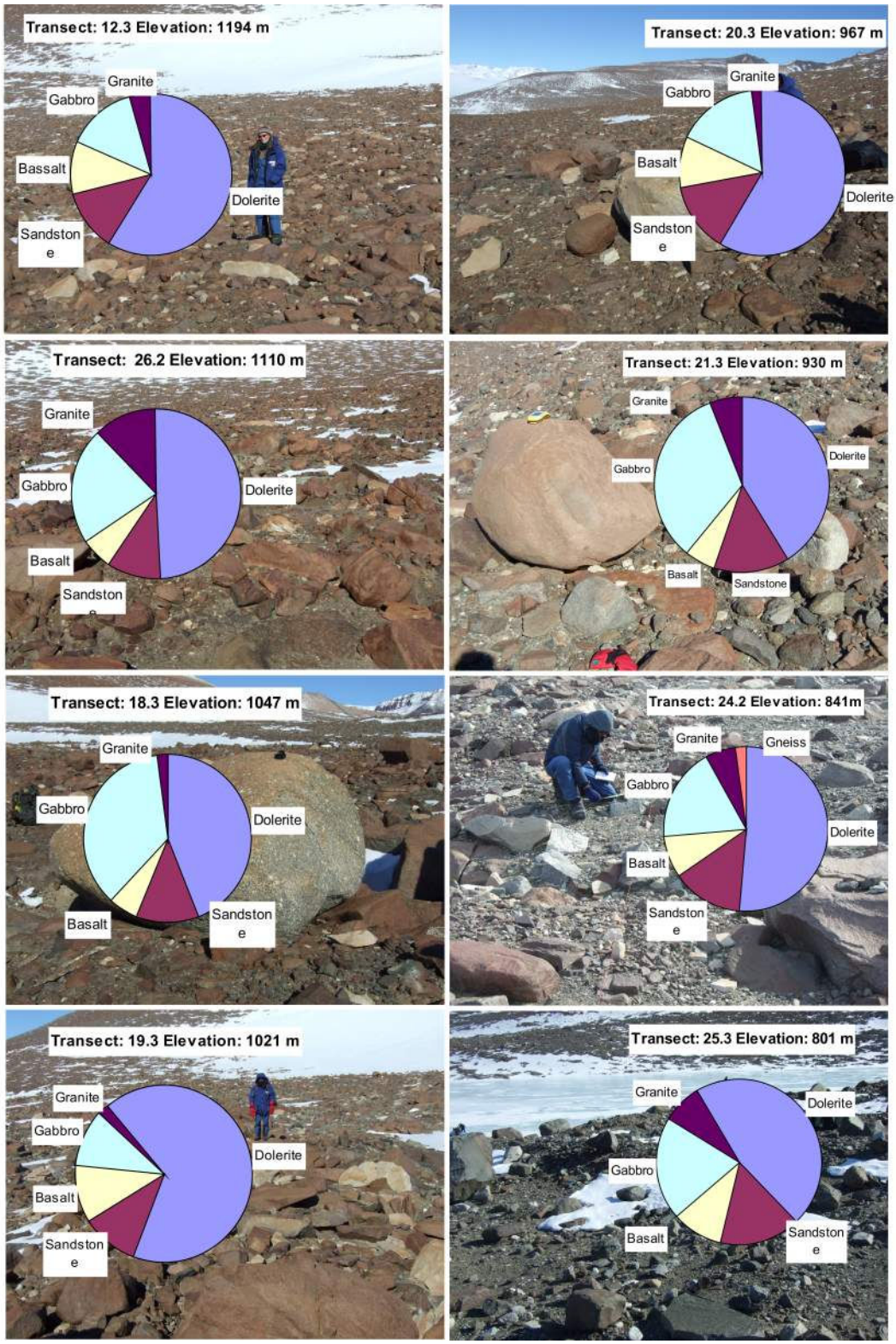

Figure 57. The proportions of different lithologies based on numbers of rocks of each type at each transect location in the Lake Wellman area.

4.3.2. Hardness

Results for the Schmidt hammer tests are shown for two rock types, sandstone and granite (Figure 58 and Figure 59). The rebound data for sandstone showed no correlation with elevation ($R = 0.0480$; $df = 26$; $p>0.05$), indicating that hardening due to weathering on the sample surfaces was not affected by altitude or distance from the present glacier (Figure 58). However, the granite samples showed a distinct decrease in rebound values as elevation increased (Figure 59; $R = 0.5448$; $df = 26$; $p<0.01$). The results from the Schmidt hammer tests therefore indicated that the rind produced by weathering of granite rocks was harder at lower elevations closer to the glacier.

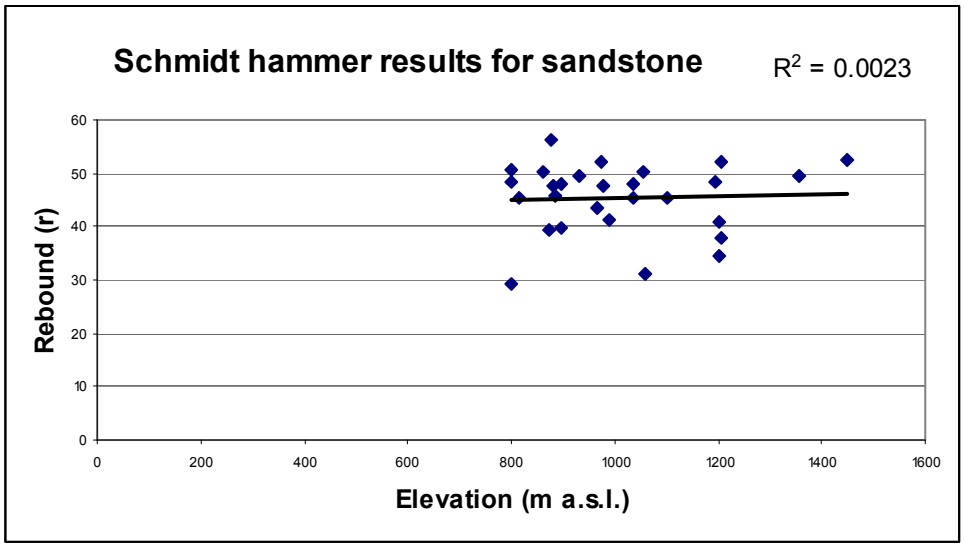

Figure 58. Schmidt hammer results for sandstone samples.

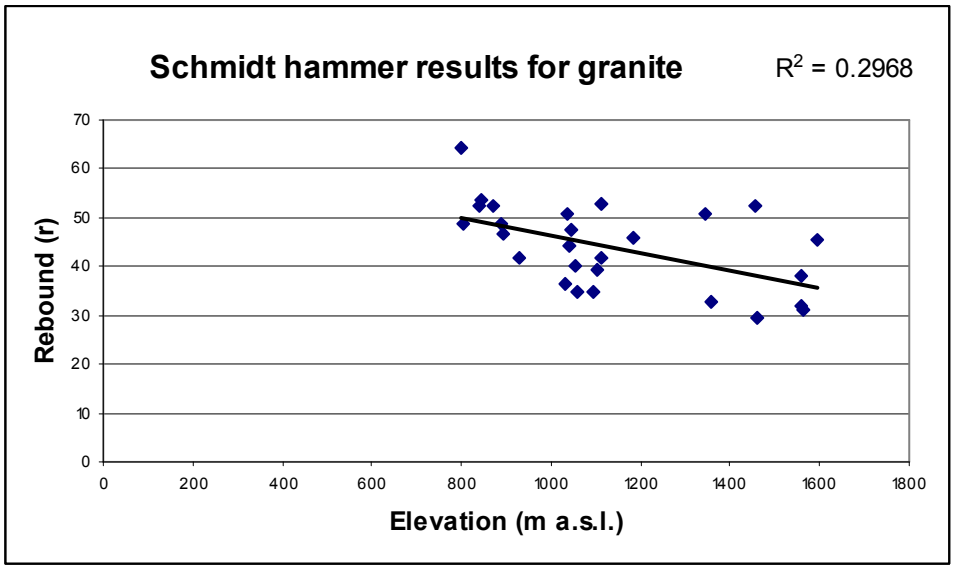

Figure 59. Schmidt hammer results for granite samples.

4.3.3. Transect line results

Graphs of angularity, weathering and clast size information are presented below. Lithologies of dolerite, sandstone and gabbro are the most common in the study area and these were therefore used to make the main comparisons between sites. Comparisons were only made between the same lithologies.

4.3.4. Angularity

The angularity plot for dolerite in the study area is shown in Figure 60. Variation among transects was significant ($p = 0.007032$). The graph indicates that there was an increasing trend for roundness as elevation increased. With the exception of the transect at 841 m, there was a general decrease in the proportion of sub-angular clasts with greater elevation, and a corresponding increase in the proportion of sub-rounded rocks (Figure 60).

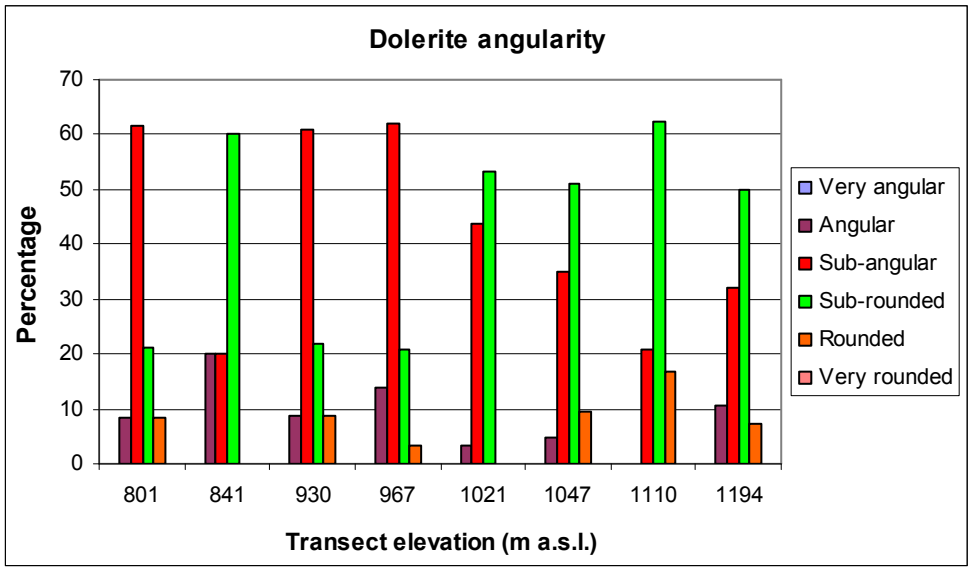

Figure 60. Percentage angularity for dolerite clasts at different transect elevations in the Lake Wellman area. There are eight transects displayed and each elevation indicates a different transect line.

The sandstone angularity plot (Figure 61) followed a similar pattern to the dolerite angularity plot (Figure 61), although the trend was barely significant, as shown by the reduced p value ($p = 0.0304$). The effect is mainly demonstrated by the sub-angular clasts which again decreased in proportion as elevation increased. Conversely, the proportion of sub-rounded rocks increased with altitude, except at the two highest transect elevations. The overall trend in sandstone angularity is therefore a change from relatively sub-angular clasts below 1000 m to a mixed distribution with sub-rounded clasts becoming more dominant at higher elevations (Figure 61).

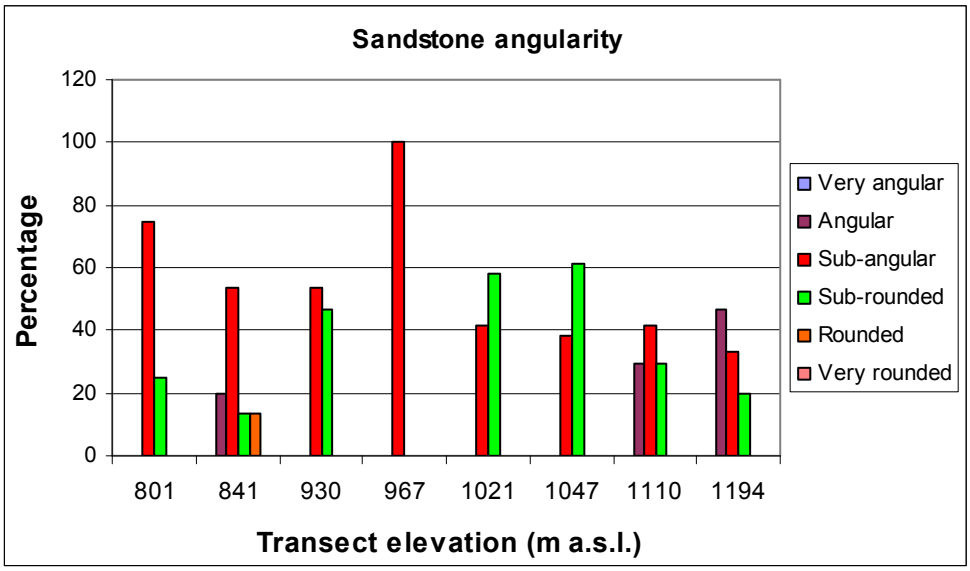

Figure 61. Percentage angularity for sandstone clasts at different transect elevations in the Lake Wellman area. There are eight transects displayed and each elevation indicates a different transect line.

Rocks of gabbro in the Lake Wellman area also tended to show a pattern of increasing roundness and decreasing sub-angularity with increasing transect elevation (Figure 62).

Angularity results for basalt and granite are not shown, as they were not represented in sufficient amounts in all transects. There was no significant variation among transects for either basalt or granite ($p>0.05$).

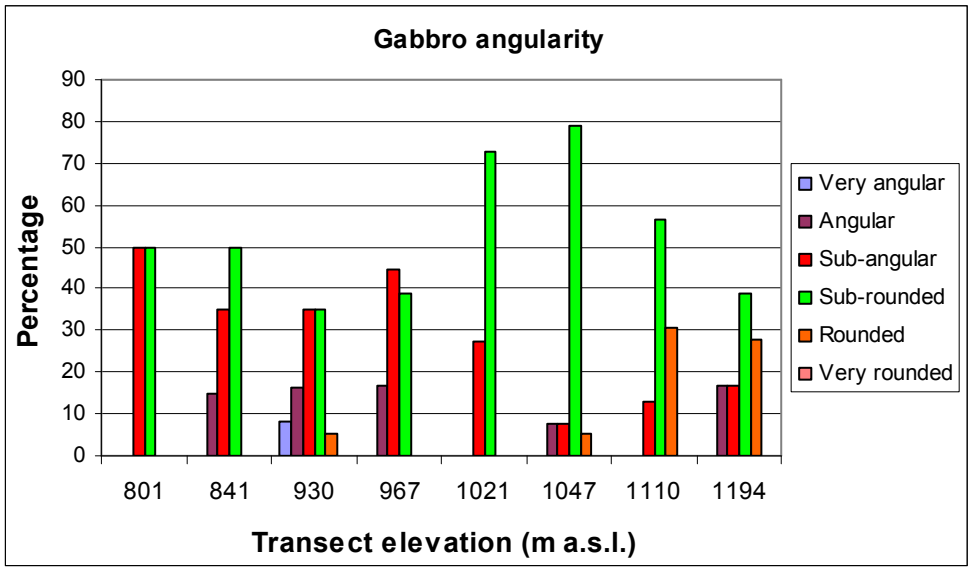

Figure 62. Percentage angularity for gabbro clasts at different transect elevations in the Lake Wellman area. There are eight transects displayed and each elevation indicates a different transect line.

4.3.5. Weathering

Results for the degree of weathering of rocks in the study transects are presented in the graphs below. In general, the results demonstrated a pattern of increased weathering as elevation increased.

Weathering of the dolerite clasts is shown in (Figure 63). For dolerite, the degree of weathering differed significantly among transect elevations ($p = 0.001207$). The graph shows that the proportion of highly weathered and oxidised clasts increased with greater elevation. Conversely, apart from the two lowest transects, moderately weathered clasts decreased in proportion with altitude. The proportion of lightly weathered clasts also decreased and then disappeared as altitude increased (Figure 63).

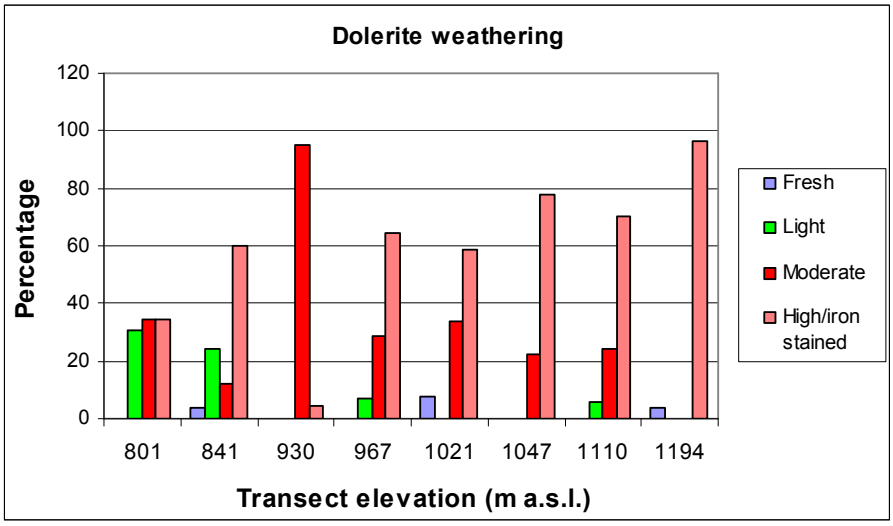

Figure 63. Percentage weathering for dolerite clasts at different transect elevations in the Lake Wellman area. There are eight transects displayed and each elevation indicates a different transect line.

The proportions of weathering classes for the sandstone clasts are shown in (Figure 64). For sandstone, too, the degree of weathering increased with elevation, and the proportions among transects were highly significant ($p = 1.905 \times 10^{-12}$). This was mainly because highly weathered and oxidised clasts were only present at elevations at 967 m and above (the proportion increasing with altitude), while moderately weathered rocks were absent at these higher elevations, being found only at altitudes of 1047 m or less.

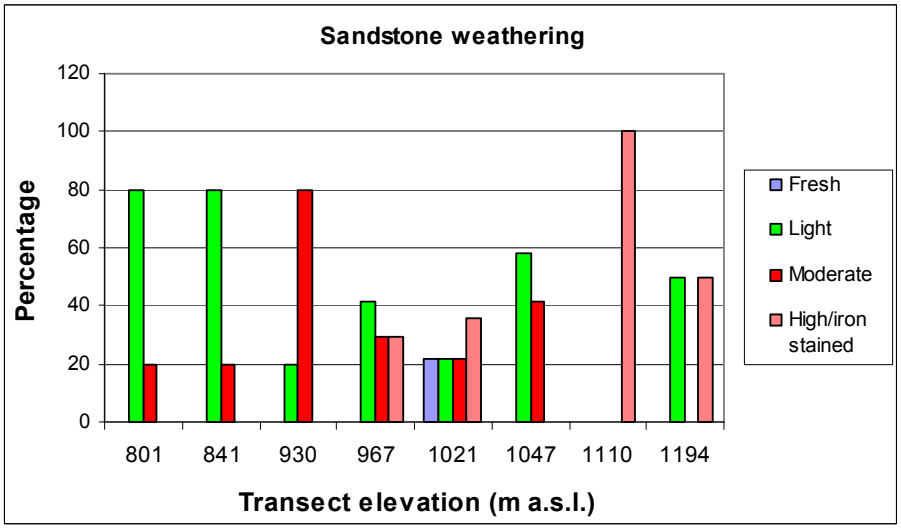

Figure 64. Percentage weathering for sandstone clasts at different transect elevations in the Lake Wellman area. There are eight transects displayed and each elevation indicates a different transect line.

For gabbro, few patterns could be discerned among the proportions of the different weathering classes as elevation increased (Figure 65). This is reflected in the p value which was not significant ($p>0.05$). Clasts of granite and basalt also showed no significant variation in weathering between transects.

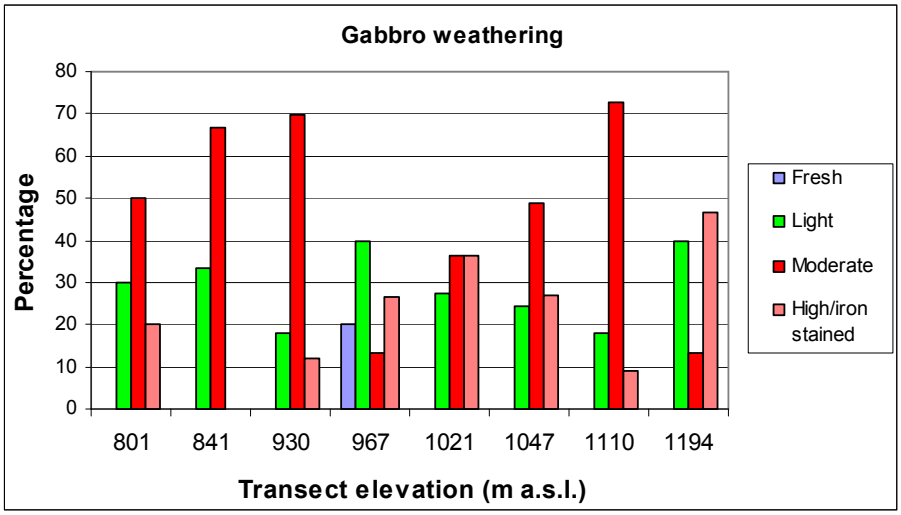

Figure 65. Percentage weathering for gabbro clasts at different transect elevations in the Lake Wellman area. There are eight transects displayed and each elevation indicates a different transect line.

4.3.6. Clast size distribution

The average size distribution along the 'a' 'b' and 'c' axes of rock samples at each transect elevation are plotted below for all lithologies (Figure 66) and for each lithology separately (Figure 67). In general, rocks were larger in transects in the intermediate elevations between 967m and 1047m. For instance, at elevations between 801 and 930 m a.s.l. the length along the a-axis fluctuated between 31 and 39 cm (Figure 66). The a-axis length then tended to increase with elevation to a maximum of 54 cm at 1047 m altitude, after which it decreased to a minimum of 27 cm at 1194 m elevation.

When considering each lithology type separately, it can be seen that this observed trend of greater size at middle elevations applied to sandstone, dolerite and granite, but less so to gabbro and basalt (Figure 67).

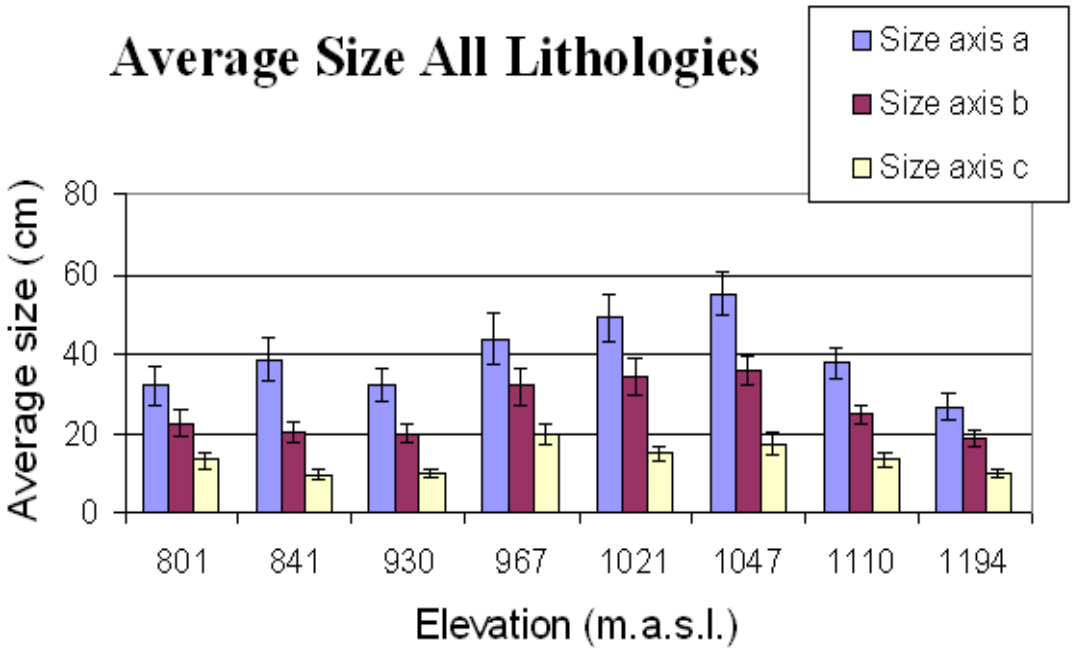

Figure 66. Average size in centimetres of the a, b, and c axes for all lithologies at different transect elevations. The error bars indicate the standard deviation around the mean.

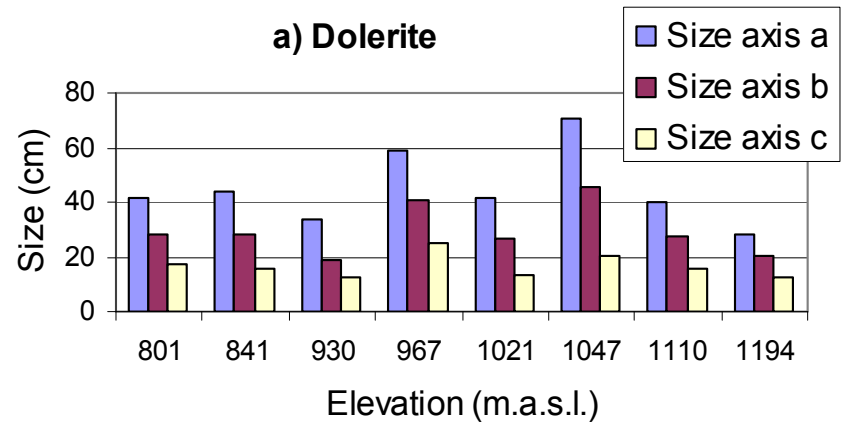

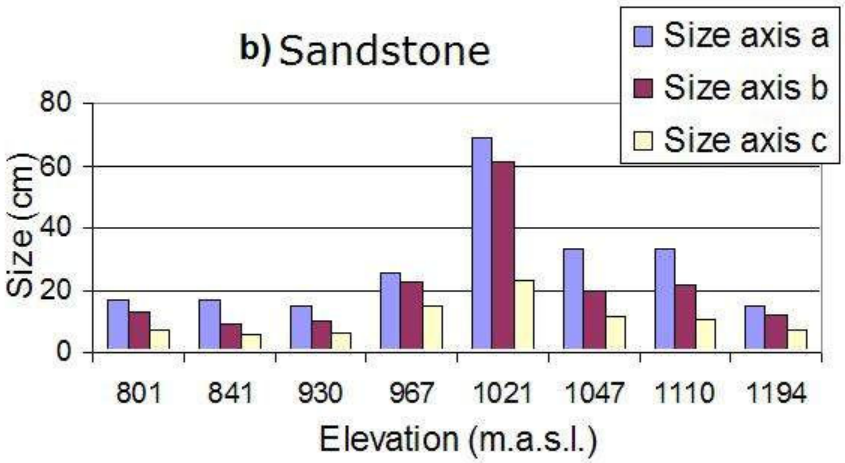

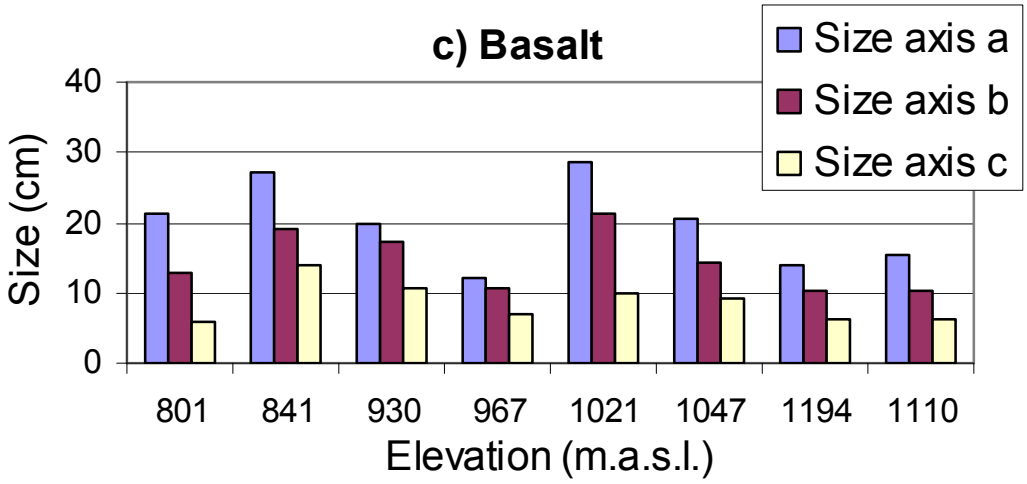

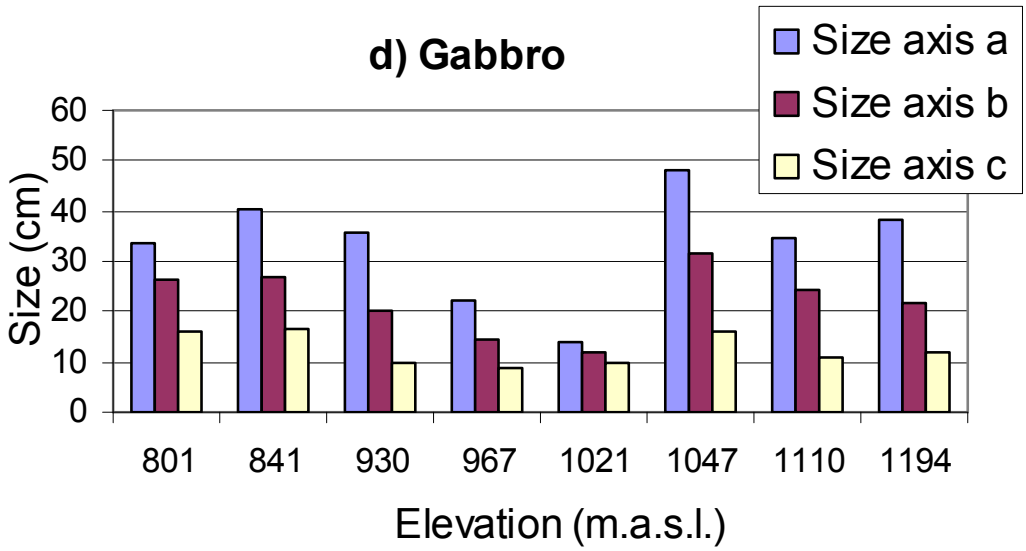

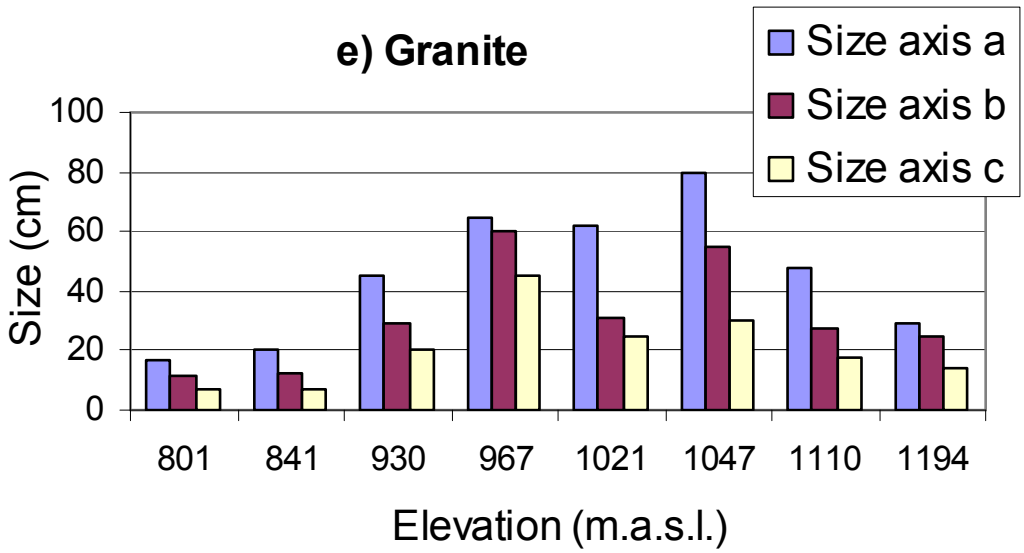

Figure 67. Average clast size for lithology: a) dolerite, b) sandstone, c) basalt, d) gabbro, e) granite.

4.4. Polygonal pattern ground

The distribution of polygon pattern ground presented in the map below follows two very strong trends (Figure 68). The first, a south-north trend, shows the polygon diameter increasing in size with increasing elevation from the Hatherton Glacier margin up to a maximum at 1400 m a.s.l. Large polygons (> 18 m diameter) are located between 1400 m and 1300 m a.s.l. and decrease to medium sized polygons (12 - 18 m diameter) from ca. 1160 m a.s.l. down to the margins of Lake Wellman. The transition coincides with the position of Moraine 5 (page 43) (Figure 22). Along the margins of the Hatherton Glacier the polygons become small, bound upslope by Moraine 2 (page 43).

The second trend follows an east-west orientation (Figure 68). Areas with small polygons are located along the margin of the Midnight Plateau, and were mapped at high elevations close to the current margin of the plateau at grid references 156°33'13.391"E 79°53'20.54"S, 156°32'24.851"E 79°54'27.896"S, 156°37'8.134"E 79°52'6.972"S, and 156°47'20.079"E 79°52'0.63"S. These are bordered to the east by areas with large size polygons. This pattern is repeated in three separate valleys (Figure 68).

In addition, polygonal pattern ground occurs in the cirque basins located on the north side of the Hatherton glacier that were previously described (on page 56). These polygons are small (< 12 m diameter) and do not appear to follow either the south - north or east–west trends shown by the other polygonal pattern ground in the Lake Wellman area.

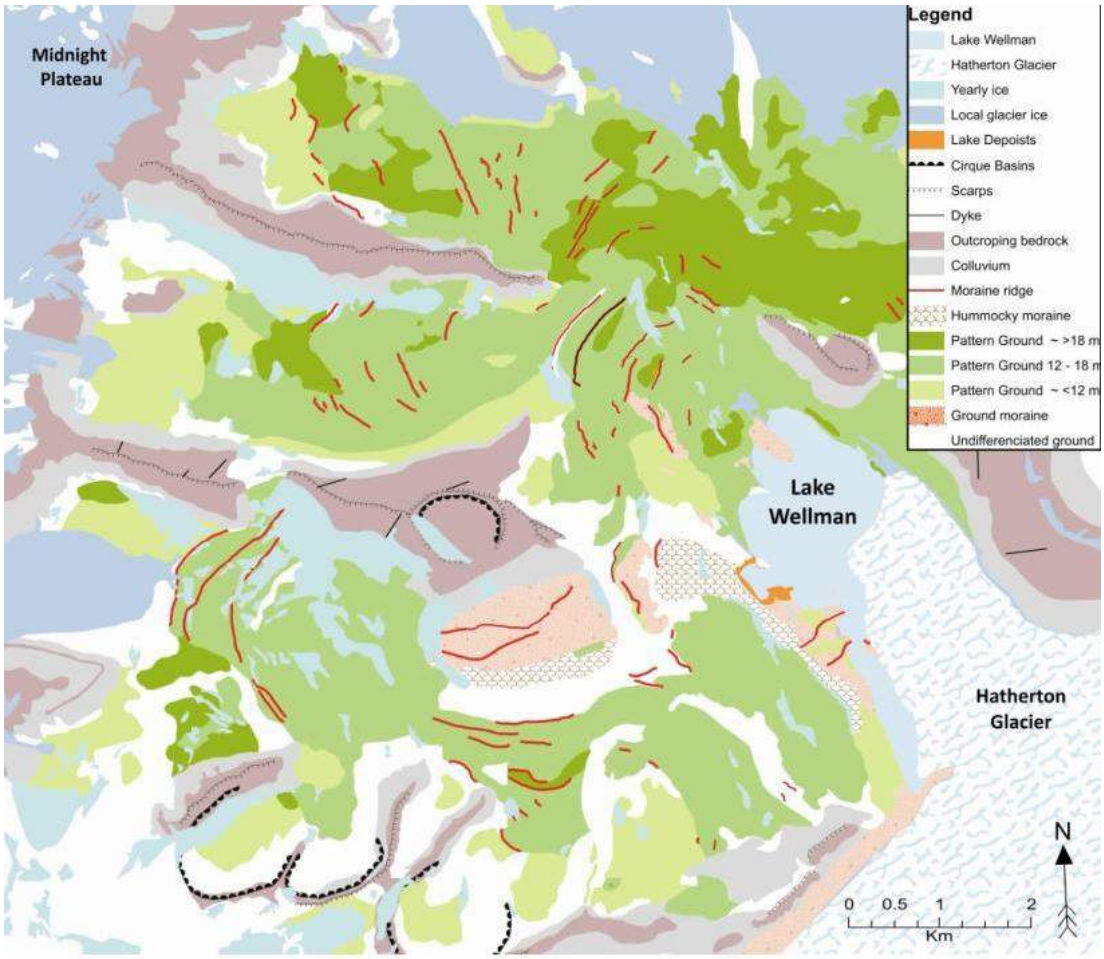

Figure 68. Polygonal pattern ground mapped based on polygon diameter. Polygons are separated into small (< 12; yellow-green), medium (12 – 18 m; pale green), and large (> 18 m; dark green) size categories.

4.5. Glacial chronology results

4.5.1. Samples for Surface Exposure Dating (SED)

Table 3 summarizes the locations, lithologies and dimensions of the 23 rock samples collected in order to determine the rate of recession of the Hatherton Glacier. As shown earlier (Figure 11, page 26 and 27) these samples were taken from three general areas or zones covering the full range of the previously named drift sequences around Lake Wellman (Bockheim et al., 1989). Each of the sample ID record sheets and photographs providing full information on each sample and its location can be found in the Appendix (section 8; page 127).

Table 4. Sample number, site, map grid coordinates, lithology and size of boulders used for cosmogenic dating in the Lake Wellman study area.

Sample number (LW number in Appendix)	Grid reference	Lithology	Size (L×W×H) (cm)
Zone A			
23.1	156°54'35.758"E 79°55'0.404"S	Sandstone	12 × 8 × 5
23.2	156°54'43.355"E 79°55'0.901"S	Granite	12 × 8 × 5
24.1	156°54'11.142"E 79°55'20.247"S	Granite	1.2 × 1.6 × 0.5
24.2	156°53'55.03"E 79°55'17.449"S	Granite	2 × 2 × 1
25.1	156°55'23.586"E 79°55'11.265"S	Granite	1.3 × 0.9 × 0.5
25.2	156°55'28.302"E 79°55'13.316"S	Sandstone	1.3 × 1.0 × 0.5
Zone B			
2.1	156°52'2.144"E/79°55'53.806"S	Granite	8 × 5 × 3
2.2	156°52'2.144"E/79°55'53.806"S	Sandstone	12 × 12 × 10
9.1	156°49'6.91"E 79°56'25.927"S	Sandstone	2.6 × 2.9 × 1.3
9.3	156°48'48.976"E 79°56'25.585"S	Granite	1.3 × 1.7 × 0.5
15.1	156°47'54.204"E 79°55'17.809"S	Sandstone	1.1 × 1.6 × 1.9
11.1	156°46'34.189"E 79°56'41.995"S	Granite	10 × 15
Zone C			
12.1	156°44'3.524"E 79°53'18.538"S	Sandstone	1.8 × 1.1 × 0.9
12.2	156°43'50.028"E 79°53'18.887"S	Granite	1.8 × 2.1 × 0.9
13.2	156°45'26.649"E 79°53'25.73"S	Sandstone	1.8 × 2.1 × 1.0
13.3	156°45'12.572"E 79°53'24.899"S	Granite	1.6 × 1.6 × 0.9
14.2	156°45'31.079"E 79°53'25.886"S	Sandstone	24 × 60 × 51
18.1	156°46'1.183"E 79°53'29.847"S	Sandstone	2.9 ×1.8 × 2.0
18.3	156°46'0.997"E 79°53'30.7"S	Granite	1.8 × 0.8 × 1.1
20.1	156°48'6.714"E 79°53'37.465"S	Sandstone	2.8 × 1.8 × 1.3
20.3	156°48'9.444"E 79°53'48.017"S	Granite	1.5 × 1.1 × 0.6
21.1	156°49'8.192"E 79°53'51.297"S	Granite	0.8 × 0.9 × 0.9
21.2	156°49'10.11"E 79°53'54.718"S	Sandstone	1.8 × 0.8 × 0.6

4.5.2. Sample preparation

The grinding and acid washing procedure worked effectively for most of the rock samples and yielded a product suitable for cosmogenic dating. However, problems occurred with two very crucial samples from the large Moraine 5 ridge (samples 14.2 and 14.3). These samples were found to contain abnormally high levels of aluminium. This element is bonded chemically within the quartz crystal lattice, and additional acid washing was unsuccessful in reducing levels to the degree required for dating. Matter is lost during acid digestion, and with these two samples so much processing was required that insufficient material remained at the end. Data are therefore presented only for the samples that were successfully processed.

4.5.3. SED results

The exposure ages determined cosmogenically are presented in Table 4, showing the results for both the ^{10}Be and ^{26}Al isotope analyses. Although not all the results for the ^{10}Be and ^{26}Al dates agree perfectly for the same samples, it can be seen that in most cases there is a general correspondence between them. For instance, values for samples 12.1, 12.2, 20.3 and 25.2 are each within the error range for both nuclides, and so give acceptable dates. Sample 12.2 has clearly been exposed for a much longer period than sample 20.3 (Table 4). For accuracy and reliable interpretation, data were rejected if the two values for each sample did not agree. Therefore, besides samples 14.2 and 14.3 (see previous section), data were rejected from the following samples due to excessive variation between ^{10}Be and ^{26}Al values: 2.1, 9.3, 11.1, 15.1, and 18.3. Remaining data were accepted and plotted onto aerial photographs in order to reveal trends in age of exposure across the study area (Figure 69).

At zone C, in the upper valley area (Figure 11), there was a broad general trend of increasing age of exposure with altitude and distance from the present glacier (Figure 11). Ages ranged from around 33 ka B.P. at 900 m a.s.l., nearer to Lake Wellman (sample 21.1.), to ca. 400 ka B.P. (sample 12.2) towards the 1200 m a.s.l. contour line. Exceptions occurred with occasional younger dates that tended to contradict this trend (Figure 69). In some cases such discrepancies may have been caused by reburial of rocks for periods following first exposure, which has protected them from cosmic rays, resulting in artificially younger dates following retreat of the glacier.

Table 5. ^{10}Be and ^{26}Al cosmogenic isotope exposure ages for the Lake Wellman study area, Darwin Mountains, Antarctica.

Sample	Site	Altitude (m)	^{10}Be CONC	^{26}Al CONC	^{26}Al/^{10}Be RATIO	Scaling factor	Correction factor	^{10}Be min exposure age (ka)	^{26}Al min exposure age (ka)
11.1	B	1595	0.187	1.03	0.0185	4.995	5.250	882 ± 66	241 ± 20
09.1	B	1450	0.242	0.30	0.0392	4.457	4.684	2047 ± 199	1978 ± 365
09.3	B	1457	0.009	0.53	0.2465	4.625	4.711	1983 ± 204	396 ±37
02.1	B	1195	0.013	0.33	0.1824	3.590	3.806	76 ± 5	137 ± 12
02.2	B	1186	0.035	0.14	0.0798	3.440	3.778	22 ± 2	25 ± 3
15.1	B	1085	0.860	0.53	0.2309	3.297	3.469	604 ± 45	491 ± 48
24.1	A	844	0.497	1.05	0.8024	2.679	2.815	64 ± 4	51 ± 4
24.2	A	841	0.428	0.53	0.4752	2.720	2.808	3 ± 0	2 ± 0
23.1	A	801	0.648	0.53	0.987	2.624	2.709	1 ± 0	1 ± 1
23.2	A	799	0.574	0.58	1.2794	2.563	2.706	19 ± 1	16 ± 1
25.1	A	801	0.628	0.49	1.2155	2.579	2.710	1 ± 0	1 ± 0
25.2	A	794	2.772	0.30	1.6121	2.563	2.694	14 ± 1	16 ± 2
12.1	C	1099	1.206	2.11	0.5724	3.353	3.510	125 ± 10	115 ± 10
12.2	C	1104	3.540	0.13	0.8439	3.309	3.526	382 ± 25	340 ± 30
13.2	C	1056	6.047	0.66	1.6711	3.221	3.385	75 ± 5	77 ± 7

Sample	Zone	Altitude (m)	^{10}Be CONC	^{26}Al CONC	^{26}Al/^{10}Be RATIO	Scaling factor	Correction factor	^{10}Be min exposure age (ka B.P.)	^{26}Al min exposure age (ka B.P.)
13.3	C	1061	8.867	1.24	26.54	3.308	3.400	221 ± 15	157 ± 13
14.2	C	1064	2.077	0.43	13.84	3.243	3.408	400 ± 27	254 ± 24
18.1	C	1036	5.909	1.67	9.068	3.151	3.328	39 ± 3	37 ± 4
18.3	C	1050	0.385	1.62	7.87	3.189	3.368	178 ± 11	No value!
20.1	C	967	1.368	1.44	288.72	3.038	3.137	42 ± 3	46 ± 4
20.3	C	974	30.17	0.06	20.94	3.056	3.155	37 ± 2	34 ± 3
21.2	C	931	30.70	0.06	479.66	2.955	3.037	29 ± 2	31 ± 3
21.1	C	930	30.70	0.06	479.66	2.955	3.037	33 ± 2	34 ± 4

Altitude = elevation above sea level where samples were collected (governs the production rate of the ^{10}Be).

^{10}Be CONC = PPM concentration of ^{10}Be.

^{26}Al CONC = PPM concentration of ^{26}Al.

^{26}Al/^{10}Be ratio = the ratio of values of ^{26}Al/^{10}Be from which the amount of ^{10}Be per gram of quartz is calculated.

Scaling factor = combined scaling factor for altitude and latitude, including geomagnetic corrections.

Correction factor = corrects for horizon shielding and thickness, based on geometry of sample.

Min exposure age = the minimum age from the ^{10}Be and ^{26}Al isotopes, with degree of error.

The same general trend, as shown in the upper valley (zone C), was also present in the data from the two acceptable samples taken from the benched slope of zone B (Figure 11 and Figure 69, Figure 70). Here ages increased from values around 22 ka B.P. near the 1200 m a.s.l. contour (sample 2.2) to ca. 2 Ma B.P. towards the 1400 m a.s.l. contour (sample 9.1), with the same unexpected younger ages showing up possibly as a result of past disturbance.

Ages obtained with samples from the Hatherton Drift close to the present glacier edge near the lake shore (zone A, Figure 11) were all less than ca. 50 ka B.P. When data from rejected samples are excluded, the age range is reduced to less than ca. 20 ka (Figure 72).

The relationship between the ages determined cosmogenically in this study and previously identified glacial drifts (Bockheim et al., 1989) are shown in Figure 69 and Figure 70. These indicate that the Hatherton drift was deposited ca. 1-20 ka B.P., and the Britannia I and Britannia II drifts, between the period ca. 22-42 ka B.P. The upper age limits for the Isca and Danum drifts extend to ca. 400 ka B.P. Finally, rock samples taken outside the boundary of the Danum drift (Figure 69; zone B in Figure 11), gave an even greater exposure ages of ca. 2000 ka B.P. These conclusions ignore data from the samples that were rejected because of divergence between the two nuclide values. The ages determined by the SED values are generally older than those recorded by Bockheim et al. (1989), who used ^{14}C dating of algal deposits (Section 1.3.2). For instance, these authors aged the Hatherton drift at 5 ka B.P., and placed the Britannia II drift into the late Wisconsin period, about 12-24 ka B.P. or something like 20 ka later than that indicated by the SED data (approximately half the age determined by the SED results).

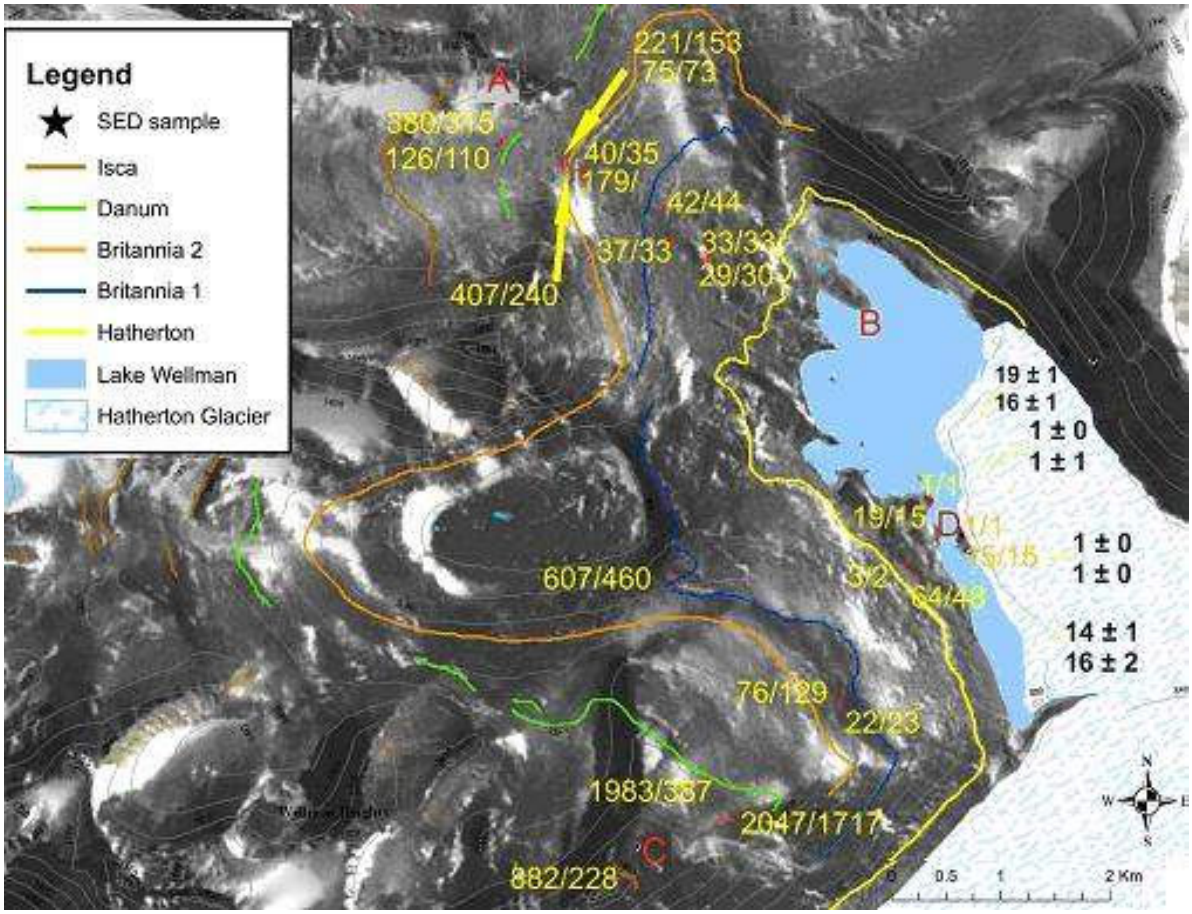

Figure 69. The SED results are indicated by the numbers, the upper in each pair being the ^{10}Be age and the lower the ^{26}Al age in ka B.P. The locations of previously mapped drifts are delineated by the coloured lines (after Bockheim et al., 1989). The locations of the cross sectional profiles in Figure 70 are indicated by red upper case letters (A-B, C-D).

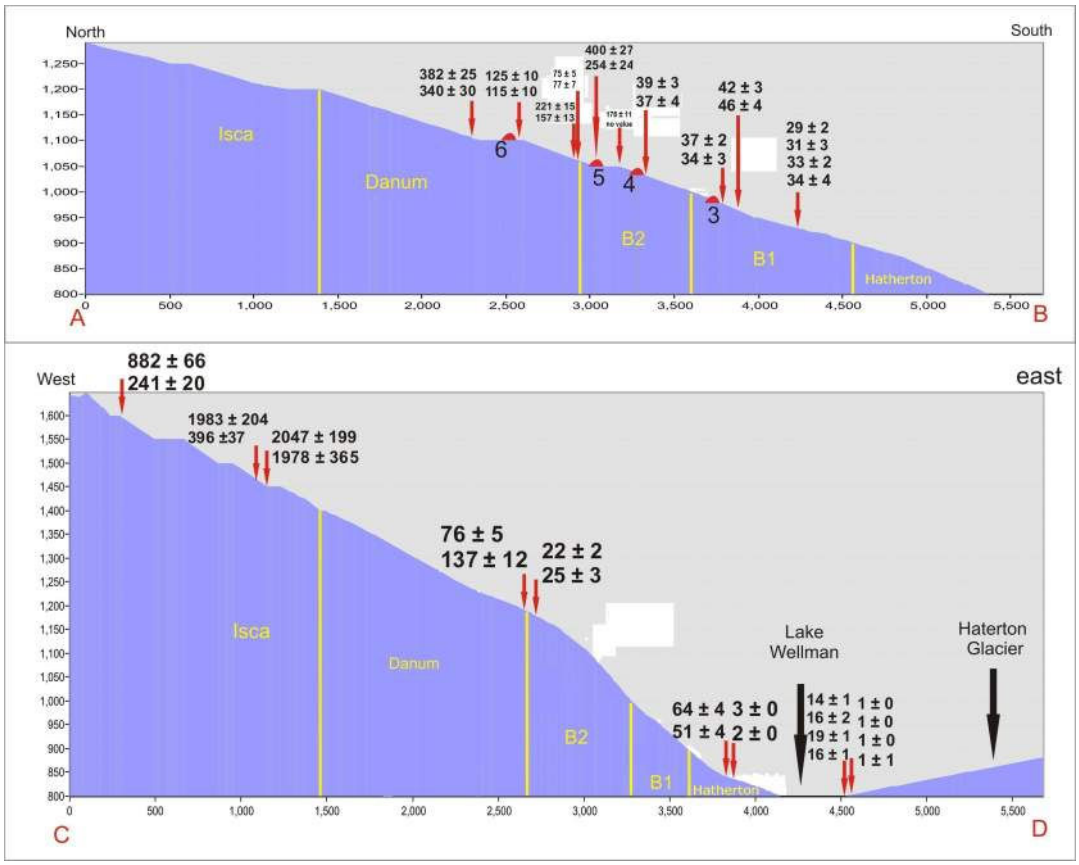

Figure 70. The SED results in relation to the locations of the previously mapped glacial drifts of Bockheim et al. (1989) (portrayed along the profiles A-B and C-D positions shown in Figure 69). Ages are presented in ka B.P. (the top value in each pair determined from the ^{10}Be nuclide and the lower from the ^{26}Al nuclide). Elevations and distances (vertical and horizontal axes) are in meters. B1 and B2 represent the respective Britannia I and II drifts, and Moraines 3-6 are shown as numbers in the A-B profile (top) Please note that the Britannia II drift and Danum drifts are at slightly higher elevations in the lower cross-section (C-D) because the ice was slightly thicker in this section of the valley.

Graphs of SED results by age and the elevation above the present Hatherton Glacier ice surface are shown in Figure 71. There is a clear trend of greater age at higher levels above the glacier surface.

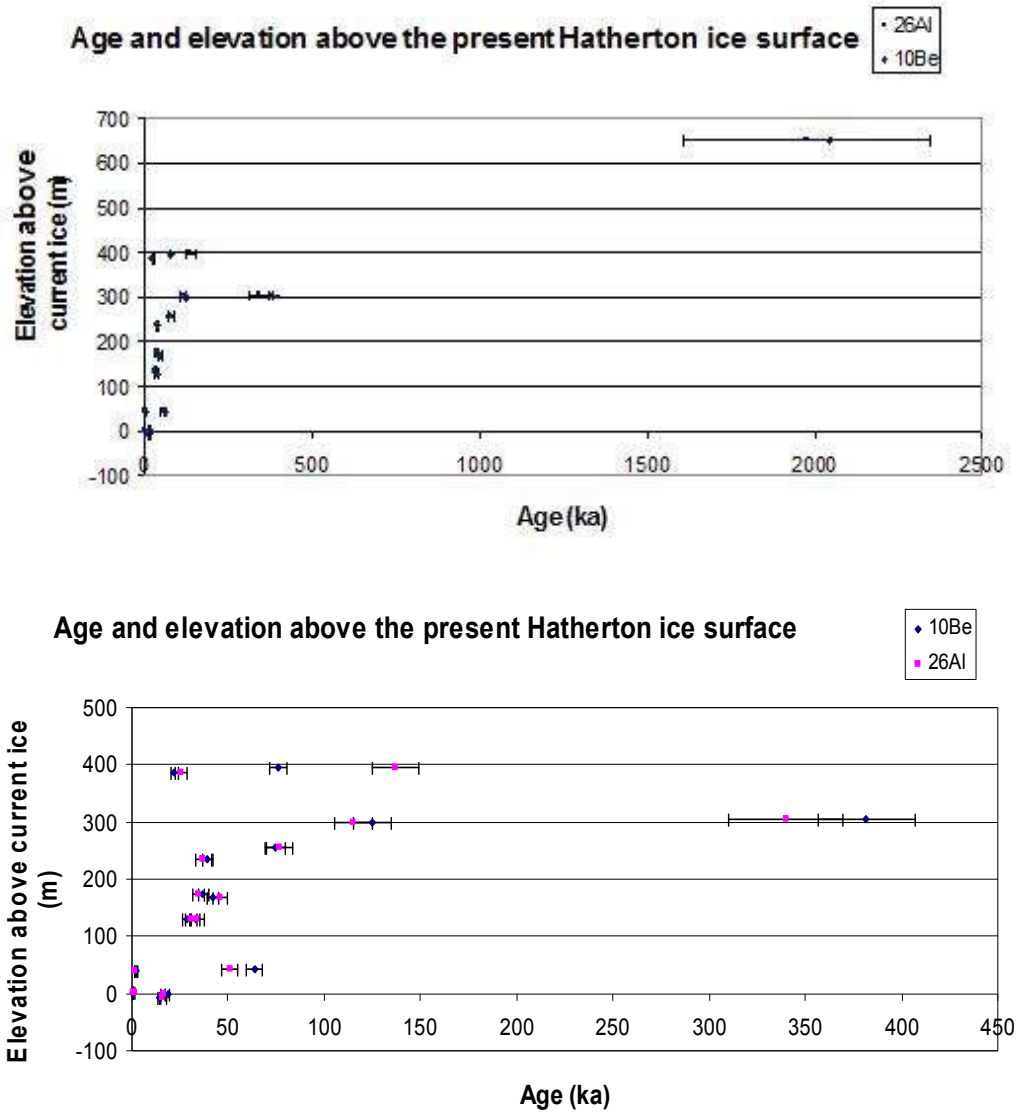

Figure 71. SED results for both the ^{10}Be and ^{26}Al nuclides plotted by age and elevation. Top, accepted data for all samples. Bottom, data from samples up to age 450 ka B.P., only (for increased resolution of data at lower end of age range).

5. Discussion

5.1. General

The Lake Wellman area was an ideal location to study the response of the Darwin-Hatherton outlet glaciers to climate fluctuations in the recent past. At its maximum prior to the LGM, the Hatherton Glacier was connected through the Lake Wellman valley to the Darwin Glacier, and reached its greatest ice elevation ca. 800 m (1600 m a.s.l.) higher than the present ice surface. The results from this study confirmed that the landscape has gradually become free from retreating ice in stages over the last two million years.

This research was the first time that the Surface Exposure Dating (SED) technique has been used in the Lake Wellman area. Samples for dating were collected with the specific aim of identifying the timing of the glacial recession before and subsequent to the LGM. The cosmogenic dates obtained indicated that the glacial drifts in the Lake Wellman area are older than was previously estimated. The SED results and the geomorphology mapping also pointed to the occurrence of fluctuations of the ice margins during the glacial retreat between ca. 40 and 30 ka B.P.

In this chapter, the results obtained from the study are considered in relation to the global perspective and their implications for climate change. The chapter first examines the field sedimentology results from different drifts and considers their implications. This is followed by a discussion of the cosmogenic dating and its interpretation. The chapter then considers and puts into perspective the ^{14}C ages of Bockheim et al. (1989) and examines the broader implications of the results, first in terms of the Lake Wellman area of the Darwin Mountains, and then more widely in relation to the Ross Ice Shelf. Finally, a summary of the conclusions is provided.

5.2. Sedimentology interpretations

This section discusses the sedimentology results presented in Chapter 4. Trends in these data are considered in the context of the different geomorphology features and the way they were distributed in the Lake Wellman area. It is assumed that the

information obtained from the different drifts is representative of the overall field area studied.

5.3. Angularity transects

As boulders are transported within glacial ice they become worn and smoothed through friction and abrasion. The relative shape, roundness and texture effects the formation of sedimentary particles (Benn and Ballantyne, 1993). The degree of rounding is proportional to the duration of transportation (Lindsey et al., 2007), so that the longer they are in the glacier the greater the rounding. However, clasts are also constantly being broken apart during transport, increasing their angularity. Therefore, the degree of rounding reaches a maximum determined by the period between crushing events and the force applied (Bennett and Glasser, 1997). Debris will remain angular if it is carried on the ice surface (supra-glacial transport). This is because these rocks do not experience the crushing and grinding forces within the ice. The results from the angularity transects are discussed below for each rock lithology.

5.3.1. Angularity of dolerite

Examination of the dolerite angularity plot suggested a significant trend for increasing roundness with elevation (Figure 60). Greater percentages of sub-rounded clasts occurred between 1000 and 1200 m a.s.l. and there were correspondingly reduced percentages of sub-angular clasts over the same range. Clasts tended to be less rounded between 800 and 1000 m a.s.l. However, this trend should be considered in relation to the distribution of the different drifts at different elevations in the valley (Bockheim et al., 1989).

Transects at 1021 and 1047 m a.s.l. were located in the Britannia II drift of Bockheim et al. (1989), and those above 1100 m a.s.l. in the Danum and Isca drifts (Figure 70). Clasts in these drifts showed a stronger pattern of roundness (50% or more of clasts were sub-rounded) than those in the lower Britannia I drift which lay between 900 m a.s.l. and 1000 m a.s.l., bounded at its upper limit by Moraine 3. Only

ca. 20% of clasts in the Britannia I drift were sub-rounded, where as ca. 60% were sub-angular.

The transects in the Britannia II drift (1000-1100 m a.s.l.) were placed just below Moraine 5. It is one hypothesis that Moraine 5 was a re-advance moraine that overran moraine 4. The resultant reworking of the dolerite clasts at this location would explain their reduced angularity. The transects in the Danum and Isca drifts lay above Moraine 5 (Figure 70).

The transects below 900 m a.s.l. were located within the Hatherton drift (Figure 70), the youngest moraine in the study area. The angularity in this drift was more variable, ranging from sub-angular (ca. 60% of clasts) at the 801 m a.s.l. transect to sub-rounded (ca. 60% of clasts) at the 841 m a.s.l. transect. This latter transect was situated just below Moraine 2, which represents a still-stand period that was followed by retreat. This is discussed further in the context of the SED results later in this chapter. The overall angularity pattern at different elevations for dolerite clasts was supported by similar trends with the sandstone and gabbro clasts (see Sections 5.3.2 and 5.3.3, below).

5.3.2. Angularity of sandstone

Sandstone clasts were very angular (more than 50% were sub-angular) at elevations below 1000 m a.s.l. (Hatherton and Britannia I drifts; Figure 61). Within the Britannia I drift, sandstone there was less angularity in the lower 930 m a.s.l. transect than at 967 m a.s.l., where all clasts were sub-angular. Such a high concentration of sub-angular material suggests it was very young and had not been transported a great distance form the source. Or, alternatively, it may possibly have been carried as supra-glacial material.

The transect lines at elevations 1021 m a.s.l. and 1047 m a.s.l. (Britannia II drift) (Figure 70) formed a distinct group dominated by sub-rounded (ca. 60% of clasts) and some sub-angular clasts (ca. 40% of clasts). The upper boundary of the Britannia II drift was considered to mark the LGM limit by Bockheim et al. (1989), and the transect data support a change in the drift characteristics at this location. Sandstone

clasts in the transects above 1100 m a.s.l. also formed a distinctive group with greater angularity than in the Britannia II drift transects. While the percentage of sub-angular rocks was comparable to that in the Britannia II drift, an additional 25 - 45% of clasts were classed as angular.

5.3.3. Angularity of gabbro

Although the differences between transects were not significant for the gabbro angularity (Figure 62), clasts in the transects at 1021 m a.s.l. and 1047 m a.s.l. elevations (Britannia II drift) stood out as being largely sub-rounded (ca. 70-80% of clasts). As noted previously, this drift is bounded at its upper limit by a large asymmetrical re-advance ridge (Moraine 5; Figure 70). The change to predominately sub-rounded clasts in this drift supports the re-advance hypothesis (section 5.3.1). At this position, it appears there was only locally-derived material transported during the re-advance. This is supported by the result that no clasts of granite were present in Moraine 5.

Above 1100 m a.s.l. rounded and sub-rounded clasts made ca. 70% or more of all gabbro material. However, angularity was greater below 1000 m a.s.l., with sub-angular and sub-rounded boulders present in approximately equal proportions. These categories made up nearly all clasts in transects on the younger Hatherton drift. When compared between lithologies, there tended to be greater proportions of rounded gabbro clasts compared to those of sandstone and dolerite at the same elevation. One explanation is that gabbro is more resistant than the other lithologies to erosion.

5.3.4. Angularity conclusion

There was a broad trend for reduced angularity and increased roundness in transects at greater elevations. However, angularity also contrasted noticeably between transects on adjacent drifts. Therefore, clast angularity probably reflects the way each of the drifts has developed and formed in the past as much as its elevation. For instance, the angularity of clasts in the vicinity of Moraine 5 may result from a reworking of rocks caused by a temporary re-advancement of the glacial ice.

5.4. Weathering transects

The degree of weathering was also evaluated using clasts in the same transects as those used for angularity. These were placed across a central part of the Lake Wellman area which displayed numerous moraine ridges. Evaluation was subjective, so to ensure consistency all data were assessed by one person. The degree of weathering depends on both the time the clasts have been exposed and their type of lithology. Certain lithologies weather faster than others. Boulders also become more weathered with exposure time. Since it was assumed that moraine drifts were older at greater distances (and elevations) from the current glacial margin, it was expected that boulders should become increasingly weathered at higher elevations.

A difficulty emerged during the evaluation of the weathering data that partly affected their interpretation. The assessment scale used to estimate the degree of weathering varied from fresh (little weathering), through light and then moderate, to highly iron stained. The Lake Wellman area had a large proportion of highly iron stained boulders throughout a range of elevations, indicating that the level of iron staining did not reflect the rate of weathering. This issue was therefore taken into account during interpretation of the weathering results for each of the clast lithologies.

5.4.1. Weathering of dolerite

The data for dolerite clasts showed a significant trend for less weathering at lower elevations, as expected for boulders that have been exposed for shorter periods (Figure 63). Thus, the least weathered boulders were present mainly in the transects below 900 m a.s.l. within the Hatherton drift (Figure 70). Since this represented the youngest drift in the sequence it would be expected to have freshly weathered material present. However, there were also boulders in this drift that showed moderate and high weathering. Also, clasts at all elevations showed a moderate to high degree of iron staining, even to some extent in the Hatherton drift. It is therefore likely that this moraine material has been affected by rapid iron staining, or re-worked material, which increased the difficulty of assessing the weathering patterns.

5.4.2. Weathering of sandstone

The level of weathering varied more significantly with transect position for sandstone clasts than for dolerite (Figure 64). A high proportion of fresh, lightly weathered boulders (ca. 80% of clasts) dominated the transects at elevations below 900 m a.s.l. within the Hatherton drift of Bockheim et al. (1989). Moderately weathered clasts predominated in the transect at 930 m a.s.l. (80% of clasts) when compared to the transect at 967 m a.s.l., at a higher elevation, both within the Britannia I drift (Figure 70). This pattern of a high proportion of moderately stained boulders at 930 m a.s.l., and a reduced level of weathering but a higher degree of iron staining at 967 m a.s.l., is repeated for the dolerite and gabbro clasts. The consistency of this pattern across different lithologies suggests that the weathering data are reliable and not greatly affected by the iron staining. The lower transect is near the boundary between the Hatherton and the Britannia I drifts which occurs at ca. 900 m a.s.l. The upper limit of the Britannia I drift is marked by Moraine 3 (Bockheim et al., 1989). This represents a still stand period which will be discussed in context of the SED results in a following section (page 111).

Between elevations 1000-1100 m a.s.l., there appears to be a slightly greater degree of weathering at the higher elevation transect (1047 m a.s.l.). Fresh, unweathered clasts (ca. 10%) are only present at the lower transect position (1021 m a.s.l.), while at the higher elevation there is twice the proportion of moderately weathered clasts (but, conversely, no iron staining, as in the lower position). The upper transect is located just below Moraine 5, and the greater proportion of light-weathered boulders at this position may be explained by the re-advance that created this asymmetrical moraine. The dolerite and gabbro boulders are more resistant to crushing, and do not show the increase in lightly weathered boulder so clearly. The uppermost transects situated at 1110 m and 1194 m a.s.l. elevations displayed a shift from 100 % moderately weathered boulders to 50 % lightly and 50 % highly weathered boulders. The lithology proportions for clasts in these two transect locations were similar (Figure 64), so it is difficult to explain the contrast in levels of weathering between them.

5.4.3. Weathering of gabbro

Trends between transects for weathering of gabbro clasts were largely unclear and there was no significant pattern (Figure 65). The transects below 900 m a.s.l. within the Hatherton drift show a moderate degree of weathering (50% or more of clasts), which is a little unexpected for the youngest material in the sequence. The lower level of weathering of clasts at 967 m a.s.l. is consistent with the trend at this elevation for diorite and sandstone, as previously noted. From positions at elevations between, and including, 967 m a.s.l. and 1110 m a.s.l., there appears to be a steady increase in the proportion of moderately weathered clasts, generally consistent with a greater period of exposure. Iron-stained clasts were moderately prevalent throughout most of the transects. Since iron staining occurs more rapidly, this may have hampered assessment of the degree of weathering for the gabbro lithology, making the patterns less clear.

5.4.4. Weathering conclusion

Evaluation of the degree of weathering of clasts was hindered by the rapid iron staining of boulders that were not necessarily greatly eroded. Despite this, for some lithologies there appeared to be a broad pattern of increased weathering with higher elevation and hence greater time of exposure. However, this apparent trend was modified by fluctuations of the glacier margin and associated disturbance, burial and re-exposure. For instance, there was a reduced level of clast weathering consistent for all lithologies in the 967 m a.s.l. elevation transect, near Moraine 3 of Bockheim et al. (1989), suggesting temporary coverage in the past that reduced the time exposed to weathering.

The pattern of weathering does not conflict with the uniformity in proportions of different lithology types observed over the full range of elevations (Section 4.3.1). The data in that section were based on numbers of rocks in each type, regardless of degree of weathering. Perhaps the regularity between transect elevations simply reflects the general proportion of lithology types present in the wider area of the Darwin Mountains.

5.5. Clast dimensions

The relative size of boulders in moraine drifts reflects their origin, the nature of their lithology type, and the period they have been subjected to crushing forces within the glacier ice. Therefore measurement of clast dimensions provides another means of comparing different drifts, besides angularity, weathering, and clast lithology. In this study, clasts were measured at regular intervals along each transect line and their dimensions along all three axes (a, b and c) were recorded. The results matched well to the geomorphology boundaries that are represented by Moraines 1 – 5 (Figure 22, page 43 and Figure 70), and the transect results (page 82).

When considering rocks of all lithologies, there were distinct differences between clast sizes in the different drifts (Figure 66). In the Hatherton drift, below 900 m a.s.l., clasts averaged less than 40 cm in length, with slightly larger and narrower boulders present at the upper transect just below Moraine 2 (Hatherton drift). A similar pattern was found in the drifts between Moraine 2 and Moraine 3 (mainly in the Britannia I drift between elevations 900 m a.s.l. and 1000 m a.s.l.; Bockheim et al., 1989). Here the rocks in the upper transect (967 m a.s.l.), just below Moraine 3, were slightly larger (and also broader), averaging between 40 and 50 cm in length.

The transects located within the Britannia II drift at elevations of 1021 m and 1047 m a.s.l. displayed a large significant increase in size in comparison with the Britannia I drift clasts, reflecting changing glacial dynamics and the process of debris entrainment. This pattern again corresponds with changes during a possible re-advance of the ice which formed Moraine 5. There is granite clasts present in the drifts up-glacier and down-glacier of Moraine 5, however no granite clasts are present within Moraine 5; this suggests its source material was locally derived. In the Danum drift position, at an elevation of 1110 m a.s.l., clasts were reduced in size confirming the different nature of this moraine drift described by Bockheim et al. (1989). Clasts at the transect at elevation 1194 m a.s.l. were still smaller, supporting the identity of a distinct Isca drift. Clast dimensions for individual lithologies supported the different nature of each of these drifts, although patterns for different lithologies were not always the same. For instance, gabbro boulders tended to be smaller in the region between the Britannia I and II drifts (elevations 967 m and 1021

m a.s.l.), but larger in the Danum and Isca drift positions (elevations 1110 m and 1194 m a.s.l.; Figure 67, Figure 70).

However, the generally smaller size of the majority of the clasts within the Isca drift suggests that they were transported for a longer time in the ice than those measured at other elevations, or alternatively have been derived from a different source location. The longer the clast is in the ice the smaller its dimensions will become. This implies that the material above Moraine 5 has been transported for greater distance than the material below this position. At mid elevations (950-1050 m a.s.l.) rocks of sandstone, diorite and granite are all at their largest. This supports the idea of a glacier re-advance in the middle level of the field bringing up new material.

5.6. Surface hardness

The Schmidt hammer was used to supplement the weathering data by providing a more objective test of surface erosion. Normally, a tough rind forms around a weathering boulder and the surface becomes harder. Accordingly, the Schmidt hammer should display an increasing rebound on rocks that have weathered over longer periods. Thus, it can also be used as a relative age dating tool.

Results from the study in the Lake Wellman area are shown in (Figure 58; Figure 59). For granite clasts, the gradual decreasing rebound with increasing elevation indicated a distinct aging, and therefore longer exposure time with elevation and distance from the present glacier. The results for the granite tests suggest that greater weathering leads to a lower rebound value. However, for sandstone there was no trend with altitude. It is possible that the sandstone boulders have been weathering by spalling, whereby the outer weathered layer periodically peels or flakes away, continually exposing a fresh surface. This affects the interpretation of the Schmidt hammer results. Sandstone boulders that become spalled give the appearance of a fresh surface that has not been exposed for a long duration. As no weathering rind is forming the outer surface does not become harder, and the Schmidt hammer rebound value does not increase with time or elevation. Sandstone rocks were present in comparatively low proportions at all elevations.

5.7. Striations

Striation data provide clues as to the degree of weathering and therefore the period of exposure, and also indicate whether the parent glacier was warm- or cold-based at the time (ie. whether-or-not the parent glacier was frozen to the base rock). Striated clasts do not however provide information about the direction of ice movement. Striations were more prominent and easily identified on the less weathered and more angular clasts found at lower elevations. They occurred in great concentrations on the surface of boulders of this type located in the Hatherton Drift. This confirmed the younger age of the low elevation drifts, since their presence meant there had been less time for exposure to weathering. It also indicated that the glacier was warm-based at this time, since cold-based ice does not form striations to the same extent (Atkins and Dickinson, 2007).

5.8. Polygonal pattern ground

The expansion and contraction of freezing and thawing water within soil and finer moraine debris free from glacial ice leads to selective movement or creep, which gradually sorts and separates out the different sized particles (Washburn, 1973). During the winter cold temperatures cause contraction in the permafrost resulting in the formation of cracks up to 5 cm wide and several metres deep (Berg and Black, 1966). These are filled with melt water and sand in the summer, and repetition of this cycle causes the polygons to form (Berg and Black, 1966). This becomes apparent in the form of a regular geometric pattern over extensive areas, such as the polygonal pattern ground that occurs over much of the Lake Wellman area (Figure 68). It has been found that the diameter of the polygons increases over time (Mellon et al., 2007), enabling differentiation of the relative ages, and so in theory providing another method of estimating the maturities of the associated moraine drifts. The polygonal pattern ground in the Lake Wellman area was mapped and divided into three groups of small (< 10 m), medium (10 - 20 m) and large (>20 m) diameters. It was found that the polygon pattern ground followed two patterns of distribution, each in a different part of the study area. The first trend was for a distinct east - west configuration in which the polygons decreased to a small size at a high elevation close to the current margin of the Midnight Plateau.

There are two possible explanations for the location of smaller polygons close to the margins of glacier ice flowing from the Midnight Plateau. This ice is likely to have fluctuated in extent, possibly advancing further into the valley at some period in the more recent past. This would result in a reduced moraine exposure time and hence smaller polygons. The second possible reason for these small diameter polygons is their relatively close proximity to the underlying bedrock (Washburn, 1973; Mellon et al., 2007). It has been suggest that adjoining bedrock will interfere with and reduce the rate of development of polygonal pattern ground.

The second trend was a north - south orientation in the polygon size distribution in a different part of the study area. Here, large polygons (> 20 m diameter) located between 1400 m and 1300 m a.s.l. elevation, decreased into medium-sized polygons (10-20 m diameter) from ca. 1180 m a.s.l. elevation down to lake level. The transition point occurred along boundary of Moraine 5, and this would support the greater age of the drifts above this position. Their elevation would put the larger polygon area into the Danum drift zone of Bockheim et al. (1989), and the SED results suggested that the age of this moraine is > 75 ka B.P.. The large diameter polygons were additionally concentrated on the western side of the field area suggesting that their size may be associated with large scale ice movement from the Hatherton Glacier.

5.9. Surface Exposure Dating (SED)

Cosmogenic Surface Exposure Dating (SED) was used to date samples of rocks collected from different locations in order to supplement the data recorded in the field. The results from both approaches were compared in order to broaden our knowledge of the way the Hatherton Glacier has fluctuated in the past and to better understand ice movement in this part of Antarctica in response to effects of changing global climate. Carefully selected rock samples taken from a series of different moraines in the Lake Wellman area were processed in the university laboratories in Christchurch, and dated at the cosmogenic facility at ANSTO in Sydney, Australia.

The SED technique was used in the Lake Wellman area in order to extend the information obtained previously by Bockheim et al. (1989) using the ^{14}C dating

method, which has several limitations. Firstly the ^{14}C method is restricted to approximately the last 50 ka years B.P., so that older samples cannot be dated in this way. Secondly, the application of the ^{14}C method to algal remains from former pond deposits (as done by Bockheim et al., 1989) provides only a minimum age for each drift surface. This is because the time between recession of glacial ice and subsequent pond formation is not known, and the date when the drift became exposed by the retreating ice may be older than that determined from algal dating.

5.9.1. Factors affecting the SED technique

Bierman et al. (1999) demonstrated that care is needed in interpreting the ages calculated using single nuclides by the SED procedure in the light of the processes of erosion and reburial by soil, rocks, snow or ice. Any unrecognized reburial which for a while shields the rock from cosmic radiation, so causing nuclide production to temporarily cease, will result in an unmeasured reduction in the amount of a nuclide due to its natural decay (Beirman et al., 1999). This will lead to underestimation, giving rise to a minimum value for the true age at which it was first exposed. Other processes which may cause the SED age to appear younger than expected include rolling, exhumation, and freezing and thawing. On the other hand, if a boulder previously exposed to cosmic radiation is engulfed by glacial ice before there has been sufficient surface erosion to remove existing nuclides then the date from when it is re-exposed will be overestimated due to the presence of the inherited nuclides. Great care is therefore necessary in determining reliable exposure ages using the SED procedure.

The ratio of the concentrations of ^{26}Al and ^{10}Be provides an indication of possible reburial. Values normally encountered vary consistently, as ^{26}Al decays about twice as fast as ^{10}Be. However, a period of reburial will cause a greater loss of this nuclide, shifting the ratio in favour of the ^{10}Be. Questionable values can therefore be checked by graphing the curve of this ratio against the ^{10}Be concentration.

The SED technique is costly, and the amount of work required restricts the number of samples that can be prepared for dating. In addition, there was a limit on the quantity of material that could be transported from the Lake Wellman study area,

placing a constraint on the number of collections that could be made in the field. It was therefore necessary to ensure that the sample points were well placed and distributed so as to give good coverage of the drifts at more than one location.

5.10. Interpretation of SED chronology

The SED project in the Lake Wellman area yielded a reasonably consistent pattern of ages. Despite some irregularities, there was an overall pattern of increasing age with elevation and distance from the current ice margin (Figure 69, Figure 70, Figure 71). This trend indicated a broad glacial recession with time, with fluctuations and temporary advances within the general retreat.

An unexpected outcome from this study was that some of the samples returned ages significantly older than those determined in the same relative drift positions by Bockheim et al. (1989) using ^{14}C dating of blue-green algae from former lakes associated with these drifts. Nevertheless, the consistency in the data indicates that some of the Lake Wellman drifts are in fact much older than was previously thought, and there appears to be no reason to doubt this conclusion.

In this section the SED data are discussed in more detail, in relation to the locations of the samples from which they were obtained (Figure 69; Figure 70; section 4.5.3). The ^{10}Be ages are considered first, because this nuclide is the primary element for determining the exposure period. The ^{26}Al ages are dealt with secondarily, as a check on the reliability of the ^{10}Be age or to judge if there has been any prior exposure (overestimation) or burial (underestimation; see previous section). Where there was a lack of correspondence between each of the two values, then other factors that may have influenced the result were considered. Also, if there was any reason to doubt the authenticity of the clast sample, itself, it was discounted for the purposes of interpretation.

The oldest SED result in the study was obtained from sample 9.1 collected on the upper benches south west of Lake Wellman, in an area (SED Site 2; Zone B, Figure 11) that was not previously dated by Bockheim et al. (1989). Two other samples in the same area (9.3 and 11.1) each gave inconsistent ^{10}Be and ^{26}Al ages, and were

discounted. The ages obtained for sample 9.1 were 2047 ± 199 ka B.P. for ^{10}Be and 1978 ± 365 ka B.P. for ^{26}Al (Figure 69; page 96). The consistency between the two values implies that they are reliable, and indicates that they were not affected by prior inheritance of nuclides. Collected at ca. 1400 m a.s.l. (Danum drift; Figure 70), sample 9.1 was almost the highest elevation sample collected in the study area. The highest was the rejected sample 11.1 taken from a large, granite erratic at an altitude of 1590 m a.s.l. The respective ^{10}Be/^{26}Al ages determined for the rejected samples were 882 ± 66/241 ± 20 ka B.P. (sample 11.1) and 1983 ± 204/ 396 ±37 ka B.P. (sample 9.3), suggesting that these samples may have experienced reburial following exposure from the retreating glacier. On the other hand, the ^{10}Be value of 1983 ka B.P. for sample 9.3 is comparable to that for nearby sample 9.1, suggesting it may be genuine and the ^{26}Al result faulty.

Further down the slope, at elevations between 1195 and 1186 m a.s.l., two samples (samples 2.1 and 2.2) were collected within 10 m of one another and a third (sample 15.1) was taken off to one side from a large sandstone boulder balanced on a dolerite rock. Sample 2.2 was the highest in this group, being a sandstone clast perched on a dolerite slab close to the moraine surface level within the Britannia II drift zone (Figure 11, page 26), while sample 2.1 was taken from a large granite erratic. Two of the three samples are rejected because of abnormally high aluminium concentrations and a lack of consistency between the ^{10}Be and ^{26}Al dates, these being 604 ± 45/ 491 ± 48 Ka B.P. (sample 15.1) and 76 ± 5/137 ± 12 ka B.P. (sample 2.1). However, the corresponding values for sample 2.2 (22 ± 2/ 25 ± 3 ka B.P.) were consistent and therefore acceptable (Figure 69).

At the base of this slope a cluster of samples was taken from around the edge of Lake Wellman, all within the youngest Hatherton drift moraine (SED site 1; Zone A, Figure 11). These were samples 24.1 and 24.2, just on the slope at an elevation of ca. 840 m a.s.l.; samples 23.1 and 23.2, collected at the same elevation from the apex of Moraine 2; and samples 25.1 and 25.2, located across a narrow portion of the lake at an elevation of between 794 m and 801 m a.s.l. within Moraine 1 next to the present glacier. All these samples gave consistent ^{10}Be/^{26}Al ages except sample 24.1 (64 ± 4/ 51 ± 4 ka B.P.), which was therefore rejected (Figure 69). The difference between the two values for sample 24.1 is not marked, but the clast that the sample was taken

from appears to have been transported into position by glacial ice from elsewhere. Ages for the other samples were 3 ± 0/ 2 ± 0 ka B.P. (sample 24.2), 1 ± 0/1 ± 0 ka B.P. (sample 25.1), 14 ± 1/16 ± 2 ka B.P. (sample 25.2), 1 ± 0/1 ± 1 ka B.P. (sample 23.1), and 19 ± 1/16 ± 1 ka B.P. (sample 23.2). These samples from the youngest drift, nearest the present glacier, were all less than 20 ka in age, and three were dated 3 ka or less. Even so, it is interesting that the ages for samples 25.1 and 25.2, which were collected within 20 m of one another, were significantly different. Sample 25.1 was partially removed from the end of a large, weathered, striated, sandstone boulder. It is therefore possible that its age has been underestimated if it was shaded from full radiation exposure.

The third group of samples (Site 3; Zone C, Figure 11) were taken to the northwest of Lake Wellman, from an altitudinal sequence that crossed Moraines 3, 4, and 5, and which spanned the Britannia I and Britannia II drifts of Bockheim et al. (1989). The SED results in this location provided the best sequence of dates from this study (Figure 69). Over a range of elevations decreasing from 1064 m to 900 m a.s.l. below Moraine 5, these samples gave respective $^{10}Be/^{26}Al$ ages of 39 ± 3/37 ± 4 ka B.P. (sample 18.1), 42 ± 3/46 ± 4 ka B.P. (sample 20.1), 37 ± 2/34 ± 3 ka B.P. (sample 20.3), 29 ± 2/31 ± 3 ka B.P. (sample 21.2), and 33 ± 2/34 ± 4 ka B.P. (sample 21.1). Only one sample is rejected, sample 18.3 (^{10}Be age, 178 ± 11 ka B.P.), as it failed to return an ^{26}Al age. So, over this sequence the ^{10}Be ages ranged between 42 ka and 29 ka B.P. This sequence is consistent with the geomorphology, and suggests that the glacier retreated down the slope over a period of 13 thousand years after a temporary re-advance that created Moraine 5 prior to 42 ka B.P..

Above this sequence, three samples were collected for dating from the apex of Moraine 5, at the upper margin of the Britannia II drift, because this was recognised as a significant feature to aid in the interpretation of past glacier movement. However, two of these samples (samples 13.2 and 13.3) failed during the first stage of the laboratory processing as the aluminium concentrations could not be brought below the 500 ppm threshold required to ensure a reliable date. It is speculated that the aluminium atoms were bound tightly within the quartz lattice, making removal impossible. Sample 14.2 was processed successfully, but unfortunately, the $^{10}Be/^{26}Al$ ages (400 ± 27/254 ± 24 ka B.P.) were not consistent, and so were also rejected.

Even so, the values obtained suggest that Moraine 5 is older than the Britannia I and II drifts below it, which tends to support the concept that it was formed by a temporary re-advance before the subsequent retreat of the ice. The alternative is that Moraine 5 is bit older than 40 ka B.P., as this was the oldest SED result from the top of the Britannia II drift. Furthermore the polygonal pattern ground observed on the Britannia II and Danum drifts, below and above Moraine 5, respectively, was not seen within Moraine 5, itself. This may indicate the action of different thermal properties between the ground moraine and the moraine ridge.

Consistent with this interpretation, the two samples (samples 12.1 and 12.2) taken above Moraine 5 at an altitude around 1200 m a.s.l. returned much older $^{10}Be/^{26}Al$ dates of 125 ± 10/115 ± 10 ka B.P. and 382 ± 25/340 ± 30 ka B.P., respectively (Figure 69). These values appear to indicate the ages of the respective Danum and the Isca drifts previously identified by Bockheim et al. (1989). However, in the upper slopes of the study area there was no distinctive change in the ground moraine appearance or geomorphology features which would have helped in distinguishing a boundary between the different drifts (refer earlier field results). However, the SED results have helped to indicate an approximate time frame for these upper drifts, and have shown that they are much older than the sequence below Moraine 5.

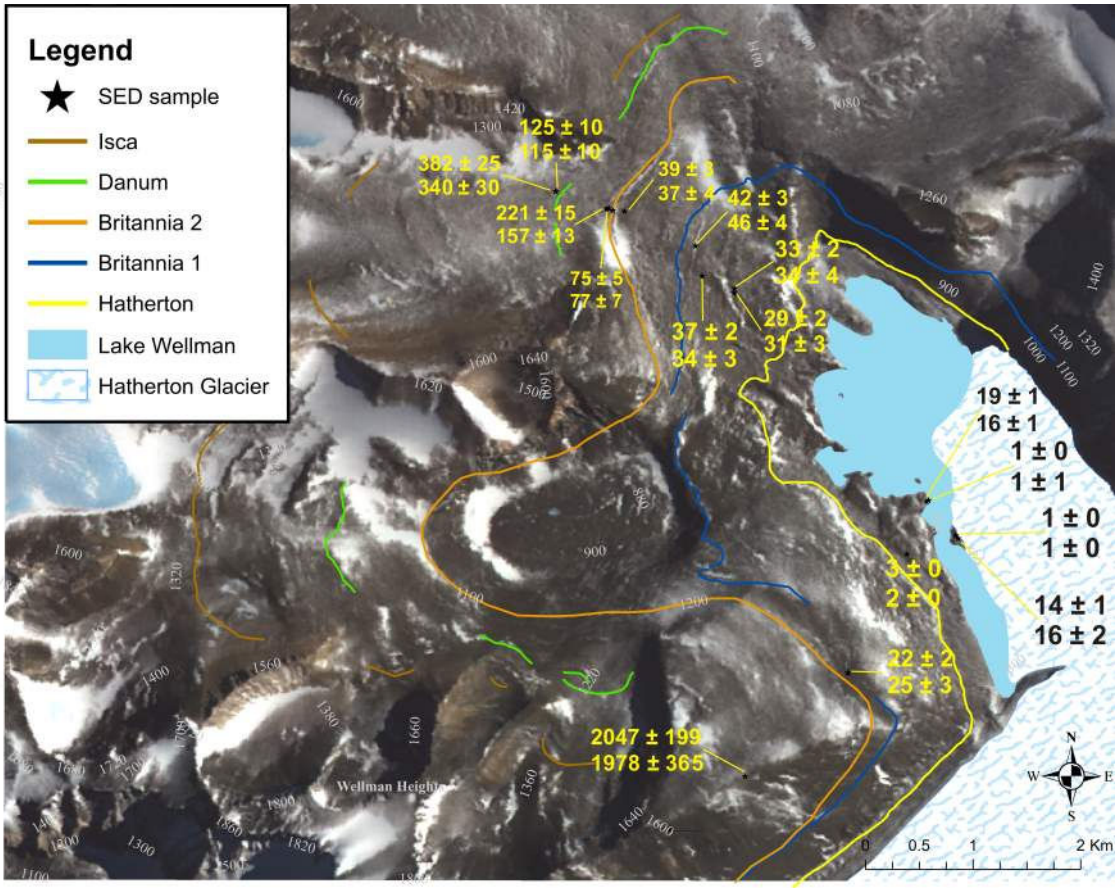

Figure 72. Final SED results. Discordant ages have removed from the map as discussed in the sections above. The location of Bockheims drifts are represented by the coloured lines; Britannia (yellow), Britannia I (blue), Britannia II (orange), Danum (green), and Isca (brown).

5.11. Previous research

Figure 72 shows the distribution of the sample positions where the SED dates are accepted as reliable, in order to assist in the interpretation of past ice movement in the Lake Wellman study area. Bockheim et al. (1989) used ^{14}C dating to derive ages for the Lake Wellman drifts. They determined the Hatherton drift to be early Holocene (ie. up to ca. 5 ka B.P.), the Britannia drifts as late Wisconsin (ie. ca. 16-20 ka B.P.), and the Danum drift as marine oxygen isotope stage 6 (MIS 6; ie. 130-200 ka B.P.), and suggested from other evidence that this last drift could be ca. 200 ka in age. These ranges for the older Danum and the younger Hatherton drifts appear broadly comparable to those obtained for the SED data, which, however, imply that the ^{14}C dates may to some degree be underestimated. Data obtained in this study

indicate ages for the Danum drift of 125/115 ka or 382/340 ka B.P., which span the ^{14}C value. SED dates for samples from the Hatherton drift ranged 1-3 Ka B.P., but with two at 14/16 and 19/16 ka B.P., significantly older than the upper limit of Bockheim et al. (1989). These authors suggested that the undifferentiated Isca drifts at higher elevations could be early Pliocene (ie. approaching 2 Ma B.P.), which is also within the approximate range of the oldest study SED date of 2047/1978 ka B.P. at ca. 1400 m a.s.l. The finding of a large granite boulder at an elevation of 1595 m a.s.l. provided an indication of the maximum extent of ice, and was clear evidence it had reached a maximum elevation 795 metre higher than the present glacier.

However, for the intermediate Britannia I and Britannia II drifts, the SED age ranges were substantially greater than those derived by Bockheim et al. (1989) using ^{14}C dating. These authors allocated a period of ca. 24-12ka for these drifts, whereas the SED dates obtained in this study ranged between 42-29 ka. As previously noted, the SED dates at this position appear reliable, being consistent for the ^{10}Be and ^{26}Al dates within each sample and forming a coherent set between samples. There is no reason to assume that these samples appear older because they have carried nuclides inherited from an earlier period of exposure.

The field results from this study do agree with the conclusions of Bockheim et al. (1989) with respect to the differentiation of the various geomorphology drift sequences and their boundaries. There were distinct differences between drifts in boulder angularity and weathering. This is also endorsed by the distribution trend for the polygonal pattern ground, which supports the concept of a much older and elevated glacier elevation around 2000 ka B.P. The SED data and field results from the Britannia drifts between 1064 m and 900 m a.s.l. also match, and taken together bear out the suggestion that Moraine 5 is a re-advance moraine formed as the temporarily expanding glacier overran the older Moraine 4, as discussed in the previous section. The asymmetrical shape of Moraine 5 shows that it is clearly a re-advance moraine caused by a minor period of increased cold, while Moraine 4 is small and has a degraded and ice-overrun appearance as a result of being overtopped during this minor re-advance. However, although there is agreement about the geomorphology and its interpretation, the timing of this event is in question. The

SED data indicate that it occurred at an earlier time than that suggested by Bockheim et al. (1989).

Below Moraine 5, the glacier receded steadily over a period of approximately 13 ka from around 42 ± 3 ka B.P., down to a position just above Moraine 1 at an elevation of 900 m a.s.l. Since this retreat, the ice has not re-advanced back over this position. During this period there was a still-stand interval represented by Moraine 3. It is unclear how long this stationary period lasted, but the size of the moraine ridge (2.5m high by 4.5 m wide) indicates it was significant. A lack of SED sample points at this point limits the interpretation of this still stand.

Bockheim et al. (1989) marked the boundary between the Hatherton and Britannia I drifts in the Lake Wellman area as being within 100 m from the present glacial margin. In this study the Hatherton drift was clearly recognisable in the zone outlined by these authors, by means of its fresh surface appearance and readily identifiable geomorphology features. The latter included the numerous striations found concentrated on the surfaces of boulders in this drift. Within the Hatherton drift, clear boundaries could be identified close to Moraines 2 and 1 from a combination of SED and field transect results. Although some inconsistencies remained even after rejecting some data as explained above, the SED results make it possible to age the Hatherton drift material at ca. 1 – 3 ka B.P. (Figure 72).

5.12. Wider implications

The Lake Wellman area is the second largest ice-free region in the Transantarctic Mountains after the Dry Valleys. It is a strategic location for understanding the factors that have influenced past fluctuations of the glaciers that drain the East Antarctic Ice Sheet (EAIS) to the Ross Ice Shelf. Identifying the location, timing and rate of recession of glacial ice in this area is relevant to knowledge of how the EAIS has responded to climate change, especially during the LGM. This is because the extent to which these glaciers advance within the TAM is determined by the volume of this ice sheet. Secondly, these factors also indirectly provide information on the movement of the Ross Ice Shelf grounding line, which governs the degree to which the glaciers thicken if they become impeded at the point where they exit. The quantity of ice in the Ross Embayment depends on the extent of the West Antarctic

Ice Sheet. This opens into the Ross Sea by means of fast moving ice streams and is less stable than the EAIS, which is constrained by the TAM. Understanding the functioning of the WAIS is important, because it holds an immense volume of frozen water (the equivalent of 5 m rise in sea level, which would have significant global effects were it to melt (Bentley et al., 1981).

Recent reconstructions presented by Conway et al. (1999) and Denton and Hughes (2000), suggest that a rise in sea level due to the melting of Northern Hemisphere glaciers initiated the rapid onset of a Ross Ice Shelf recession at the end of the LGM. This was because of the manner in which the Ross Ice Shelf grounding line margin responds to sea level fluctuations. Sea level rise causes sub-glacial decoupling resulting in a retreat of the grounding line margin accompanied by ice berg carving at the floating ice margin (Reusch and Hughes, 2003). This recession continued in the Holocene although it eventually decreased following a reduction in sea level forcing (Conway et al., 1999). Conway et al. (1999) even suggested that another rise in sea levels might cause the collapse of the WAIS. Understanding the current rate of ice recession will help to quantify any similar such recession in the future and the impact it is likely to have on the WAIS.

In order to resolve how the ice did recede, attempts have been made to determine chronological relationships between a number of the glaciers in the TAM by comparing data on soil characteristics and ^{14}C dates of algal deposits (Bockheim et al., 1989; Denton et al., 1989). As noted, Bockheim et al. (1989) placed the position of the Hatherton Glacier ice surface within the Britannia drifts in the Lake Wellman area at the time of the LGM (late Wisconsin, within the MIS 2 period, ca. 16-20 ka B.P.).

Anderson et al. (2004) created a model for the progress of the Darwin and Hatherton Glaciers which determined that the best fit position for the maximum ice elevation of the Darwin Glacier-Ross Ice Shelf transition during the LGM was 800 m higher than the present Ross Shelf ice surface (Figure 6, page 15). They disputed the higher value determined by Bockheim et al. (1989), and considered that the Ross Ice Shelf had retreated at an earlier period than suggested by these authors. This appears to be supported by the work of Todd et al. (2007) in the Reedy Glacier. However, the

absence of a prominent LGM feature in the Lake Wellman landscape is a problem. There are therefore two possibilities: Model A, which places the LGM position of the glacier surface lower than that of Moraine 5, which itself is dated older than 40 ka B.P. Or, Model B, which sites the LGM location as concurrent with that of Moraine 5 (age 18-20 ka B.P.), as suggested by Bockheim et al. (1989).

The results from this new study using the comparatively recent technique of cosmogenic dating concur with the conclusion of Anderson et al. (2004) and imply that the position of the glacier surface during the LGM was lower than that proposed by Bockheim et al. (1989). The regular trend in the SED data over a wide area shows that it is unlikely that these are inherited ages obtained from boulders of an older drift carried in by the ice advance. The SED and field data indicate that Moraine 5 does not relate to the LGM, but instead represents an earlier expansion of the glacier that occurred during a colder period at ca. 42 ka B.P., or earlier. Ice core data indicate a gradual oscillating decline in temperatures over a period of 40 ka to a minimum during the LGM, after which they rose more rapidly until ca. 10 ka B.P. (Barnola et al., 2003). It is likely that Moraine 5 formed during one of the more pronounced descending temperature fluctuations prior to the LGM. The position of the glacier margin during the LGM was thus lower, in the Britannia I drift area, possibly between Moraines 2 and 4. It may have coincided with Moraine 3, but the nature of the SED sampling positions makes it impossible to check this without further investigation. Since the glacier surface was lower than previously thought in the vicinity of Lake Wellman during the LGM, it was also lower at its outlet at about this time. This is based on the assumption that the EAIS was reasonable stable with little elevation change during the LGM as presented by Denton and Hughes (2000). Polar Plateau ice would therefore have had no effect on the thickness of the glacier, which would have been influenced solely by grounded shelf ice at the outlet. Thus, the work of this project supports the earlier retreat of the Ross Ice Shelf, as proposed by Anderson et al. (2004).

6. Conclusions

6.1. General

The Lake Wellman area was an appropriate locality to apply the relatively new Surface Exposure Dating (SED) technology, in order to gain new insights on past changes in the extent of the Hatherton and Darwin Glacier system. This procedure analyses the concentrations of the cosmogenic nuclides ^{10}Be to ^{26}Al in order to determine how long rock samples from moraines have been exposed to cosmic rays after release from the ice of a receding glacier margin. During the project, geomorphology features were studied in the field, lithologies and physical properties of clasts from moraine drifts were recorded and evaluated, and rock samples were collected and dated cosmogenically. The results of this project have improved our understanding of the past ice movement in this region, by yielding the following information.

1. The moraine drifts described by Bockheim et al. (1989) were generally confirmed by means of their physical and chemical clast properties. In addition, six moraine ridges which formed during periods of temporary re-advance and recession were identified and numbered.

2. The SED dates of the drift deposits were broadly comparable to those obtained using ^{14}C dating by Bockheim et al. (1989), but with indications that their values were partly underestimated. In particular, the data indicated that the ice had receded from below a large moraine ridge, Moraine 5, over a period between approximately 42 ka and 29 ka B.P., not later, as previously believed. This was based on the ages determined for the residual Britannia drift deposits.

3. Instead, Moraine 5 was formed by a temporary re-advance at or earlier than ca. 42 ka B.P., which over-rode an earlier ridge, Moraine 4.

4. The margin of the glacier ice during the LGM (18 – 20 ka B.P.) was therefore not located at Moraine 5, as suggested by published ^{14}C data, but at a lower

position between Moraine 2 (3 ka B.P.) and Moraine 3 (31 ka B.P.) (Figure 22).

5. There was a relatively short stationary period in ice recession at ca. age 19 ka B.P. indicated by a further, lower elevation ridge, Moraine 3.

6. There were slight fluctuations in the current margin of the Hatherton Glacier during the last 1 ka.

7. The repositioning of the glacier surface resulting from the new SED data obtained in this study indicates that the glacier was not as thick as indicated by Bockheim et al. (1989) during the LGM. Instead, the results of this project support the modelled outcome of Anderson et al. (2004) that the glacier was thinner at this time due to the unrestricted access of ice at the glacier outlet into the Ross Sea. These findings therefore endorse a more rapid recession of the Ross Ice Shelf grounding line subsequent to the LGM.

6.2. Further research

In order to refine the outcomes from this project, investigation into the following is suggested:

1. Additional SED sample collection and dating from sediments at different location on the margins of the Darwin-Hatherton Glacier System, and from adjacent valleys east of the Hatherton, to compare these data to those found in this study area.

2. Further SED sampling from the Lake Wellman area to increase the accuracy and of the dates found in this study, in particular in the vicinity of Moraines 2 and 3, where greater enhancement is needed to identify the position of the ice during the LGM.

3. U-Pb SHRIMP analysis of the large granite erratic boulders to identify provenance and derive their source.

7. References

Allibone, A.H., Forsyth, P.J., Sewell, R.J., Turnbull, I.M., and Bradshaw, M.A., 1991. Geology of the Thundergut Area, Southern Victoria Land, Antarctica. DSIR Geology and Geophysics, PO Box 30368, Lower Hutt.

Anderson, B.M., Hindmarsh, R.C.A. and Lawson, W.J., 2004. A modelling study of the response of Hatherton Glacier to Ross Ice Sheet grounding line retreat. Global and Planetary Change, 42(1-4): 143-153.

Anderson, J. B., 1999. Antarctic Marine Geology. New York: Cambridge University Press.

Atkins, C.B., Barrett P.J. and Hicock, S.R., 2002. Cold glaciers erode and deposit: Evidens from Allan Hills, Antarctica. Geological Society of America, 30(7): 659-662.

Atkins, C.B., 2004. Photographic atlas of striations from selected glacial and non-glacial environments. Antarctic Data Series No.28, Antarctic Research Centre, Victoria University of Wellington, PO Box 600, New Zealand.

Atkins, C.B and Dickinson, W.W., 2007. Landscape modification by meltwater channels at margins of cold-based glaciers, Dry Valleys, Antarctica. Boreas, 36, 47-55.

Balco, G., Stone, J., Lifton, N., and Dunai, T., 2008. A simple, internally consistent, and easily accessible means of calculating surface exposure ages and erosion rates from Be^{10} and Al^{26} measurements. Quaternary Geochronology, 3, 174-195.

Barnola, J.-M., D. Raynaud, C. Lorius, and N.I. Barkov. 2003. Historical CO2 record from the Vostok ice core. In Trends: A Compendium of Data on Global Change. Carbon Dioxide Information Analysis Center, Oak Ridge National Laboratory, U.S. Department of Energy, Oak Ridge, Tenn., U.S.A.

Barret, P. J. and Kohn, B.P., 1975. Changing sediment transport directions form Devonian to Triassic in the Beacon Supergroup of South Victorier Land, Antarctica. In: Campbell, K. S. W. ed. Gondwana geology. Third Gondwana Symposium, Canberra, Australia. pp. 15-35.

Barrett, P.J., Florindo, F. and Cooper, A.K., 2006. Introduction to Antarctic climate evolution: View from the margin. Palaeogeography, Palaeoclimatology, Palaeoecology, 231(1-2): 1-8.

Behrendt, J.C. and Cooper, A. K., 1991. Evidence of rapid Cenozoic uplift of the shoulder escarpment of the West Antarctica rift system and a speculation on possible climate forcing. Geology, 19, 315-319.

Bennett, M. R. and Glasser, N. F., 1997. Glacial geology: Ice sheets and landforms. Chichester, New York: Wiley.

Benn, D. I. and Evans D. J. A., 1998. Glaciers & glaciation. London: Arnold; New York : Wiley.

Benn, D.I., and Ballantyne, C.K., 1993. The description and representation of particle shape. Earth Surface Processes and Landforms, 18, 665-672.

Bentley, C.R. and Jezek, K.C., 1981. RISS, RISP and RIGGS: Post-IGY glaciological investigations of the Ross Ice Shelf in the U.S. programe. Journal of the Royal Society New Zealand, 11(4): 355-372.

Berg, T. E. and Black, R. F. 1966. Preliminary measurements of growth of nonsorted polygons, Victoria Land, Antarctica. In: Tedrow, J. C. F. (Ed.), Antarctic Soils and Soil Forming Processes. Antarctic Research Series 8: 61-108.

Bierman, P.R., and Steig, E., 1996. Estimating rates of denudation and sediment transport using cosmogenic isotope abundances in sediment. Earth Surface Processes and Landforms, 21, 125-139.

Bierman, P. R., Marsella, K. A., Davis, P. T., Patterson, C. and Caffee, M., 1999. Mid-Pleistocene cosmogenic minimum-age limits for pre-Wisconsinan glacial surfaces in southwestern Minnesota and southern Baffin Island a multiple nuclide approach. Geomorphology, 27(1/2): 25-40.

Bockheim, J.G., Wilson, S.C., Denton, G.H., Andersen, B.G. and Stuiver, M., 1989. Late Quaternary ice-surface fluctuations of Hatherton Glacier, Transantarctic Mountains. Quaternary Research, 31(2): 229-254.

Budzikiewicz, H. and Grigsby, R. D., 2006. Mass spectrometry and isotopes: A century of research and discussion. Mass Spectrometry Reviews, 25, 146-157.

Conway, H., Hall, B.L., Denton, G.H., Gades, A.M. and Waddington, E.D., 1999. Past and future grounding-line retreat of the West Antarctic Ice Sheet. Science, 286(5438): 280-283.

David, R. J. and Schaeffer O. A., 1955. Chlorine^{36} in nature. Annals of the New York Academy of Sciences, 62, 105-122.

Denton, G.H., 1979. Glacial history of the Byrd-Darwin Glacier area, Transantarctic Mountains. Antarctic Journal of the United States, 14(5): 57-58.

Denton, G.H., Bockheim, J.G., Wilson, S.C. and Stuiver, M., 1989. Late Wisconsin and early Holocene glacial history, inner Ross Embayment, Antarctica. Quaternary Research, 31(2): 151-182.

Denton, G.H. and Hughes, T.J., 2000. Reconstruction of the Ross Ice Drainage System, Antarctica, at the Last Glacial Maximum. Geografiska Annaler, Series A, Physical Geography, 82(2/3): 143-166.

Drewry, D., 1986. Glacial geologic processes. London: Arnold.

Evans, D.J.A., 2002. Glacial geology and geomorphology. In: Encyclopedia of Physical Science and Technology, 3rd ed. Accademic Press, 6, 719-731.

Haskell, T.R., Kennett, J.P. and Prebble, W.M., 1964. Basement and seimentary geology of the darwin glacier area. In: Adie, J.R. (Ed.), SCAR - IUGS Symposium of Antarctic Geology; Cape Town, South Africa, 348-351.

Hulbe, C.L. and MacAyeal, D.R., 1999. A new numerical model of coupled inland ice sheet, ice stream, and ice shelf flow and its application to the West Antarctic Ice Sheet. Journal of Geophysical Research B: Solid Earth, 104(B11): 349-366.

Kellogg, T.B., Hughes, T. and Kellogg, D.E., 1996. Late Pleistocene interactions of East and West Antarctic ice-flow regimes: Evidence from the McMurdo Ice Shelf. Journal of Glaciology, 42, 486-499.

Lindsey, D.A., Langer, W.H. and Van Gosen, B.S., 2007. Using pebble lithology and roundness to interpret gravel provenance in piedmont fluvial systems of the Rocky Mountains, USA. Sedimentary Geology, 199(3-4): 223-232.

McKelvey, B.C. and Webb, P.N., 1977. Stratigraphy of the Taylor and lower Victoria groups (Beacon Suprergroup) between the Mackay Glacier and Boomerang Range, Antarctica. New Zealand Journal of Geology and Geophysics, 20(5): 813-863.

Mellon, M. T., Searls, M. L., Martinez-Alonso, S., and the HiRISE Team, 2007. HiRISE observations of patterned ground on mars. 7th International Conference on Mars; Pasadena: California, LPI Contribution No. 1353, p.3285

Moriwaki, K., Yoshida, Y. and Harwood, D.M., 1992. Cenozoic glacial history of Antarctica - a correlative synthesis. In: Yoshida, Y, Kaminuma, K., and

Shiraishi, K. (Eds.), Recent Progress in Antarctic Earth Science - Proceedings of the 6th International Symposium on Antarctic Earth Science; Tokyo (Terra Sci. Publ. Co.), 773-780.

Mustoe, G. E., 1982. The origin of honeycomb weathering. Geological Society of America Bulletin, 93(2): 108-115.

Olmsted, J. and Williams, G.M., 2006. Chemistry, 4th ed.. New York: Whiley, p 47.

Reusch, D. and Hughes, T., 2003. Surface waves on Byrd Glacier, Antarctica. Antarctic Science, 15(4): 547-555.

Rodriguez-Navarro, C., Doehne, E. and Sebastian, E., 1999. Origins of honeycomb weathering: The role of salts and wind. Bulletin of the Geological Society of America, 111(8): 1250-1255.

Stern, T.A. and Ten Brink, U.S., 1989. Flexural uplift of the Transantarctic Mountains. Journal of Geophysical Research, 94(B8): 10315-10330.

Storey, B.C.; MacDonald, D.I.M.; Dalziel, I.W.D.; Isbell, J.L.; Millar, I.L. (1996): Paleozoic sedimentation, magmatism, and deformation in the Pensacola Mountains, Antarctica: the significance of the Ross Orogeny. *Geological Society of America Bulletin 108 (6)*: 685-707.

Smith, N.D., 1985. Proglacial fluvial environments. In: Ashley, G.M., Shaw, J., and Smith, N.D. (Eds.), Glacial sedimentary environments: Society of Economic Paleontologists and Mineralogists, Short Course, 16, 85-126.

Sugden, D. E. and John, B. E., 1985. Glaciers and Landscape. London: Butler and Tanner.

Todd, C. E.; Stone, J.; Bromley, G.; Hall, B.; Conway, H. (2007): Late Quaternary evolution of Reedy Glacier, Antarctica. GSA Denver Annual Meeting, No. 27-17. *Geological Society of America Abstracts with Programs 39 (6)*: 80.

Van-den Berg, J., Van de Wal, R.S.W. and Oerlemans, J., 2006. Recovering lateral variations in lithospheric strength from bedrock motion data using a coupled ice sheet-lithosphere model. Journal of Geophysical Research, 111, B05409.

Waller, R.I., 2001. The influence of basal processes on the dynamic behaviour of cold-based glaciers. Quaternary International, 86, 117-128.

Washburn, A. l., 1973. Periglacial processes and environments. London: Arnold.

Windley, B. F., 1984. The Evolving Continents. (2nd) Edition. New York: John Wiley and Sons.

Winkler, S., 2005. The Schmidt hammer as a relative-age dating technique: Potential and limitations of its application on Holocene moraines in Mt. Cook National Park, Southern Alps, New Zealand. New Zealand Journal of Geology and Geophysics, 48, 105-116.

Zreda, M., 2000. Paleoclimate: are terrestrial and marine records concordant? Annual Packard Fellows Meeting; Monterey, USA.

Zreda, M.G., and Phillips, F.M., 2000. Cosmogenic nuclide buildup in surficial materials. In: Noller, J.S., Sowers, J.M and Lettis, W.R. (Eds.), Quaternary Geochronology: Methods and Applications, AGU Reference Shelf 4, American Geophysical Union, 61-76.

8. Appendix

8.1. SED sample ID sheets and photographs

SAMPLE ID The sample ID correspond to LW numbers used in tables and in the main text.	
Date	
Geographical locality	
Grid reference (Lat/Long)	
Altitude (m.a.s.l.)	
Rock type/lithology	
Glacial stage/age	
Site description	
Surface character	
Depth/thickness	
Boulder dimensions	
Topographic shading Example. All compass readings are from magnetic north. No correction has been applied.	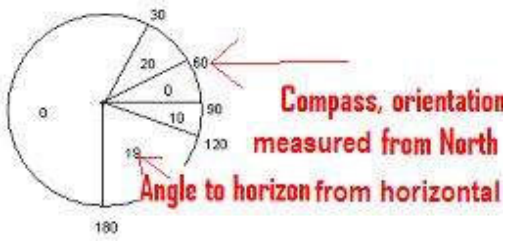
Surface slope	
Picture numbers	
Comment	

SAMPLE ID	**NZ 0365** (LW13.3)
Date	10.12.2007
Geographical locality	As 1
Grid reference (Lat/Long)	795325.93351 S / 1564522.42325 E
Altitude (m.a.s.l.)	1112.058 m
Rock type/lithology	Granite, cracked
Glacial stage/age	
Site description	As 1
Surface character	Weathered, rounded
Depth/thickness	2-3 cm
Boulder dimensions	158 x 157 x 93 cm
Topographic shading	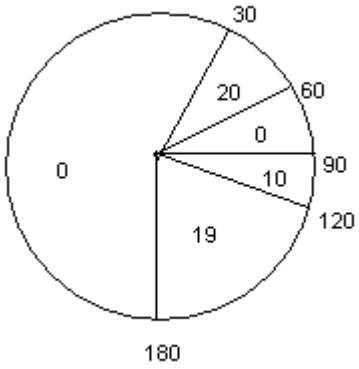
Surface slope	Sub-horizontal
Picture numbers	506-507
Comment	

SAMPLE ID	**NZ 0382** (LW11.1)
Date	09.12.2007
Geographical locality	As LW10 but a bit further up slope at the end of drift (CL8)
Grid reference (Lat/Long)	795641.59490 S / 1564632.06894 E
Altitude (m.a.s.l.)	1646.225 m
Rock type/lithology	Granite perched on basalt rocks
Glacial stage/age	
Site description	As LW10
Surface character	Weathered, slightly stained
Depth/thickness	
Boulder dimensions	
Topographic shading	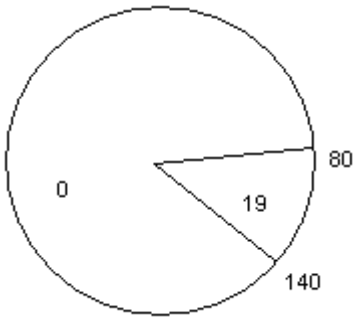
Surface slope	
Picture numbers	-441
Comment	Sample ‘LW11.1b’ of basalt at the same location

SAMPLE ID	**NZ 0384** (LW09.3)
Date	09.12.2007
Geographical locality	As 1
Grid reference (Lat/Long)	795625.67586 S / 1564852.19147 E
Altitude (m.a.s.l.)	1508.449 m
Rock type/lithology	Granite
Glacial stage/age	
Site description	As 1
Surface character	High degree of weathering, although not as much as other types of rock, heavy iron staining
Depth/thickness	1-2 cm
Boulder dimensions	130 x 170 x 45 cm
Topographic shading	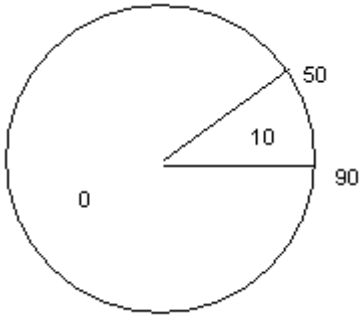
Surface slope	Sub-horizontal
Picture numbers	417-418
Comment	

SAMPLE ID	**NZ 0372** (LW20.3)
Date	12.12.2007
Geographical locality	As 1
Grid reference (Lat/Long)	795348.22461 S / 1564809.11753 E
Altitude (m.a.s.l.)	1024.943 m
Rock type/lithology	Granite, split in two
Glacial stage/age	
Site description	
Surface character	Iron stained
Depth/thickness	3 cm
Boulder dimensions	150 x 110 x 60 cm
Topographic shading	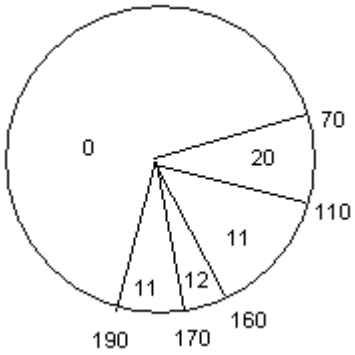
Surface slope	
Picture numbers	605-606, 1003040
Comment	Soil sample + transect

SAMPLE ID	**NZ 0373** (LW21.1)
Date	12.12.2007
Geographical locality	On terrace between T02 and T01
Grid reference (Lat/Long)	795352.58402 S / 1564906.00887 E
Altitude (m.a.s.l.)	981.510 m
Rock type/lithology	Granite (subrounded)
Glacial stage/age	
Site description	
Surface character	Iron stained
Depth/thickness	2-3 cm
Boulder dimensions	74 x 93 x 84 cm
Topographic shading	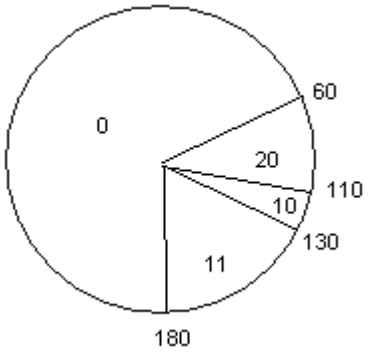
Surface slope	Sub-horizontal
Picture numbers	608-609
Comment	

SAMPLE ID	**NZ 0370** (LW18.3)
Date	12.12.2007
Geographical locality	As 1
Grid reference (Lat/Long)	795329.37657 S / 1564553.63371 E
Altitude (m.a.s.l.)	1101.008 m
Rock type/lithology	Granite (subrounded)
Glacial stage/age	
Site description	
Surface character	Weathered, brown stained
Depth/thickness	
Boulder dimensions	180 x 83 x 110 cm
Topographic shading	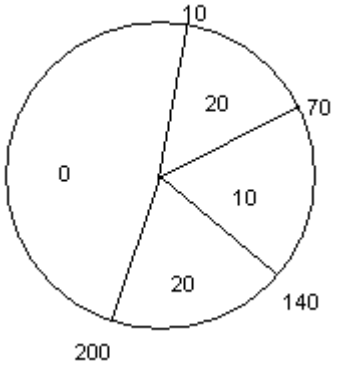
Surface slope	
Picture numbers	591-592
Comment	Soil sample and transect

SAMPLE ID	**NZ 0371** (LW20.1)
Date	12.12.2007
Geographical locality	Just down valley from T03
Grid reference (Lat/Long)	795338.66895 S / 1564759.29028 E
Altitude (m.a.s.l.)	1019.342 m
Rock type/lithology	Sandstone with dolorite on top
Glacial stage/age	
Site description	
Surface character	Iron stained, fresh striations
Depth/thickness	3 cm
Boulder dimensions	
Topographic shading	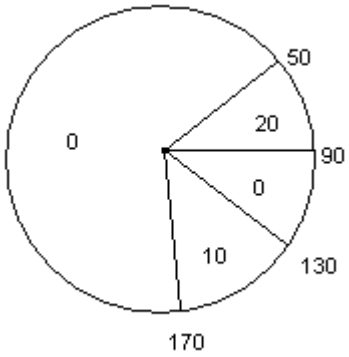
Surface slope	
Picture numbers	602-603
Comment	

SAMPLE ID	**NZ 0374** (LW21.2)
Date	12.12.2007
Geographical locality	As 1
Grid reference (Lat/Long)	795353.97033 S / 1564905.28732 E
Altitude (m.a.s.l.)	982.281 m
Rock type/lithology	Beacon sandstone
Glacial stage/age	
Site description	
Surface character	Striated
Depth/thickness	2-3 cm
Boulder dimensions	177 x 78 x 56 cm
Topographic shading	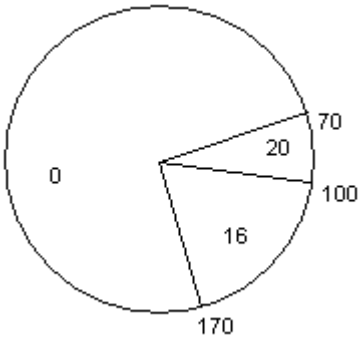
Surface slope	
Picture numbers	
Comment	

SAMPLE ID	**NZ 0375** (LW24.1)
Date	13.12.2007
Geographical locality	1st terrace from camp
Grid reference (Lat/Long)	795520.60881 S / 1565407.68442 E
Altitude (m.a.s.l.)	894.977 m
Rock type/lithology	Granite with stones on top (including sample LW24.1b)
Glacial stage/age	
Site description	Flat terrace with an abundance of striated and rounded boulders
Surface character	Iron stained, weathered
Depth/thickness	From edge – 5 cm
Boulder dimensions	115 x 160 x 50+
Topographic shading	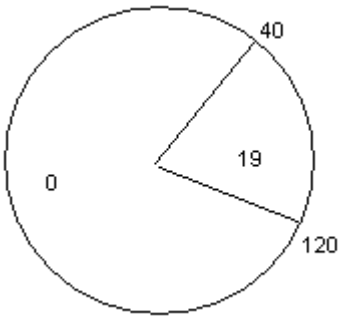
Surface slope	Sub-horizontal
Picture numbers	661-662
Comment	

SAMPLE ID	**NZ 0376** (LW24.2)
Date	13.12.2007
Geographical locality	As 1
Grid reference (Lat/Long)	795517.81137 S / 1565357.69160 E
Altitude (m.a.s.l.)	892.903 m
Rock type/lithology	Granite (subrounded)
Glacial stage/age	
Site description	
Surface character	Slight iron staining
Depth/thickness	3 cm
Boulder dimensions	
Topographic shading	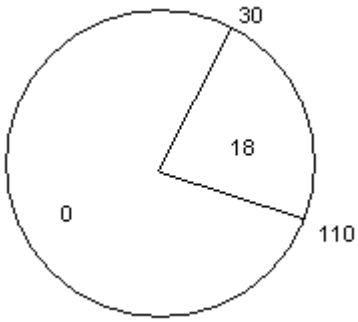
Surface slope	
Picture numbers	Soil sample + transect
Comment	

SAMPLE ID	**NZ 0377** (LW23.1)
Date	13.12.2007
Geographical locality	On top of ridge named ‘LW T01’
Grid reference (Lat/Long)	795500.82679 S / 1565439.38766 E
Altitude (m.a.s.l.)	851.966 m
Rock type/lithology	Beacon sandstone (angular)
Glacial stage/age	
Site description	
Surface character	Fresh
Depth/thickness	3 cm
Boulder dimensions	33 x 18 x 14 cm
Topographic shading	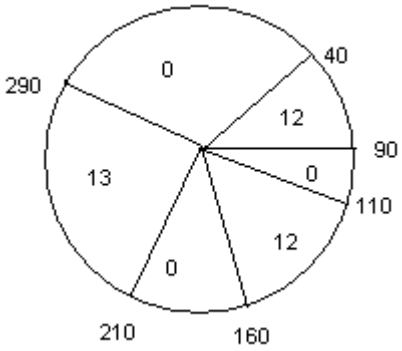
Surface slope	
Picture numbers	626-627
Comment	

SAMPLE ID	**NZ 0379** (LW25.1)
Date	13.12.2007
Geographical locality	Drift behind camp
Grid reference (Lat/Long)	795512.34441 S / 1565525.96534 E
Altitude (m.a.s.l.)	852.690 m
Rock type/lithology	Granite
Glacial stage/age	Hatherton
Site description	An abundance of striated rocks
Surface character	Iron stained
Depth/thickness	5 cm
Boulder dimensions	125 x 86 x 44 cm
Topographic shading	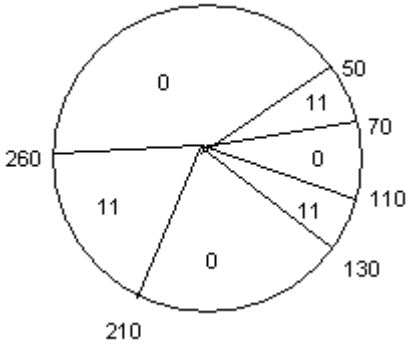
Surface slope	16 degrees SE
Picture numbers	672-673
Comment	

SAMPLE ID	**NZ 0366** (LW14.1)
Date	10.12.2007
Geographical locality	On apex of T05
Grid reference (Lat/Long)	795326.40287 S / 1564533.54117 E
Altitude (m.a.s.l.)	1119.346 m
Rock type/lithology	Beacon sandstone on top of dolorite
Glacial stage/age	
Site description	Angular – subangular rocks, no fines on surface
Surface character	Slightly iron stained
Depth/thickness	
Boulder dimensions	10 x 6 x 8 cm
Topographic shading	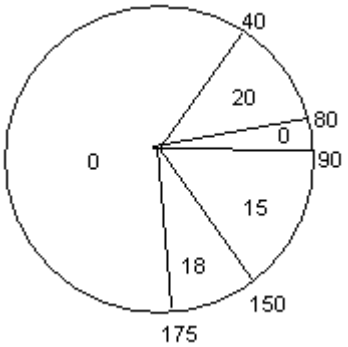
Surface slope	Sub-horizontal
Picture numbers	508-512
Comment	Transect

SAMPLE ID	**NZ 0368** (LW14.3)
Date	10.12.2007
Geographical locality	As 1
Grid reference (Lat/Long)	795326.62957 S / 1564533.40033 E
Altitude (m.a.s.l.)	1116.140 m
Rock type/lithology	Beacon sandstone on top of dolorite
Glacial stage/age	
Site description	As 1
Surface character	Slight iron staining
Depth/thickness	6 cm
Boulder dimensions	17 x 17 x 8 cm
Topographic shading	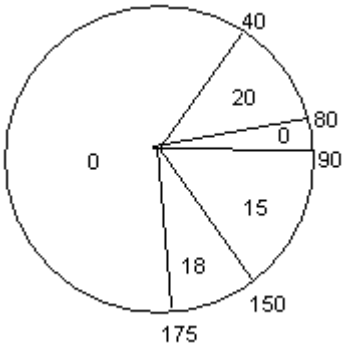
Surface slope	
Picture numbers	514-516
Comment	

SAMPLE ID	**NZ 0385** (LW02.1)
Date	05.12.2007
Geographical locality	On top of slope (lunch spot)
Grid reference (Lat/Long)	795553.77144 S / 1565217.67073
Altitude (m.a.s.l.)	1245.887 m
Rock type/lithology	Granite, subangular / angular (check picture)
Glacial stage/age	Britannia / Danum
Site description	Fewer large boulder compared to previous site
Surface character	Iron stained, fresh rock
Depth/thickness	5-7 cm
Boulder dimensions	800 x 500 x 300 cm
Topographic shading	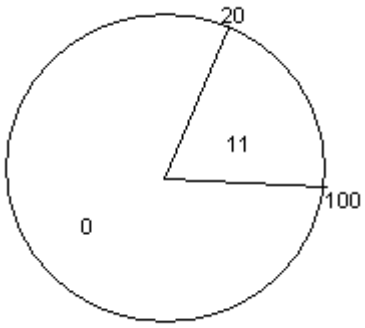
Surface slope	15 degrees
Picture numbers	
Comment	Leaning on rocks

SAMPLE ID	**NZ 0369** (LW18.1)
Date	12.12.2007

Geographical locality	Just down valley from T05
Grid reference (Lat/Long)	795326.94287 S / 1564554.12007 E
Altitude (m.a.s.l.)	1087.005 m
Rock type/lithology	Beacon sandstone
Glacial stage/age	Britannia?
Site description	
Surface character	Weathered, bash marks, iron stained, cavernous weathering
Depth/thickness	
Boulder dimensions	290 x 177 x 203 cm
Topographic shading	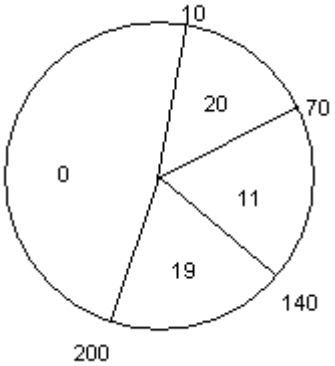
Surface slope	Sub-horizontal
Picture numbers	587-588
Comment	

SAMPLE ID	**NZ 0378** (LW23.2)
Date	13.12.2007

Geographical locality	As 1
Grid reference (Lat/Long)	795501.11192 S / 1565435.64305 E
Altitude (m.a.s.l.)	850.463 m
Rock type/lithology	Granite
Glacial stage/age	
Site description	
Surface character	
Depth/thickness	Whole stone sampled
Boulder dimensions	12 x 8 x 5
Topographic shading	

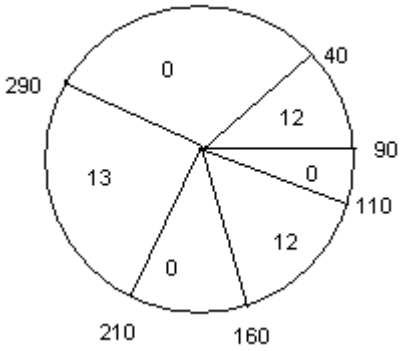

Surface slope	
Picture numbers	628-629, 1003062
Comment	Soil sample

SAMPLE ID	**NZ 0380** (LW25.2)

Date	13.12.2007
Geographical locality	As 1
Grid reference (Lat/Long)	795513.44598 S / 1565530.54614 E
Altitude (m.a.s.l.)	845.559 m
Rock type/lithology	Beacon sandstone
Glacial stage/age	Hatherton
Site description	
Surface character	Plucked, bashed, striated, edges recently rounded
Depth/thickness	5 cm
Boulder dimensions	125 x 96 x 45 cm
Topographic shading	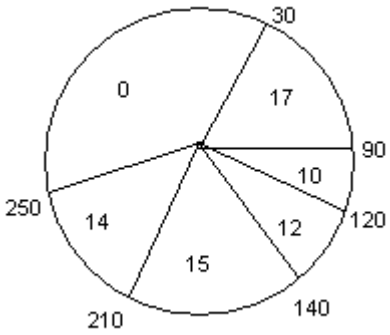
Surface slope	
Picture numbers	674-675
Comment	

SAMPLE ID	**NZ 0367** (LW14.2)
Date	10.12.2007
Geographical locality	As 1
Grid reference (Lat/Long)	795326.54600 S / 1564533.80748 E
Altitude (m.a.s.l.)	1114.881 m
Rock type/lithology	Beacon sandstone
Glacial stage/age	
Site description	As 1
Surface character	Slight iron staining
Depth/thickness	
Boulder dimensions	24 x 60 x 51 cm
Topographic shading	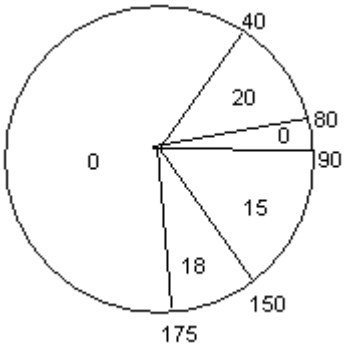
Surface slope	
Picture numbers	513-516
Comment	

SAMPLE ID	**NZ 0362** (LW12.1)

Date	10.12.2007
Geographical locality	~ 500 m up valley from T05
Grid reference (Lat/Long)	795319.79819 S / 1564353.58644 E
Altitude (m.a.s.l.)	1149.722 m
Rock type/lithology	Beacon sandstone (beding, blocky) perched on stones
Glacial stage/age	Danum?
Site description	Patterned ground, undulating topography, an abundance of iron stained and cavernous weathered rocks
Surface character	Iron stained, brown weathered
Depth/thickness	~ 4 cm
Boulder dimensions	174 x 105 x 84 cm
Topographic shading	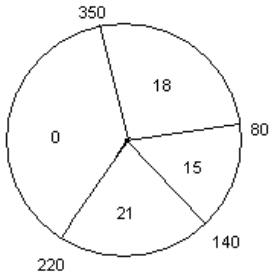
Surface slope	
Picture numbers	494-495
Comment	Outcrop of sandstone in the cliffs above. Soil sample

SAMPLE ID	**NZ 0363** (LW12.2)
Date	10.12.2007

Geographical locality	4 m from LW12.1
Grid reference (Lat/Long)	795319.78570 S / 1564352.76899 E
Altitude (m.a.s.l.)	1154.062 m
Rock type/lithology	Granite
Glacial stage/age	
Site description	As 1
Surface character	Iron stained, slight cavernous weathering
Depth/thickness	- 6cm
Boulder dimensions	180 x 212 x 84 cm
Topographic shading	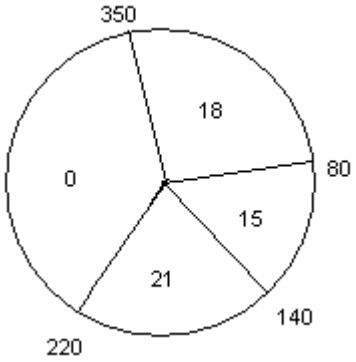
Surface slope	Sub-horizontal
Picture numbers	496-497
Comment	

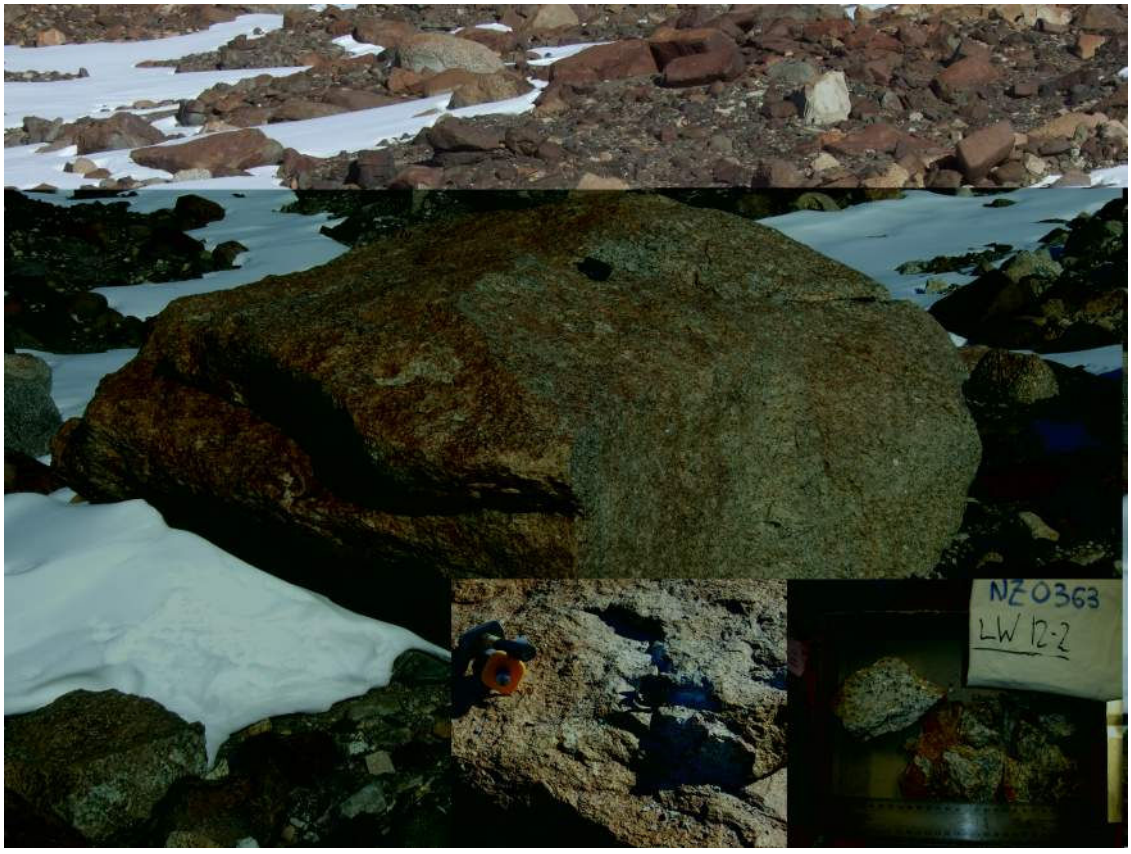

SAMPLE ID	**NZ 0364** (LW13.2)
Date	10.12.2007

Geographical locality	As 1
Grid reference (Lat/Long)	795325.81355 S / 1564526.79864 E
Altitude (m.a.s.l.)	1107.076 m
Rock type/lithology	Beacon sandstone
Glacial stage/age	
Site description	As 1
Surface character	Slight iron staining, slight exfoliation
Depth/thickness	5 cm
Boulder dimensions	180 x 211 x 103 cm
Topographic shading	

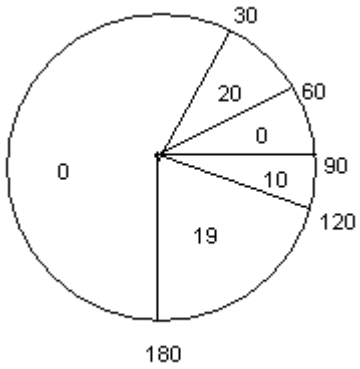

Surface slope	Sub-horizontal
Picture numbers	504-505
Comment	

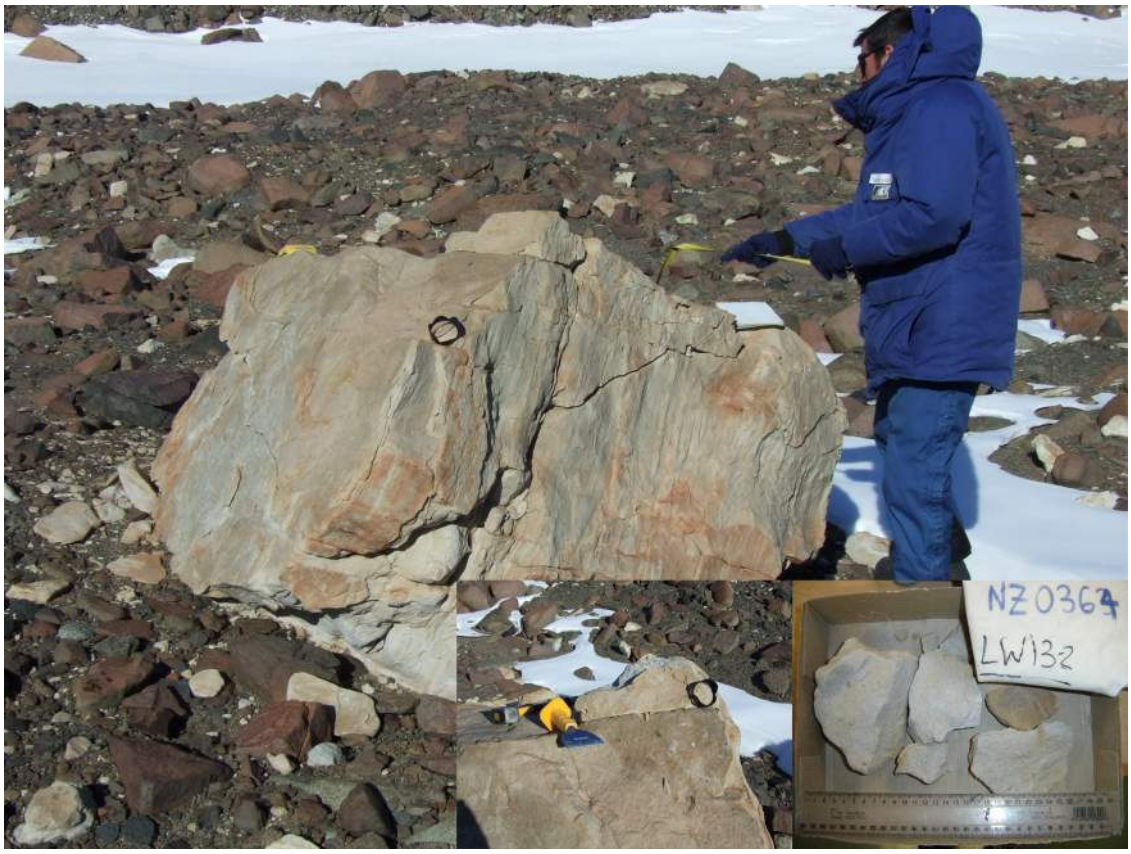

SAMPLE ID	**NZ 0381** (LW15.1)
Date	11.12.2007

Geographical locality	Just below moraine (lateral) on slope above depression
Grid reference (Lat/Long)	795519.23653 S / 1564754.99538 E
Altitude (m.a.s.l.)	1135.652 m
Rock type/lithology	Beacon sandstone (subangular) perched on dolorite boulder
Glacial stage/age	
Site description	Cavernous weathering on some of the surrounding boulders
Surface character	Brown stained
Depth/thickness	4 cm
Boulder dimensions	105 x 156 x 185 cm
Topographic shading	

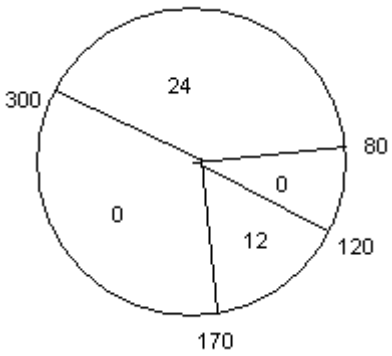

Surface slope	
Picture numbers	544-545
Comment	

SAMPLE ID	**NZ 0386** (LW02.2)
Date	05.12.2007

Geographical locality	10 m from LW02.1
Grid reference (Lat/Long)	795553.77480 S / 1565216.79445 E
Altitude (m.a.s.l.)	1237.447 m
Rock type/lithology	Beacon sandstone perched on a flat dolerite
Glacial stage/age	Britannia / Danum
Site description	As 1
Surface character	Fresh, slight staining
Depth/thickness	Whole cobble
Boulder dimensions	12 x 12 x 10 cm
Topographic shading	

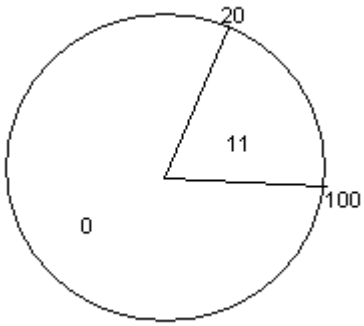

Surface slope	Sub-horizontal
Picture numbers	
Comment	Took whole cobble

SAMPLE ID	**NZ 0383** (LW09.1)
Date	09.12.2007
Geographical locality	Level number 6 from camp (CL6)
Grid reference (Lat/Long)	795625.70248 S / 1564910.13584 E
Altitude (m.a.s.l.)	1501.021 m
Rock type/lithology	Beacon sandstone
Glacial stage/age	
Site description	Boulder drift (granite, basalt, sandstone), abundance of cavernous weathering
Surface character	Iron stained, cavernous weathering, lichens (sample collected)
Depth/thickness	5 cm
Boulder dimensions	256 x 290 x 130 cm
Topographic shading	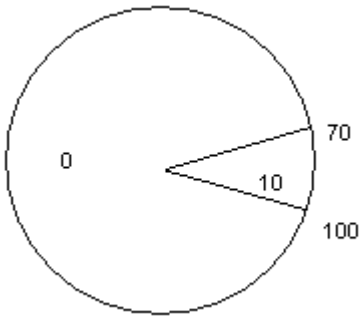
Surface slope	Sub-horizontal
Picture numbers	413-414
Comment	Soils sample

Glacial Geomorphology of the Lake Wellman area, Antarctica.

Scale 1:50 000

Produced by David J. Hood, May 2009.

This map was created at the University of Canterbury using the grid based Universal Transverse Mercator coordinate system and the World Geodetic System 1984 datum. A Trimble GPS GEO - XM unit was used to locate features within the datum and the contour interval is measured from the datum. Special thanks to the Japanese Aerospace Exploration Agency for an Advanced Land Observation Satellite image of the Lake Wellman area (© JAXA 2008) and to Land Information New Zealand for access to polygon and DEM data.